PERFORMANCE INVESTIGATION OF THE SWASH PLATE AXIAL PISTON PUMPS WITH CONICAL CYLINDER BLOCKS

Medhat Khalil

A Thesis

In

The Department of

Mechanical and Industrial Engineering

Presented in Partial Fulfillment of the Requirements

for the Degree of Doctor of Philosophy (Mechanical Engineering) at

Concordia University

Montreal, Quebec, Canada

March 2003

ABSTRACT

PERFORMANCE INVESTIGATION OF THE SWASH PLATE AXIAL PISTON PUMPS WITH CONICAL CYLINDER BLOCKS

Medhat Khalil, Ph.D.

Concordia University, 2003

In view of their excellent static and dynamic characteristics, swash plate axial piston pumps are now widely used in open and closed hydraulic circuits in both mobile and industrial applications. Recently, an improved version of the swash plate pumps was designed in which the group of pistons was assembled in a conical arrangement around the pump driving shaft within a conical cylinder block. The improved version of the pump has not been investigated in comparison to the conventional design where the group of pistons was assembled in a cylindrical array around the pump driving shaft. An analytical investigation is important in order to fully exploit the advantages of a conical arrangement.

In this thesis a mathematical model is developed in order to describe the dynamics of the variable geometric volume swash plate axial piston pumps with the conical cylinder blocks and the integrated control unit. The relevant operating conditions, fluid properties and pump design parameters are considered in the model. A simulation program based on Matlab-Simulink is constructed to solve the derived pump mathematical model numerically. The simulation program is flexible enough to

simulate both the old and new design of the pump. An experimental setup was built in the laboratory using a commercially available pump with a conical cylinder block consisting of 9 cylinders in order to verify the pump model. The model was then validated based on the agreement between the simulation and the measured results.

Using the validated model, an analytical study was conducted in order to investigate the effect of the port plate configuration on pump performance. Simulation of the change in the cylinder pressure and pump flow rate, in a systematic sequential procedure, led to an improved geometry for the suction and delivery silencing grooves on the valve plate. Cavitaion in the cylinder and pump noise were also reduced with the improved geometry. Force and vibration analysis of the pumping mechanism were carried out. This analysis presents some design recommendations regarding the moments acting on the swash plate, dynamic loads acting on the drive shaft bearings and the advantages and the limitations of using the conical arrangement of the pistons.

Pump performance is simulated using a conventional PD controller with double negative feedback loop to control the swash plate swiveling angle, as currently used in practical applications. An introductory study of implementing other control schemes is conducted. A fuzzy controller is proposed to replace the PD controller in a double feedback control loop in order to improve the robustness of the control action. A single feedback control loop is proposed to replace the double control loop in order to suppress the steady state vibration of the swash plate. The control schemes were prototyped using specially developed real-time control techniques on a personal computer. The experimental setup is also used to verify the analytical findings of the pump performance with the newly proposed control schemes.

ACKNOWLEDGMENTS

All praises are due to Allah who blessed me with kind professors and gave me support during the writing and research for this thesis.

I would like to express my deepest gratitude to Prof. Rama Bhat and Prof. J. Svoboda, Department of Mechanical and Industrial Engineering, Faculty of Engineering and Computer Sciences, Concordia University, for their continuous guidance, effective support, and suggestions during the various stages of this work.

I wish also to express my deep appreciation to Prof. Saad Kassem, Department of Mechanical Design and Production, Faculty of Engineering, Cairo University, for his effective advising in the early stages of this project.

I would like to thank the group of technicians and department secretaries for giving all the assistance needed to facilitate the work in the project.

I also wish to express my warm love and sincere appreciation to my wife Nahla, my children Karim, Sharif and Moataz, my sister Amal and my close friends Abd El-Hady and Yasser for their encouragement and support.

TABLE OF CONTENTS

LIST OF FIGURES

FIGURES IN THE APPENDICES

LIST OF TABLES

LIST OF SYMBOLS

Symbol	Description	Units
$A_d(A_s)$	Area of the openings that connect the cylinder to the delivery (suction) port on the port plate	m^2
A_{cp}	Area of the control piston	m^2
A_p	Piston cross-section area	m^2
$[a_{ck}]_0$	k^{th} piston absolute acceleration	M/s^2
B	Effective bulk modulus	Pa
C_d	Coefficient of discharge	-
D_1/R_1	Pitch circle diameter/radius of the cylinder arrangement at the base of the cylinder block	m
D_2/R_2	Pitch circle diameter/radius of the cylinder arrangement at the top of the cylinder block	m
D_3	Pitch circle diameter of the port plate	m
d_p	Piston diameter	m
F_{dt}	Piston detaching force	N
$F_{xk,yk,zk}$	Components of the resultant force acting on the swash plate due to the k^{th} piston	N
f_v	Control valve equivalent viscous friction coefficient	Ns/m
f_α	Equivalent angular viscous friction coefficient of the swash plate	Ns/m
I_e	Equivalent moment of inertia of the swash plate	$kg.m^2$
i_n	Half the maximum current given to the proportional valve solenoid	A

i_v	Proportional valve solenoid current	A
k	Piston number in the piston group arrangement	-
k_i	Proportional solenoid force-current constant	N/A
k_v	Proportional valve spring stiffness	N/m
k_α	Equivalent torsional spring stiffness of the swash plate	Nm/rad
L_1/ L_2	Lengths, referred in Fig. 2.1	m
L_{3k}	Variable length	m
L_c	Total cylinder length	m
L_p	Piston length	m
$[M_k]_0$	Moment acting on the swash plate in vector form	Nm
M_b	Moment acting on the swash plate bearing system	Nm
$M_{x,y,z}$	Components of the moment acting on the swash plate	Nm
M_{yo}	Average value of the moment acting on the swash plate	Nm
m_p	Piston mass	kg
m_v	Proportional valve spool mass	kg
N	Number of pistons	-
nof	Number of frequencies	-
nop	Number of points	-
N	Pump speed	rpm
p_c	Pressure difference across the control piston	Pa
$p_{c1,2}$	Pressure at the two sides of the control piston	Pa
p_d	Pump delivery pressure	Pa
p_k	Cylinder pressure	Pa
p_{max}	Static characteristic maximum pressure	Pa

p_s	Pump suction pressure	Pa
p_T	Tank line pressure	Pa
p_v	Control pressure	Pa
P	Value of the controlled constant power	kW
Q	Pump instantaneous delivery flow rate	m^3/s
$Q_{a,b,c,d}$	Flow rate through proportional valve ports	m^3/s
Q_d	Delivery flow rate of one cylinder	m^3/s
Q_{max}	Static characteristic maximum flow rate	m^3/s
Q_s	Suction flow rate into one cylinder	m^3/s
R_L	Leakage resistance	$Pa/(m^3/s)$
R_s	Radius of swash plate swinging	m
r_{ck}	Radius of the trace of the piston center of gravity relative to the Z_0 axis	m
$[r_{ck}]_{0/5/6}$	Position vector indicates to the k^{th} piston center of mass relative to inertial/5^{th} /6^{th} frame of reference	
$[r_{5k}]_0$	Position vector indicates to the k^{th} piston spherical head center relative to the inertial frame of reference	
s_k, s_v	The k^{th} Piston, valve spool displacement	m
$\dot{s}_k$, $\dot{x}_{cp}$, $\dot{s}_v$	Velocity of the k^{th} piston, control piston, valve spool	m/s
$\ddot{s}_k$, $\ddot{s}_v$	Acceleration of the k^{th} piston, valve spool	m/s^2
s_{sp}, (s_e)	Set point of the spool displacement (error value)	m
s_{vmax}	Maximum proportional valve spool displacement	m
t	Time	s
$V_{c1,2}$	Control volume on the two sides of the control piston	m^3

V_{ci}	Initial control volume	m^3
V_{ck}	Instantaneous cylinder volume of the k^{th} piston	m^3
V_o	Cylinder clearance volume	m^3
w	Proportional valve port width	m
$x_{cp\ (min,\ max)}$	Control piston displacement (minimum, maximum)	m
x_{5k}, y_{5k}, z_{5k}	Cartesian coordinates of piston spherical head center relative to the inertial frame of reference	m
$\dot{\alpha}$	Swash plate angular velocity	s^{-1}
α, (α_{sp}), (α_e)	Swash plate angle of inclination, (set point), (error value)	rad
β	Cylinder block cone angle	rad
θ_k	Angular position of the k^{th} piston	rad
θ_p	Angle subtended by the piston	rad
ρ	Oil density	kg/m^3
ϕ	Silencing groove angle	rad
ω / $\dot{\omega}$	Pump angular speed/acceleration	s

CHAPTER 1

INTRODUCTION AND LITERATURE REVIEW

In this chapter an introduction to the general field of the study will be given, followed by a summary of prior work done on the chosen thesis topic. The thesis objectives are then formulated and the scope of work is determined.

1.1 Introduction

Fluid power control systems use a fluid medium to transmit and control power. Systems that use hydraulic fluids are called hydraulic systems, while those that use air are called pneumatic systems. Hydraulic systems are primarily composed of a prime mover that provides the raw form of the mechanical power needed to drive a pump. The latter converts the mechanical power into hydraulic power in the form of oil discharge against load pressure. Families of hydraulic control valves are used to control the magnitude of the hydraulic power exerted by the pump and direct it towards the hydraulic actuators, which reconvert the hydraulic power into a mechanical form in order to perform certain dynamic functions.

High-pressure pumps are considered the heart of the hydraulic control systems because they are the main contributor to the system efficiency. They may be of the gear, vane or piston type. Radial and axial piston pumps are used when the hydraulic system working pressure is expected to be higher than 16 MPa, or when the pump is

expected to work under adverse operating conditions such as sudden changes in the delivery pressure or an increase in the load shocks. Figure 1.1 illustrates the earlier versions of piston pumps where a single piston was used. The basic design of the single piston pump is very simple as it has just two valves and one stuffing box. In this example, the reciprocating piston is driven back and forth by a rotating mechanism. Single piston pump design is simple, however it suffers from a disadvantaged flow rate with a high degree of fluctuation. These disadvantages resulted in subsequent designs of piston pumps with multi-pistons. A reduced flow rate fluctuation was found when an odd number of pistons were used. In multi-cylinder pumps, conventional suction and delivery valves are no longer convenient and are being replaced by one fixed valve plate on which the pump cylinders are sliding. The design of the valve plate in piston pumps is of great importance due to its direct effect on pump performance.

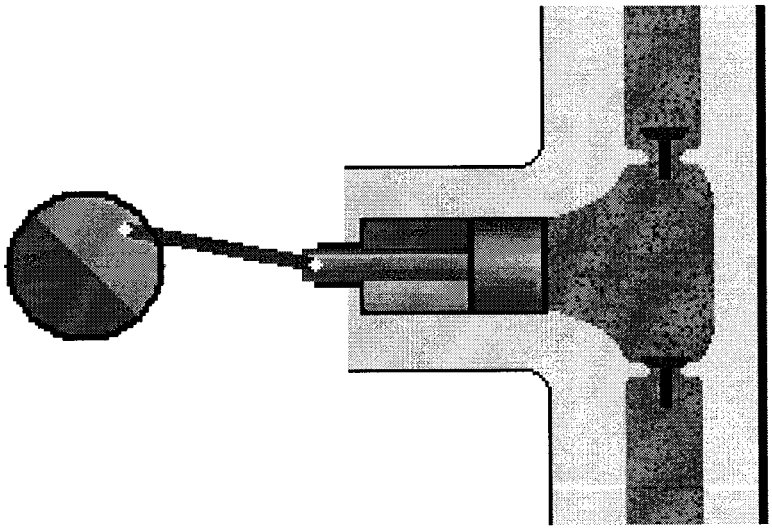

Fig. 1.1 Single piston pump

For many years, hydraulic pumps were designed with a fixed geometry that discharges a constant volume flow rate at a constant driving speed. Using such fixed geometry pumps under variable flow demand requirements causes gross power loss since the excess flow is directed to the reservoir through the pressure relief valve under maximum pressure. Power loss in hydraulic systems leads to inefficient systems and causes heat generation, which significantly affects the physical properties of the hydraulic fluid and consequently affects the system performance. Designers provided many traditional solutions to solve this problem using various combinations of hydraulic and/or electro-hydraulic components of large sizes.

Variable geometric volume positive displacement pumps are used in hydraulic drives along with control systems in order to save power and to reduce the number and/or size of the components used. Among the multi-piston pumps, swash plate axial piston pumps generally have the advantages of compactness, high specific power and good static and dynamic characteristics. They can easily be equipped with different types of controllers. Conversely, they are complicated mechanisms that are sensitive to oil contamination, a problem that can be controlled by keeping the oil clean. Due to their advantages, swash plate axial piston pumps are now widely used in open and closed hydraulic circuits, in both mobile and industrial applications.

In variable geometric volume pumps, the stroke of the pistons and consequently the pump delivery flow rate can be controlled during pump rotation by means of a control unit integrated with the pump. The control system of these pumps is generally designed to achieve different control goals. As shown in Fig.1.2a, the controller is designed to limit the pump's maximum delivery pressure. The pump delivers the

maximum discharge, irrespective to the power exerted by the pump, so long as the delivery pressure is below a certain adjustable maximum value. When maximum pressure is attained, the pump controller reduces the pump geometric volume to a lower value that satisfies the pump self-lubrication requirements. A pump equipped with this type of controller is also called a pressure compensated, or alternatively, a pressure regulated pump. As shown in Fig1.2b, the controller is designed to adjust the pump flow rate in response to an external command signal irrespective of the power exerted by the pump. This controller respects a fixed maximum pressure, at which the pump flow rate is switched to the minimum value. A constant power controller regulates the pump discharge, as shown in Fig.1.2c, in accordance with the pump delivery pressure so as to keep the pump output power constant. A pump that is equipped with this controller type is called a constant power regulated pump. There are controllers that satisfy combinations of these control goals also. Control systems also vary in construction; they can be mechanical, hydro-mechanical or electro-hydraulic. Each of these systems has significant advantages. However, electro-hydraulic controllers nowadays broadly replace the hydro-mechanical ones to be used with the microprocessor controlled industrial applications.

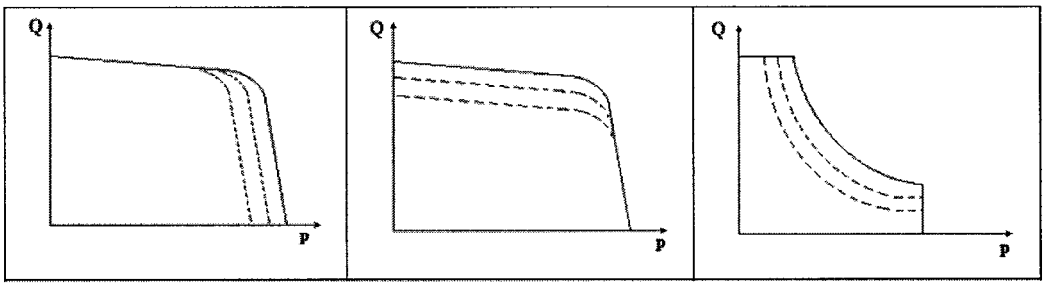

a- Pressure controller b- Flow controller c- Power controller

Fig. 1.2 Static characteristics of variable geometric pumps with different controllers

1.2 Descriptions and Principle of Operation of the Swash Plate Pumps

Figure 1.3 illustrates a schematic drawing of a swash plate pump with a circular piston arrangement. The pump must have an odd number of pistons distributed in a circular array arrangement in the cylinder block. The cylinder block is rotated by means of the pump driving shaft, and is held tightly against the port plate by the effect of the delivery pressure and a compression spring. A ball-and-socket joint connects the spherical end of each piston to a slipper pad, which is always kept in contact with the swash plate by means of the compression spring and the retaining plate. During cylinder block rotation, each piston passes periodically over the discharge and intake ports on the port plate. Since the slipper pads are held against the inclined plane of the swash plate, each piston undergoes a simple harmonic reciprocating motion in and out of the cylinder block. The increasing or decreasing volume of each cylinder, in front of its respective piston, is defined in the text as the "cylinder". As a cylinder passes over the intake port, its respective piston is retracted and fluid is drawn into the cylinder. As the cylinder passes over the discharge port, its piston advances into the cylinder and displaces the fluid out of the cylinder.

Fig.1.4 illustrates an improved design of the swash plate pump, in which pistons are arranged in a conical cylinder block. In this type of pumps, the piston line of stroke is inclined to the pump axis of rotation. An axial component of the centrifugal force acting on each piston is generated and pushes the piston towards the swash plate. This reduces the piston inertia force effect, which normally tends to detach the pistons from the slipper pads or the slipper pads away from the swash plate. With this design,

the pump can be rotated at a higher speed, thereby increasing pump specific power. Advantages of having such conical cylinder blocks will be discussed later.

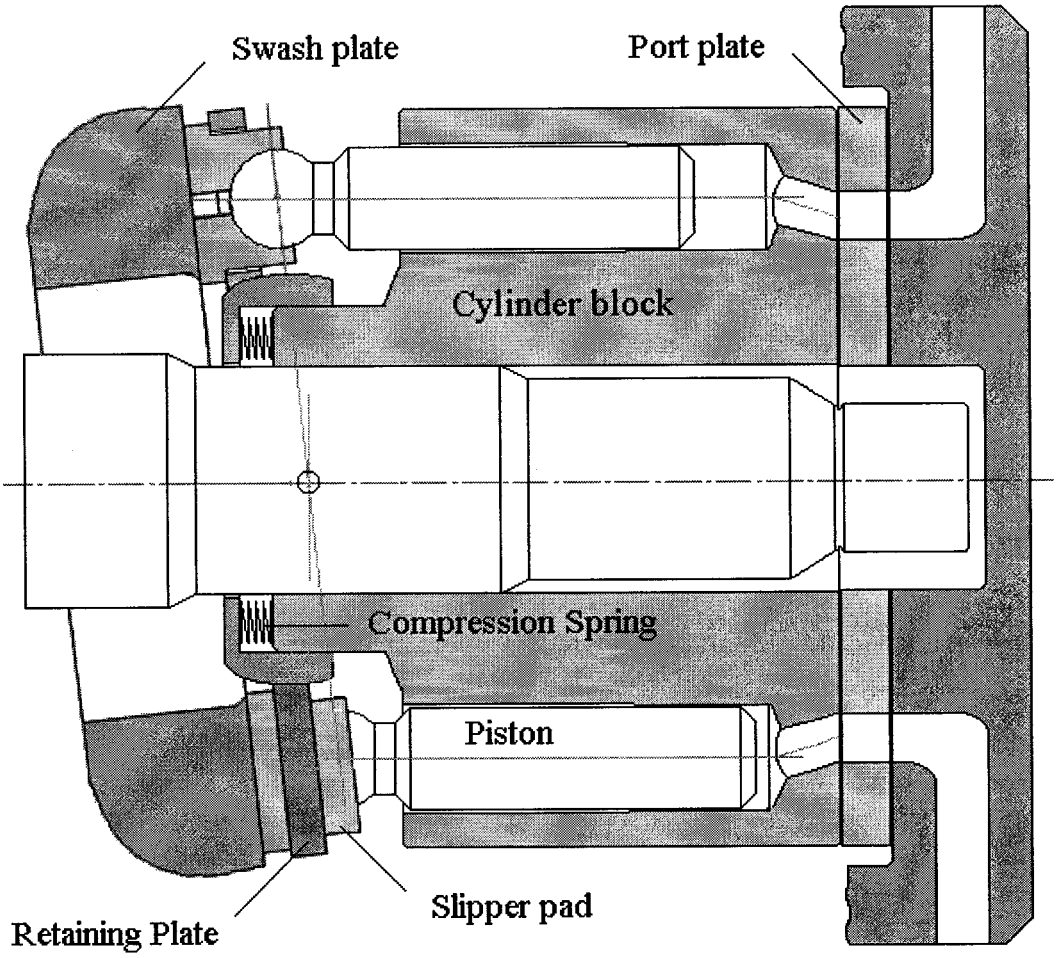

Fig. 1.3 Swash plate axial piston pump with cylindrical cylinder block

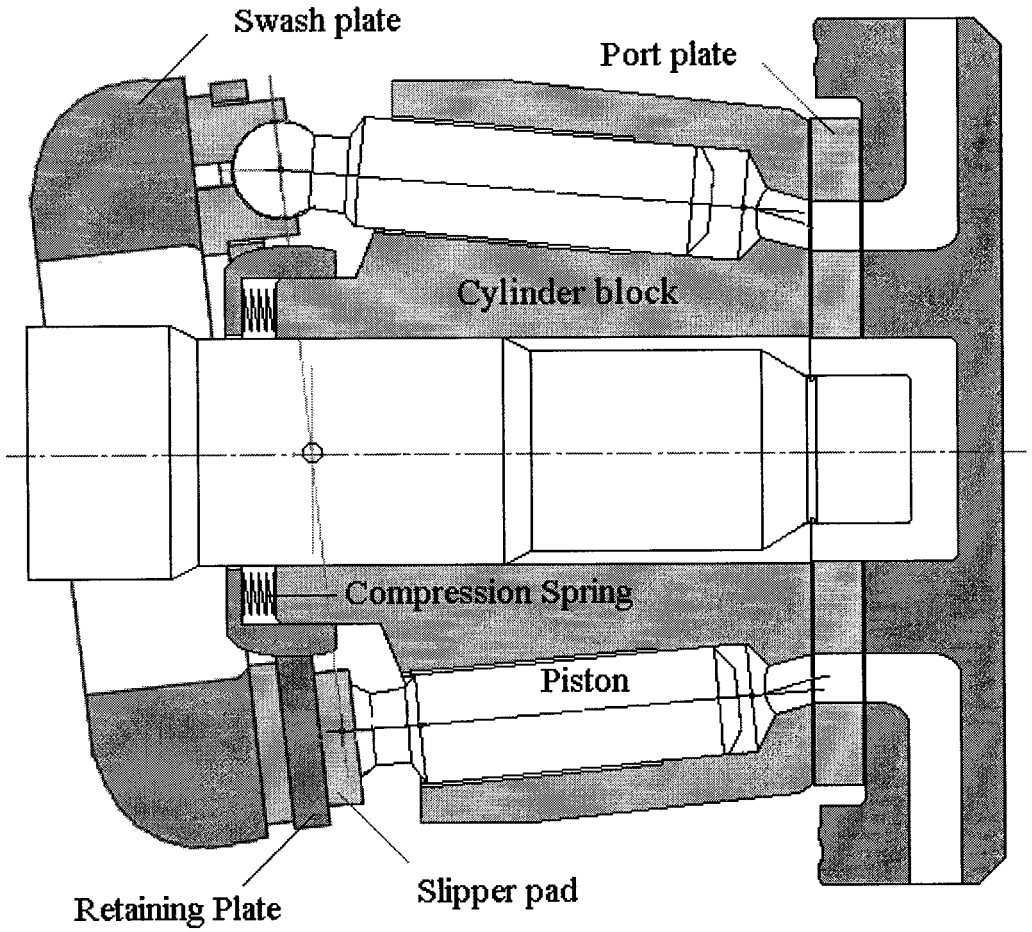

Fig. 1.4 Swash plate axial piston pump with conical cylinder block

1.3 Survey of Previous Work

The static and dynamic characteristics of swash plate axial piston pumps have been extensively studied during the past two decades. In the following survey, the relevant work is presented and classified into the various research points of view. Based on the previous work, the motives for the present study and the thesis objectives will be articulated.

(i) Pump Mathematical Modeling

Modeling of the swash plate axial piston pumps was the main focus of the following studies [13, 29, 34, 35, 42, 44 and 52]. A parameter sensitivity analysis for the dynamic model of a variable displacement axial piston pump was introduced by Kim, Cho and Lee [13].

The static and dynamic characteristics of a standard variable geometric volume swash plate pump with pressure regulator were studied by Kaliafetis and Costopoulos [29]. In this study they proposed a mathematical model and checked its validity. Their findings revealed that operating conditions are very crucial for the pump dynamic behavior and that the dynamic performance improves when the set pressure is decreased.

Modeling and design of a variable geometric volume axial piston pump were also presented by Manring and Jonson [34]. They discussed the effect of factors such as the volume of the actuator and discharge fluid line, the controller gain and system

leakage on the pump performance. Rodney D. Hugelman [35] designed a new adjustable stroke control module for axial piston hydraulic pumps that corrects the shortcomings of the typical adjustable wobble plate designs for axial piston pumps. The new control module is small, self-contained, and does not need the external tilt control mechanisms. They presented an analysis of timing error and the effects of such errors on the pump performance and noise.

Bapiraju Surampudi [42], in 2000, carried out a modeling of low-speed characteristics of swash-plate-type axial piston hydraulic motors. This study investigated the performance variations of the swash plate type axial piston motors. The author demonstrated that an alternative control algorithm can be developed using the model to change motor displacement or pressure in order to control torque within tolerance requirements. A computer aided design tool for axial piston machines was introduced by Wieczorek and Ivantysynova [44].

In 2001, X.Zhang, J. Cho, S. S. Nair and N.D. Manring [52] introduced a reduced model of a damping swash plate pumping mechanism. They validated the proposed reduced order model by comparing it to a complete nonlinear simulation of the pump dynamics over the entire range of operating conditions.

It must be noted that all of the above studies dealt with the swash plate pump in which the piston arrangement is circular around the pump-driving shaft.

(ii) Effect of the Valve Plate on the Pump Performance

Pressure transients and ripples in an axial piston pumps due to the angle between the suction and delivery port are discussed in [2, 9, 12, 19 and 46]. Atsushi [8], in 1983, experimentally studied the effect of suction pressure, rotational speed, shape and sealing conditions of the port plate on cavitation in an axial piston pump. It was found that the occurrence of cavitation could be attributed to either the separation of the shear layers after sudden contractions and/or enlargements of the flow passages, or due to the fluid have trapped, and that it can be prevented by appropriate design of the port plate. The effects of swash plate angle and suction port timing on the noise generation in an axial piston pump are investigated in [40]. In 2000, Kassem and Bahr also carried out a theoretical study [50] in which they proposed a valve plate configuration that suppressed cavitation in the cylinder and caused low pump discharge fluctuations. Manring, N. D., and Y. Zhang, [53], studied the improved volumetric efficiency of an axial-piston pump utilizing a trapped-volume design.

(iii) Pump Dynamics:

The swash plate pump mechanism attracted the attention of many researchers. To optimize the dynamic characteristics of a variable-displacement pump, one must have a thorough understanding of the moments acting on the swash plate. These moments are functions of cylinder pressure and piston kinematics, both of which are nonlinear. Among different dynamic aspects investigated, the torque acting on the swash plate was the concern of many investigations [10, 11, 14, 20, 21, 32, 39, 51 and 54]. Zeiger and Akers introduced two successive studies about the torque on the swash plate of an

axial piston pump, [10] and [11] in the years 1985 and 1986, respectively. The variation of the cylinder pressure and the moment acting on the pump swash plate was studied in [14] both theoretically and experimentally. This study was carried out for two different types of port plates. The calculated values coincided well with those that were measured when a port plate with wide, short and deep notches was used. Manring [32] in 1994 obtained an approximate solution for the moments realized by the swash plate. This solution was easy to use and readily understood by the engineers. This analysis was compared with the test data and the level of correlation was high. Manring [39] calculated the torque on the input shaft of an axial piston swash plate type hydrostatic pump in 1998. Kassem, S.A. and Bahr, M.K., [51] in 2000 investigated the dynamics of the swash plate axial piston pumps with conical cylinder blocks for the first time. Their theoretical model showed that the lateral moment that acts on the swash plate increases nearly linearly with the increase in the load pressure and/or the decrease in the swash plate inclination angle.

Friction and slipper-pad behavior in the swash plate mechanism was the focus of [41, 7, 27 and 56]. Performance of a pressure compensated swash plate pump was studied in [4]. A linearized model was developed and used to investigate the effect of specific operating parameters on the pump performance. The authors concluded that the variation of the oil temperature within the normal operating range has no significant influence on pump dynamics, while the effect on the pump running speed is considerable. Investigations of the temperature behavior of the piston-cylinder assembly in piston pumps were carried out in [43]. A study on the suction dynamics of positive displacement axial piston pumps is introduced in [31]. Investigations related to the vibration of the pump mechanism were carried out in [6 and 26].

(iv) Pump Control Scheme:

Control units of multiple control goals are widely used with variable displacement pumps. The first stage, common to all applications, is the pressure compensator. Flow and power controllers can be added as additional stages.

Baz A. [5] carried out an optimization study of the dynamics of pressure-compensated axial piston pumps. The author developed a design method for selecting the pump parameters that yield optimum dynamic performance. The developed design method would enable pump designers to select, on a rational basis, the optimum design parameters of this class of pumps so as to minimize the response time necessary to match the pump delivery flow rate with the load requirement. A lumped-parameter model for pressure regulated axial piston pumps using the bond graph technique was introduced in [17]. The TUTSIM simulation program was used to carry out a theoretical analysis for the pump dynamic performance. Gregory [33] demonstrated in this paper how the pressure compensated pump is used in forestry skidders with multitask actuators.

The practical implementation of the control circuits is a recognized practice that uses a fully hydro-mechanical or electro-hydraulic option. A general analysis of the hydro-mechanical control mechanism used in variable delivery hydraulic pumps is presented in [1, 3]. Hydro-Mechanical pressure controllers were also investigated in [16 and 18]. W. Backe and H. Ulrich [16] investigated the design of a hydro-mechanical pressure control of a variable displacement pump. A theoretical comparative study of the dynamic characteristics of three different types of hydro-mechanical constant-

pressure regulators for swash plate pumps was presented in [18]. The system with the most suitable characteristics was determined by this study.

Akers and Lin [15] applied the optimal control theory to determine the design parameters of a pressure regulator of an axial piston pump, which incorporates a single-stage electro-hydraulic servovalve. Jaecheon Lee [24] in 1992 investigated the performance of a swash plate pump equipped with an Electro-hydraulic servovalve, which adjusts the swash plate angle of the pump. The system modeling included the servovalve dynamics. They applied a robust control scheme based on the methodology of sliding mode control and feedback linearization. In this work, a fifth-order system was divided into two successive lower order systems and then the control scheme was applied. Results show that the controlled pump pressure follows the desired trajectory to meet the load condition even though the discharge flow rate of the pump changes rapidly. Using this control scheme, the ripple pressure during the transient period can be reduced by as much as is required. This work also verifies the satisfactory performance robustness regardless of uncertain fluid properties on a large range of the operating conditions. Constant pressure control of a piston pump using a model reference adaptive control scheme was investigated in [30].

The static and dynamic characteristics of a bent axis piston pump with a constant power controller was investigated theoretically in [38] by Osama, G. The proposed controller includes a nitrogen-charged accumulator to replace the spring used in the feedback path. Simulation results showed better exploitation of the available power when this type of controller is used, so long as the working temperature is constant.

Non-conventional control systems were used in fluid power systems. A knowledge-based system used for the diagnosis of faults in hydraulic systems and a simulation study of an adaptive control scheme for pressure compensated axial piston pumps are presented in [22] and [23], respectively.

The use of fuzzy logic controllers in fluid power systems and components has grown recently. Examples of fuzzy controller use for hydraulic drives are found in [25 and 48]. The modeling of hydraulic components, the control of electro-hydraulic steering systems and the hydraulic lifting systems of cranes are investigated in [45, 47 and 49], respectively.

Paoluzzi et al [36] investigated the torque and speed limiter used for the third stage in hydro-mechanical control circuits, and both show a number of limitations in handling the pump interaction on the mechanical side (i.e. interaction with the pump prime mover). The aim of this paper is to demonstrate how an electronically controlled proportional servovalve, when paired with a properly suited (both traditional and based on fuzzy logic) control strategy featuring good characteristics, can overcome those limitations to a large extent, and can also be used as an add-on to existing pumps with double (pressure and flow) hydro-mechanical compensators.

Jong-Hwan et al [28] and Fantuzzi [37] made the conclusion that a fuzzy controller can generally replace conventional PID controllers, offering simple but robust solutions that cover a wide range of system parameters and that can cope with major disturbances. Work introduced in [55] represents the first trial in implementing a fuzzy control in swash plate pumps.

1.4 Thesis Objectives

Microprocessor-controlled variable geometric volume swash plate pumps have been developed to cope with the high performance requirements of modern industrial applications and computer aided process control techniques. One category of those pumps is the electrically controlled swash plate pumps, which are widely used today in both industrial and mobile applications. Based on the survey of the previous work, the objectives of this thesis are set forth as follows:

(i) Pump Mathematical Modeling:

The novel design of the swash plate pumps with conical cylinder blocks has not been studied extensively in order to fully exploit their inherent advantages. Therefore, the basic objective of this thesis is to formulate a mathematical model and investigate the pump dynamic characteristics including the pump control unit. A mathematical model of the pump will then be validated experimentally.

(ii) Effect of the Valve Plate Design on Pump Performance:

The previous studies clearly show the great effect of the valve plate on the pump performance from different sides. However, it is necessary to integrate these studies in a one generalized systematic approach applicable to any pump size. This approach should lead to a desired valve plate design. The study will consider the variation of the cylinder pressure, cavitation in the cylinder, and pump flow rate fluctuation as measures of the pump performance.

(iii) Force and Vibration Analysis of the Pump Mechanism:

Most researchers focus their attention on the torque that acts on the swash plate in the direction of its swiveling, which should be overcome by the control unit. Those studies had to be extended to include harmonic analysis for the torque acting on the swash plate, and for calculating the moments acting on the swash plate in other inertial directions. The vibration of the cylinder block has a direct effect on the positioning of the swash plate and consequently on the pump performance. Therefore, dynamic loads acting on the drive shaft bearings will greatly help in studying pump performance and designing the bearings.

(iv) Introductory Study of the Pump Performance with Alternative Control Schemes:

The previous studies show that the electro-hydraulic hybrid (pressure, flow and power) control system is the most advanced control system that could be implemented for variable displacement pumps. Such a control system offers the industrial process control designers great flexibility in implementing the pump for use in different applications that have various modes of operations.

The control units of the electrically controlled swash plate pumps are currently implementing a double negative feedback control loop with conventional PID controllers for the valve spool and PD for the swash plate inclination angle. Dynamics of the swash plate pump with conical cylinder block will have to be investigated in

view of such control scheme that satisfies the requirements of hybrid (pressure, flow and power) control system.

In spite of the reasonable dynamic performance of these pumps under normal operating conditions, pump operation and control action is full of uncertainties. The main sources of such uncertainties are the varying fluid properties such as effective bulk modulus, fluid viscosity and density. Conventional linear control theory, which requires perfect knowledge of the system, cannot guarantee the robustness of the pump performance and stability. Unsatisfactory performance is then expected under off-design operating conditions. Therefore, the fuzzy logic controller is proposed as a replacement for the PD controller. In this thesis, the fuzzy controller will be checked to do the same basic control function as the PD one in addition to improve the robustness of the control action.

Alternative control scheme is proposed based on the satisfactory open loop static characteristics of the proportional valve. A single feedback loop is proposed to replace the currently used double feedback arrangement in order to simplify the control scheme and the associated electronics, which contribute to reduce the pump production cost. Also, a single feedback control loop scheme is proposed in order to decrease the system speed of response and hence suppress the steady state vibrations of the swash plate shown with the double feedback control loops.

An introductory study of the pump dynamic performance with different control schemes will be carried out. Analytical findings will be validated experimentally.

1.5 Thesis Outlines

The first chapter of the thesis provides a survey of previous work done and proposes thesis objectives. The second chapter focuses on the mathematical modeling of the pump. A comprehensive mathematical model is developed for a variable geometric volume swash plate axial piston pump with a conical cylinder block. The model calculates the piston stroke and absolute acceleration during its general space motion as a function of the cylinder block angle of rotation. Pump flow rate and cylinder pressure are found by solving the continuity equation for the control volume inside each cylinder. By having the calculated amounts of cylinder pressure and absolute acceleration, the forces and moments acting on the swash plate can be calculated. The model is further developed to include the dynamics of the proportional valve that leads to a specified pressure distribution across the control piston, which is mechanically attached to the swash plate. The swash plate swiveling angle is calculated by solving the equation of motion of the swash plate considering the moments acting on it.

In the third chapter, with the aid of especially developed auxiliary software, a pump model is used to investigate the effect of the silencing groove dimensions on the pump performance. The trend of change in the pump performance is monitored while one of the silencing groove dimensions is varied and the others are kept constant. This process is repeated systematically for every effective dimension of the silencing groove. Out of this systematic parametric investigation, silencing groove dimensions are improved for better pump performance over a wider range of delivery pressures.

Analysis of force and vibration of the pumping mechanism is then carried out in the fourth chapter. Features behind the novelty of using conical cylinder blocks are then investigated. The vibration of the swash plate is analyzed with regards to the moments acting on it. Dynamic loads on the drive shaft bearings due to pressure forces transmitted by the cylinder block are also evaluated.

The fifth chapter is concerned with the simulation of the pump performance with the current control scheme as well as other proposed control schemes. The pump static and dynamic characteristics are simulated when a conventional PD controller is used to control the swash plate swiveling angle, as is currently used in practical applications. The PD controller parameters were tuned to satisfy the requirements of constant pump operation with less power shocks on the prime mover. A fuzzy controller is then constructed and used to replace the PD controller within the double feedback loop arrangement. The construction of a fuzzy controller is undertaken in order to increase the robustness of the control action and to take care of uncertainties in the operating conditions. The pump dynamic characteristics are simulated with another control scheme in which a single control loop is proposed as a replacement of the currently used double control loop. The simulation results are compared and then qualitatively evaluated.

An experimental setup composed of real time control software and a hydraulic test bed is constructed for testing the pump static and dynamic performance. The units that constitute the setup are fully described in Chapter 6. The steps that should be taken to prepare for the test and to calibrate the sensors are also presented in Chapter 6. The setup is used to validate the pump mathematical model. The validity of the model is

confirmed on the basis of the agreement between the simulation and experimental results of the pump step response when the pump controller is of the PD type currently in use. The experimental setup is used afterwards for creating a prototype and to verify the pump dynamic characteristics with other proposed control schemes.

Conclusions and suggestions for future work are presented in the seventh chapter.

CHAPTER 2

PUMP MATHEMATICAL MODEL

As outlined in the previous chapter, the basic thesis objective is to derive a mathematical model for the swash plate piston pump with a conical cylinder block. The model will then be used to carry out analytical studies and simulations of the pump performance with different control schemes. In this chapter, the pump modeling will begin with a study of pump kinematics followed by the pressure variation in the cylinder. Moments acting on the swash plate are then calculated, and the equation of motion of the swash plate is derived using these calculations. Modeling of the control unit, including the dynamics of the proportional valve, will be also presented. The derived mathematical model will be validated experimentally.

2.1 Pump Kinematics

Figure 2.1 illustrates the layout and main dimensional parameters of the swash plate axial piston pumping mechanism with a conical cylinder block. The cylinder block cone angle is designated as β. Such a model can be applied to the general swash plate pumps including those with a circular arrangement of the pistons where the cone angle equals zero.

In order to study pump kinematics, a relationship between the displacement $s_k(t)$ of the k^{th} piston, relative to the cylinder, and piston angular position $\theta_k(t)$ is established. Figure 2.2 shows the frames of reference used to deduce this relationship. The initial

frame of reference $X_0Y_0Z_0$ is chosen where its origin coincides with the swash plate pivoting point O_0, the axis Z_0 coincides with the pump driving shaft axis, and Y_0 coincides with the axis around which the swash plate is swinging. Following a coordinate transformation [68], five steps of frame transformation are then carried out beginning at $X_0Y_0Z_0$ and ending with $X_5Y_5Z_5$. The objective of the coordinate transformation is to obtain the coordinates of the k^{th} piston spherical head center at the angular position θ_k, relative to the initial frame of reference. As shown in Appendix 1, the resultant transformation matrix is as follows:

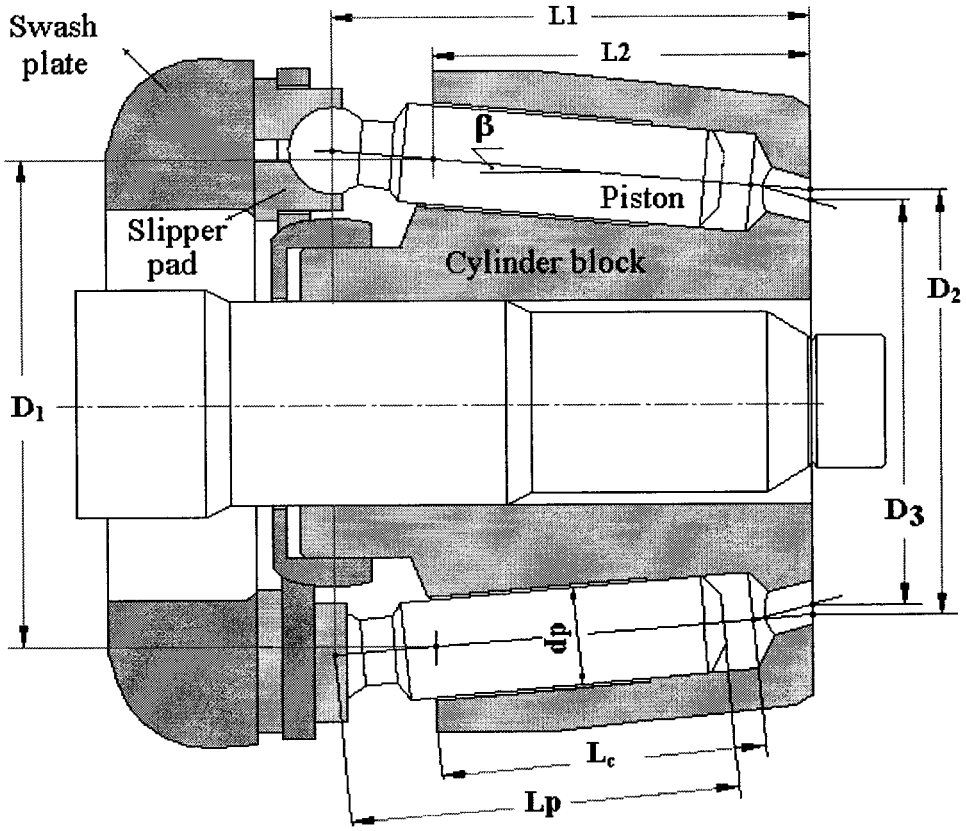

Fig. 2.1 Main dimensions of swash plate axial piston pump with conical cylinder block

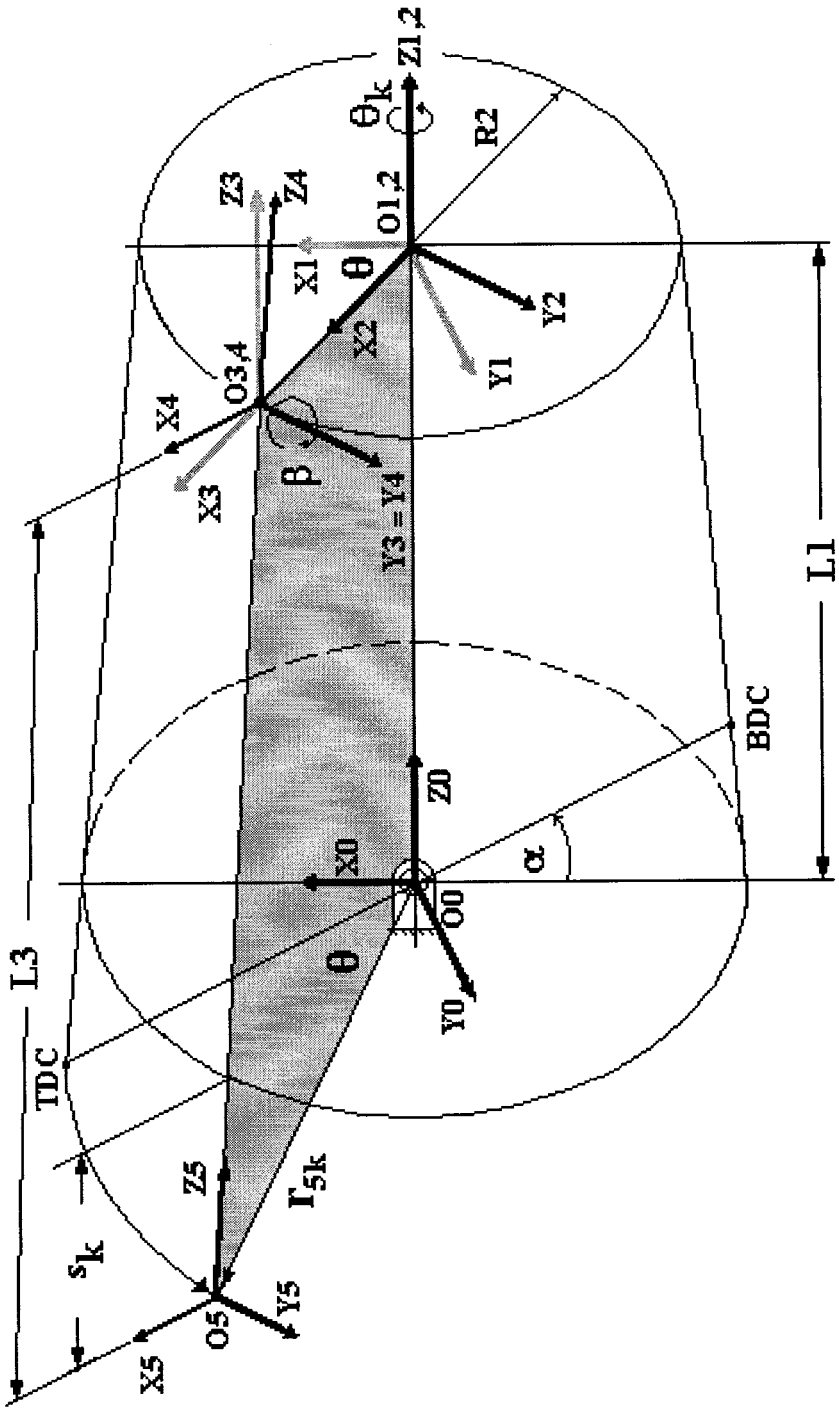

Fig. 2.2 Frames of reference for the piston motion

$$T_{05} = T_{01} \times T_{12} \times T_{23} \times T_{34} \times T_{45} = \begin{bmatrix} \cos\theta_k \cos\beta & -\sin\beta & -\cos\theta_k \sin\beta & L_{3k} \cos\theta_k \sin\beta + R_2 \cos\theta_k \\ \sin\theta_k \cos\beta & \cos\theta_k & -\sin\theta_k \sin\beta & L_{3k} \sin\theta_k \sin\beta + R_2 \sin\theta_k \\ \sin\beta & 0 & \cos\beta & -L_{3k} \cos\beta + L_1 \\ 0 & 0 & 0 & 1 \end{bmatrix}$$

Hence, the position vector $[r_{5k}]_0$ that starts at the origin point O_0 and points to the center of the k^{th} piston spherical head O_5 at any given angular position $\theta_k(t)$, and is relative to the initial frame of reference, has the following time dependent components:

$$x_{5k} = L_{3k} \cos\theta_k \sin\beta + R_2 \cos\theta_k \tag{2.1}$$

$$y_{5k} = L_{3k} \sin\theta_k \sin\beta + R_2 \sin\theta_k \tag{2.2}$$

$$z_{5k} = -L_{3k} \cos\beta + L_1 \tag{2.3}$$

The tip of the position vector $[r_{5k}]_0$ is constrained by a plane parallel to the swash plate surface and passing through the swash plate pivoting point. Hence, the coordinates of the origin O_5 must satisfy the equation of that plane which is inclined at an angle α to the vertical plane, and its equation is given by:

$$X_0 \tan\alpha + Z_0 = 0 \tag{2.4}$$

Substituting the values of x_{5k} and z_{5k} from equation (2.1) and (2.3) into equation (2.4) results in:

$$L_{3k}(t) = (R_2 \cos\theta_k \tan\alpha + L_1)/(\cos\beta - \cos\theta_k \sin\beta \tan\alpha) \tag{2.5}$$

Knowing the value of L_{3k}, the k^{th} piston displacement s_k relative to the piston cylinder along Z_5 direction can be deduced, since it can be shown from the geometry that

$$s_k(t) = -(L_{3k} - L_1/\cos\beta) \qquad (2.6)$$

where: $\theta_k(t) = \omega t + 2\pi(k-1)/N$ and $\beta = \tan^{-1} 0.5(D_1 - D_2)/L_2$

For a pump running at a constant speed of 1450 rpm, $\theta_k(t)$ is linearly dependent on the time taken for one complete revolution, which equals 0.041 s. Knowing that, the time variation of the piston displacement, velocity, and acceleration, relative to the piston cylinder, can be found.

Software based on the Matlab-Simulink simulation program has been developed to calculate and plot the k^{th} piston relative displacement, velocity and acceleration versus the angle θ_k for any pump running speed. A simulation run was carried out for a 9-piston pump of geometric volume 40 cc/rev running at a constant speed of 1450 rpm. The various dimensions of this pump are shown in Fig. 2.1 and the numerical values are included in Appendix 2. The results obtained are illustrated in Fig. 2.3.

Fig. 2.3 shows that the piston relative motion is nearly simple harmonic since β is small. The piston motion would be purely simple harmonic only if $\beta = 0$. The magnitudes of the piston maximum velocity are seen to occur where θ_k equals nearly 90° and 270°, while the magnitudes of the maximum acceleration occurs where θ_k equals 0°, 180° and 360°. When the swash plate inclination angle is 15 degrees, the value of the full piston stroke inside its chamber is 19.8 mm, the maximum velocity is approximately 1.5 m/s, and the maximum acceleration is approximately 240 m/s^2.

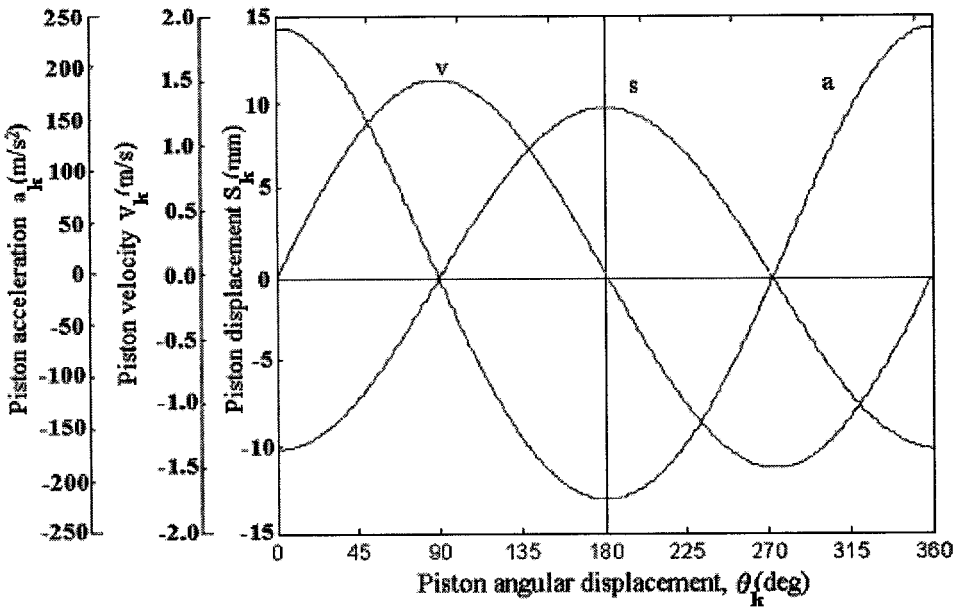

Fig. 2.3 Variation of piston displacement, velocity, and acceleration, relative to the piston cylinder, with θ_k for the 40 cc/rev pump running at 1450 rpm

The above equations are also solved using a specially developed visual basic program The developed program animates the piston movement relative to Z_5 direction during both the delivery and suction strokes. The program features and user interface are shown in Appendix 3.

2.2 Cylinder Pressure and Flow Rate

The variation of the pressure in each cylinder during one complete revolution of the pump is derived based on the following assumptions:

1. The pump rotational speed is constant
2. The pump suction and delivery pressures are constants because of pump boosting and constant external load, respectively.
3. The inertia effect of the oil column inside the cylinder is negligible

4. Leakage passages in the pump are the radial clearance between the piston and its cylinder and the clearance between the cylinder block and the valve plate. These clearances are in order of microns and hence the leakage flow rate is expected to be laminar. Therefore the total instantaneous leakage flow rate out of the pump is assumed proportional to the cylinder instantaneous pressure p_k. The leakage resistance is calculated based on the amount of the leakage flow rate reported by the manufacturer at certain operating conditions.
5. The coefficient of oil discharge from and into the cylinder is constant.
6. The oil density and bulk modulus are constants.

By applying the continuity equation [67] to the control volume (C.V.) surrounding the interior volume of the cylinder shown in Fig.2.4, we obtain the formula:

$$Q_{sk} + A_p \dot{s}_k = Q_{dk} + p_k / R_L + V_{ck}\dot{p}_k / B \tag{2.7}$$

where Q_{sk} represents the oil flow rate drawn into the cylinder from the pump suction line, and Q_{dk} is the flow rate delivered from the cylinder to the pump delivery line at any angular position θ_k. A_p is the piston cross section area and V_{ck} is the cylinder instantaneous volume. The instantaneous cylinder pressure is p_k and the oil bulk modulus is B. The leakage flow rate out of the cylinder to the pump housing Q_{Lk} is assumed to be linearly dependent on p_k and equals p_k/R_L.

The cylinder instantaneous volume is given by:

$$V_{ck} = A_p (0.5L_c - s_k) + V_o \tag{2.8}$$

where L_c is the cylinder block maximum length filled with oil, and V_o is the cylinder trapped and maintained volume as shown in Fig. 2.4. We have

$$Q_{sk} = C_d A_{sk} \sqrt{\frac{2|p_s - p_k|}{\rho}} \operatorname{sgn}(p_s - p_k) \tag{2.9}$$

and

$$Q_{dk} = C_d A_{dk} \sqrt{\frac{2|p_k - p_d|}{\rho}} \operatorname{sgn}(p_k - p_d) \tag{2.10}$$

where C_d is the coefficient of discharge and ρ is the oil density. The areas A_{sk} and A_{dk} are the instantaneous cross sectional areas of the ports communicating the cylinder to the suction and delivery ports respectively. Evidently, the port plate design should consider that when A_{sk} is of any value at any θ_k, the value of A_{dk} should be zero, and vice-versa.

Knowing the values of A_{sk} and A_{dk} at each value of θ_k, and for given constructional and operation parameters, the values of each cylinder pressure p_k and flow rate Q_{dk} can be calculated by solving equations (2.7) to (2.10) simultaneously, provided that the piston displacement and speed are determined. Superimposing Q_{dk} for the group of N pistons, the total pump delivery flow rate Q at any θ_k is then given by:

$$Q = \sum_{k=1}^{N} Q_{dk} \tag{2.11}$$

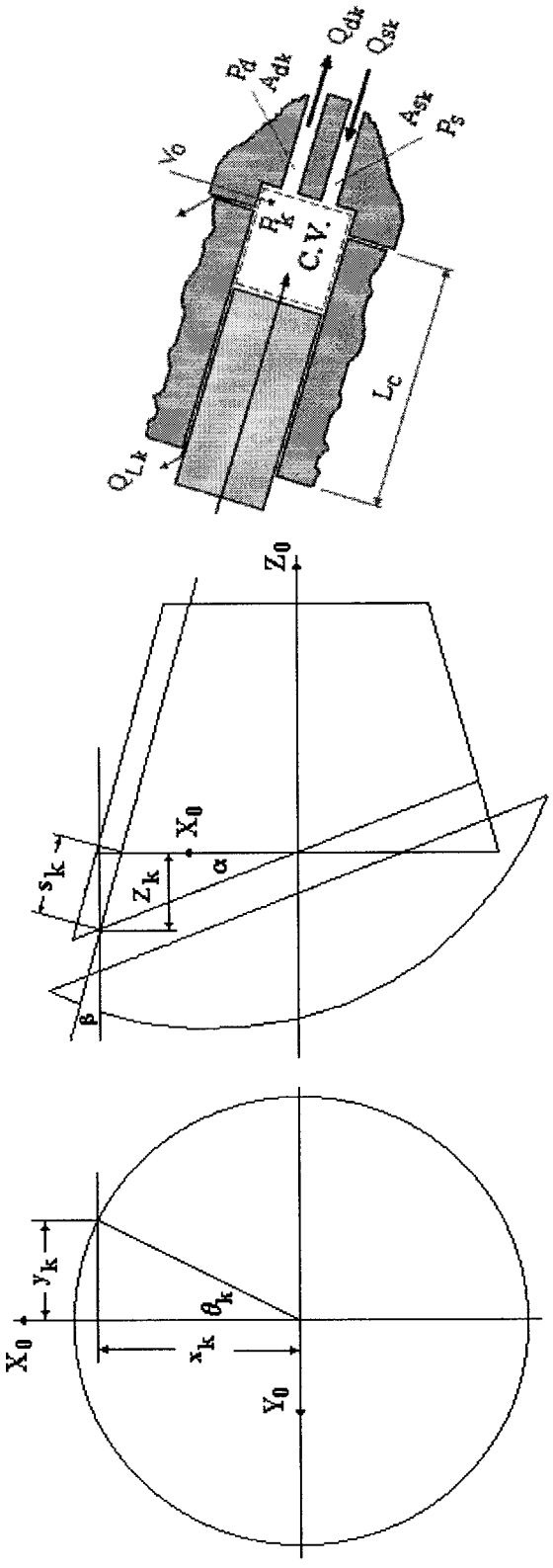

Fig. 2.4 Cylinder parameters and variables

2.3 Moments Acting on the Swash Plate

As illustrated in Fig. 2.5, the piston performs general three dimensional motion relative to the initial frame of reference $(OXYZ)_0$, which is assumed to be the inertial frame of reference. At the same time, the piston movement $s_k(t)$ is constrained in the Z_5 direction of the 5^{th} frame of reference, which is attached to the piston spherical head center O_5. During the piston general motion, it acts on the swash plate by a resultant force vector $[F_k]_0$ belonging to the inertial frame of reference. This resultant force vector acts on the swash plate at the point O_5 that is indicated by the position vector $[r_{5k}]_0$. The position vector $[r_{5k}]_0$ has the previously calculated components, which are relative to the inertial frame of reference given by equations (2.1) to (2.3). Hence, to calculate the moments acting on the swash plate relative to the inertial frame of reference, the resultant force vector $[F_k]_0$ should be multiplied by the position vector $[r_{5k}]_0$.

The resultant force vector $[F_k]_0$ by which the k^{th} piston acts on the swash plate during the piston general space motion is composed of the following:

1. The force resulting from the oil pressure inside the cylinder.
2. The piston inertia due to its absolute acceleration.
3. The friction force between the piston and the cylinder block walls which can be assumed to be viscous friction force.

An order of magnitude analysis for the values of these forces with the constructional parameters shown in Fig. 2.1 revealed that the viscous friction force is of the least and negligible amplitude. This force was disregarded during the following analysis.

The force resulting from the oil pressure inside the cylinder equals $A_p p_k$ and acts along the Z_5 axis. Hence, it can be defined in vector form relative to the 5th frame of reference to be $[F_{pk}]_5$ that has the components 0, 0 and $A_p P_k$ along the unit vectors i_5, j_5 and z_5 respectively. This force can be redefined as relative to the inertial frame of reference, by using the orientation sub-matrix from the resultant transformation matrix, as follows:

$$[F_{pk}]_0 = \begin{bmatrix} \cos\theta_k \cos\beta & -\sin\beta & -\cos\theta_k \sin\beta \\ \sin\theta_k \cos\beta & \cos\theta_k & -\sin\theta_k \sin\beta \\ \sin\beta & 0 & \cos\beta \end{bmatrix} \times [F_{pk}]_5 = A_p p_k \begin{bmatrix} -\cos\theta_k \sin\beta \\ -\sin\theta_k \sin\beta \\ \cos\beta \end{bmatrix} \quad (2.12)$$

To calculate the piston absolute acceleration, the point c_k is defined as the k^{th} piston center of mass as shown in Fig. 2.5, and the position vector $[r_{ck}]_0$ should be calculated first as follows:

$$[r_{ck}]_0 = [r_{5k}]_0 + [r_{ck}]_6 \quad (2.13)$$

where $[r_{ck}]_6$ is the fixed magnitude position vector $[r_{ck}]_5$ redefined as relative to the 6^{th} frame of reference that has an origin that coincided with the 5^{th} frame origin, and axes parallel to those of the inertial frame of reference. It can be calculated as follows:

$$[r_{ck}]_6 = \begin{bmatrix} \cos\theta_k \cos\beta & -\sin\beta & -\cos\theta_k \sin\beta \\ \sin\theta_k \cos\beta & \cos\theta_k & -\sin\theta_k \sin\beta \\ \sin\beta & 0 & \cos\beta \end{bmatrix} \times [r_{ck}]_5 = \frac{L_p}{2} \begin{bmatrix} -\cos\theta_k \sin\beta \\ -\sin\theta_k \sin\beta \\ \cos\beta \end{bmatrix} \quad (2.14)$$

At any angle θ_k, the piston absolute acceleration due to its three-dimensional general motion relative to the inertial frame of reference, [68], is given by:

$$[a_{ck}]_0 = \dot{\omega}\times[r_{ck}]_0 + \omega\times(\omega\times[r_{ck}]_0) + 2\omega\times[\dot{r}_{ck}]_0 + [\ddot{r}_{ck}]_0 \quad (2.15)$$

The first two terms in equation (2.15) represent the piston acceleration due to its rotation, while the last two terms represent the piston acceleration due to its translation. The first term is the piston tangential acceleration that equals zero due to pump rotation with constant angular speed. The second term is the piston normal (centripetal) acceleration. The third term is the piston coriolis acceleration. The last term is the second derivative of the position vector $[r_{ck}]_0$.

The resultant force vector by which the k^{th} piston acts on the swash plate has the components F_{xk}, F_{yk} and F_{zk}. It can be calculated as follows

$$[F_k]_0 = [F_{pk}]_0 + m_p[a_{ck}]_0 \quad (2.16)$$

where m is the piston mass. This force has the components F_{xk}, F_{yk} and F_{zk}.

The resultant force vector $[F_k]_0$ acts on the swash plate and causes a moment vector that is relative to the inertial frame of reference and can be calculated as follows:

$$[M_k]_0 = [r_{5k}]_0 \times [F_k]_0 = \begin{vmatrix} i_0 & j_0 & k_0 \\ x_{5k} & y_{5k} & z_{5k} \\ F_{xk} & F_{yk} & F_{zk} \end{vmatrix} \quad (2.17)$$

The moment acting on the swash plate due to k^{th} piston thus has the three components M_{xk}, M_{yk} and M_{zk} along the unit vector directions i_0, j_0 and z_0 respectively.

The total moment components acting on the swash plate due to the whole piston group are given by:

$$M_x = \sum_{k=1}^{N} M_{xk,} \tag{2.18}$$

$$M_y = \sum_{k=1}^{N} M_{yk} \tag{2.19}$$

$$M_z = \sum_{k=1}^{N} M_{zk} \tag{2.20}$$

The moment M_y tends to change the swash plate inclination angle, while the moment M_z equals the pump driving torque. The resultant of the two moment components M_x and M_z; namely M_b, acts on the swash plate bearing system and is given by:

$$M_b = \sqrt{M_x^{\,2} + M_z^{\,2}} \tag{2.21}$$

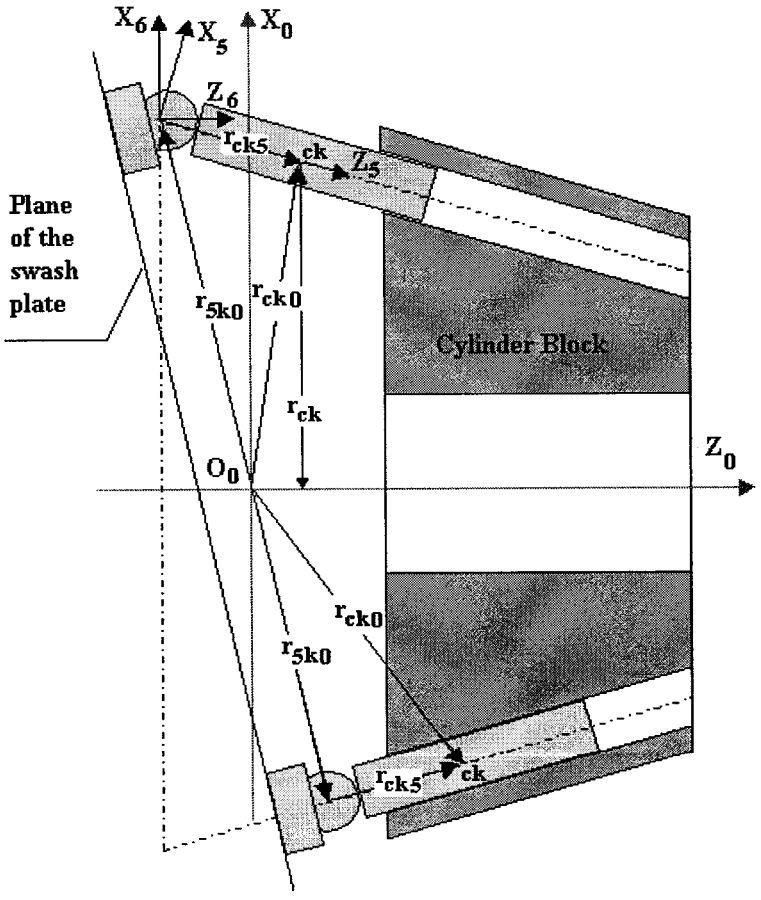

Fig. 2.5 Piston three-dimensional general space motion

2.4 Mathematical Model of the Pump Control Unit

The circuit diagram of the pump control system is shown in Fig. 2.6 as illustrated in [69], while Fig.2.8 shows a schematic drawing of the hydro-mechanical part of the control system. The system consists of a symmetrical hydraulic cylinder that has a piston connected mechanically to the swash plate. The position of the control piston is controlled by means of a hydraulic proportional valve. In open hydraulic circuits, when the proportional valve is de-energized and the control pressure p_v exists, the pump swash plate swivels to an adjustable minimum value. When the proportional valve receives an actuating electrical signal from its electronic control card, its spool moves correspondingly. Consequently, the control piston moves causing a change in the swash plate inclination angle and hence in the pump flow rate. The system incorporates three transducers. The first transducer senses the pump delivery pressure and produces a voltage proportional to it, while the other two are position transducers; one of them senses the swash plate position, while the other senses the proportional valve spool displacement. The output signals of these transducers, as well as the setting values of the constant power and the limits of the pump static characteristic curve, feed the electronic control card.

The equations governing the dynamics of the hydro-mechanical part of the control system, shown schematically in Fig.2.7, are derived in the following. When the proportional valve solenoid receives a control current i_v, an electromagnetic force proportional to this current, namely $k_i i_v$, acts on the valve spool and causes it to move. Friction inside the valve is due to viscous friction as well as the spool seal friction. Due to the complexity of finding these parameters, valve friction is assumed to be

proportional to the speed of the valve spool and an equivalent viscous friction coefficient f_v is considered in the following equation of motion of the valve spool:

$$m_v\ddot{s}_v + f_v\dot{s}_v + k_v s_v = k_i i_v \tag{2.22}$$

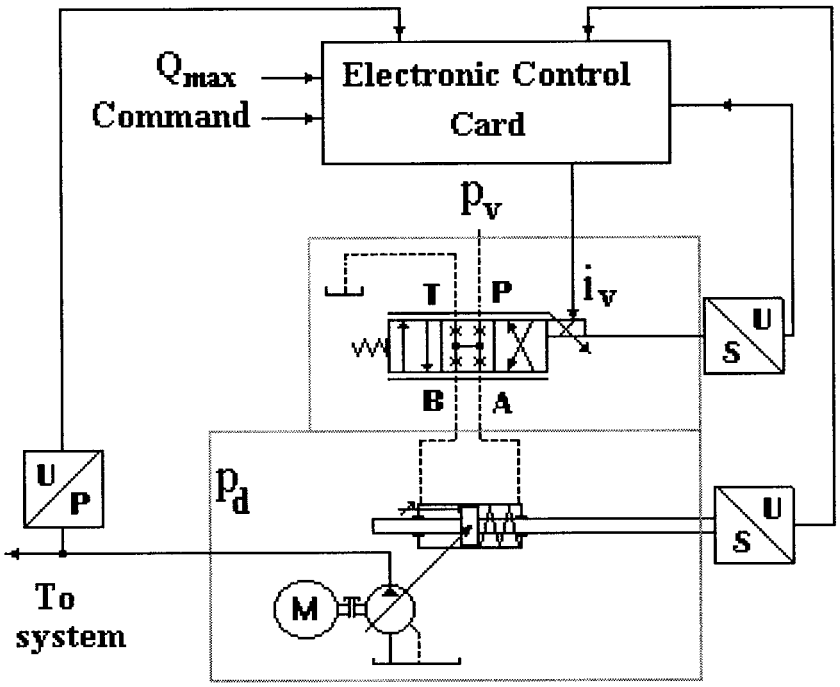

Fig.2.6 Symbolic representation of the constant power control unit

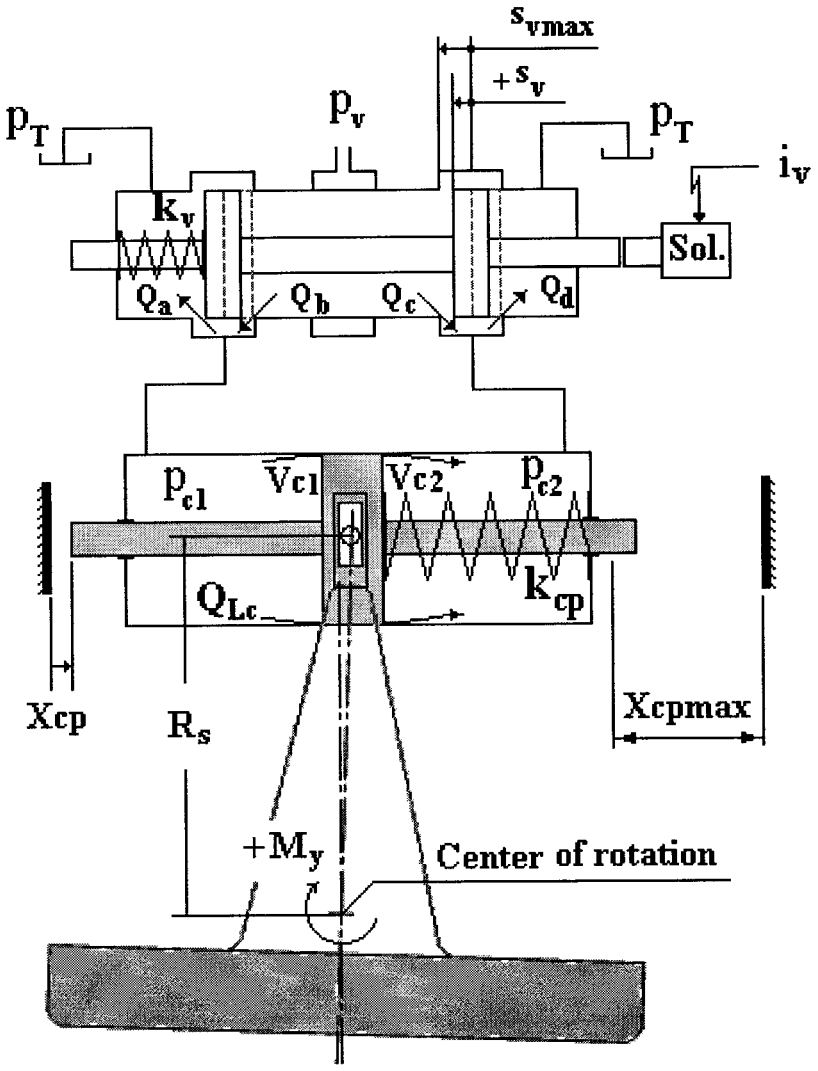

Fig.2.7 Schematic representation of the hydro-mechanical part of the control system shown in Fig. 2.6

The proportional valve spool displacement throttles the oil flow through its four control gaps since the valve is of the under-lap type. Assuming constant discharge coefficient, negligible valve leakage and under-lapped valve spool, it can be verified that the flow rates through the four control gaps, shown in Fig. 2.7, are given by the following equations:

$$Q_a = C_d w(s_{v\max} - s_v)\sqrt{\frac{2|p_{c1} - p_T|}{\rho}}\,\mathrm{sgn}\,(p_{c1} - p_T) \tag{2.23}$$

$$Q_b = C_d w s_v \sqrt{\frac{2|p_v - p_{c1}|}{\rho}}\,\mathrm{sgn}\,(p_v - p_{c1}) \tag{2.24}$$

$$Q_c = C_d w(s_{v\max} - s_v)\sqrt{\frac{2|p_v - p_{c2}|}{\rho}}\,\mathrm{sgn}\,(p_v - p_{c2}) \tag{2.25}$$

$$Q_d = C_d w s_v \sqrt{\frac{2|p_{c1} - p_T|}{\rho}}\,\mathrm{sgn}\,(p_{c2} - p_T) \tag{2.26}$$

where p_v is the proportional valve supply pressure, p_{c1} and p_{c2} are the pressures acting on the two sides of the piston of the hydraulic cylinder, and p_T is the tank pressure. The valve port width is w, the spool displacement is s_v, and the maximum spool displacement is s_{vmax}.

By applying the continuity equation to the hydraulic cylinder chambers, the pressures p_{c1} and p_{c2} can be given by:

$$p_{c1} = \frac{B}{V_{c1}}\int(Q_b - Q_a - A_{cp}\dot{x}_{cp} - \frac{p_c}{R_L})dt \tag{2.27}$$

$$p_{c2} = \frac{B}{V_{c2}}\int(Q_c - Q_d + A_{cp}\dot{x}_{cp} + \frac{p_c}{R_L})dt \tag{2.28}$$

where P_c is the pressure difference across the control piston and

$$V_{c1} = V_{ci} + A_{cp} x_{cp} \tag{2.29}$$

$$V_{c2} = V_{ci} - A_{cp} x_{cp} \tag{2.30}$$

where V_{ci} is half the cylinder total volume, A_{cp} is the cross sectional area of the control piston, x_{cp} is the piston displacement, R_L is the leakage resistance across the piston.

The pressure difference P_c on the two sides of the control piston drives it to a new equilibrium position. Swash plate is then swiveled around a center of rotation, shown on Fig. 2.7, until the valve return into its initial central position. Due to the angular displacement of the swash plate and the linear movement of the control piston, the mechanical connection between them considered a kind of sliding relation.

The instantaneous swash plate inclination angle are then given by solving the following equation of motion numerically:

$$I_e \ddot{\alpha} = P_c A_{cp} R_s + M_y - f_\alpha \dot{\alpha} - k_\alpha (\alpha + 0.09) \tag{2.31}$$

Value of I_e represents an equivalent moment of inertia of the swash plate and the parts attached to it as well as the moving mass of the control piston. In addition to the driving moment resulting from the pressure difference P_c, the lateral moment M_y acting on the swash due to pumping pistons is also considered. Last two terms of the equations consider the viscous friction and spring effect, respectively.

Value of f_α represents an angular viscous friction coefficient equivalent to the viscous damping at the control piston and the swash plate supporting bearings.

Value of k_α represents the torsion spring effect at the swash plate equivalent to the spring effect at the control piston. Pre-compression value of 0.09 N.m/rad is considered.

The above-mentioned design parameters are shown in Appendix 2 as reported by the manufacturer. Friction coefficients of the proportional valve and the swash plate are estimated in view of the dynamics reported by the manufacturer [69].

A test setup has been built in order to measure the pump performance and to validate the derived model. A description of the test setup and the steps taken to validate the model and comparison of the theoretical and measured pump performance will be discussed in detail in Chapters 5 and 6. The pump model has been validated based on the satisfactory agreement between the simulation results and the experimentally measured results.

In this chapter, an analytical model is developed. The model considered the kinematics and dynamics of the pump mechanisms and the control system. In the following, Chapter 3 will investigate the effects of the port plate configuration on the pump performance using the derived pump mathematical model.

CHAPTER 3

EFFECT OF THE PORT PLATE CONFIGURATION ON THE PUMP PERFORMANCE

Among the different measures by which one can evaluate the performance of a positive displacement pump are the mode of variation of cylinder pressure and the pump flow rate. The recommended cylinder pressure variation is a gradual rise in the delivery stroke to meet the load pressure without overshooting, and a gradual drop in the suction stroke to meet the suction pressure without cavitation. The recommended flow rate is that which has the minimal amount of fluctuations. This leads to a smooth pumping operation with less noise, which reflects on the pump service life. For swash plate and bent axis pumps, the geometry of the port plate is known to have a significant effect as was previously mentioned in the literature review.

In this chapter, a comprehensive theoretical study is carried out to investigate the effect of silencing groove dimensions on cylinder pressure and pump delivery flow rate fluctuations by numerically solving equations (2.1) to (2.11) developed in the previous chapter. The Matlab-Simulink simulation program was employed in the numerical simulation. The design parameters of a pump of a geometric volume 40 cc/rev running at a speed of 1450 rpm when the suction and delivery pressures are $0.5x\ 10^4$ Pa and 10 MPa, respectively, were fed into the simulation program. The dimensional and operational parameters of this pump are given in Appendix 2.

3.1 Calculation of the Porting Area on a Port Plate of General Configuration

Initially, a port plate of general configuration was considered. It was assumed to have two symmetric pairs of silencing grooves, as illustrated in Fig. 3.1a. One silencing groove is located at the entrance and exit of both the suction and delivery kidney ports. The angles at which the silencing grooves start and end, as well as the other angles of interest on the port plate, are also shown in Fig. 3.1a. The two silencing grooves are assumed to be of a triangular cross section, with two identical sides that meet at right angles as shown in Fig.3.1b; this configuration is widely used in practice. Knowing the dimensions of the suction and delivery ports, as well as those of the silencing grooves, the cross sectional areas of the control ports connecting the cylinder to the delivery, and suction ports on the port plate, A_{dk} and A_{sk} respectively, can be calculated at any angular position θ_k.

Appendix 4 shows the user interface of a visual basic program specially developed in order to calculate the values of both A_{dk} and A_{sk} for each piston versus its angular position θ_k during one complete revolution of the cylinder block. The program allows selection of different combinations of the silencing grooves key dimensions like transition period, notch length and notch angle. The selected dimensions are implemented in a piece-wise function that is built inherently in the program based on the geometry of the general valve plate configuration. The program is then calculates the porting area and save it in a data file to be read by the Matlab simulation program. Using this program is quite effective in reducing the required memory size and the computational time of the Matlab program that simulates the pump dynamics.

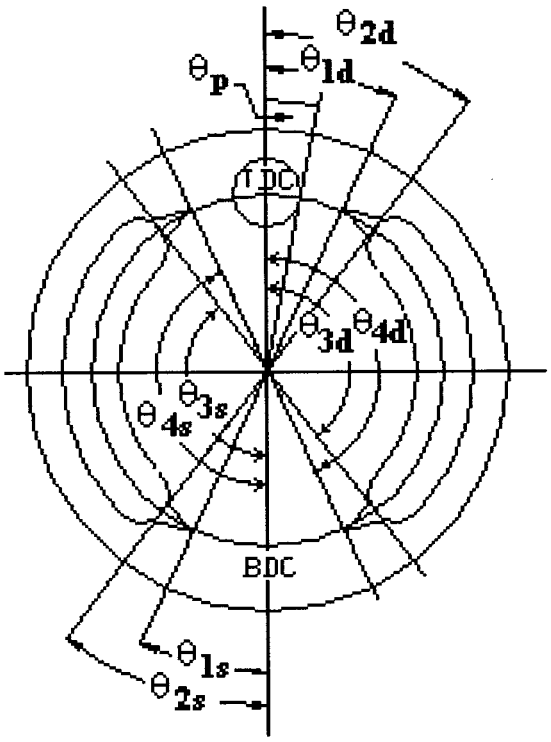

a- Port plate of general configuration

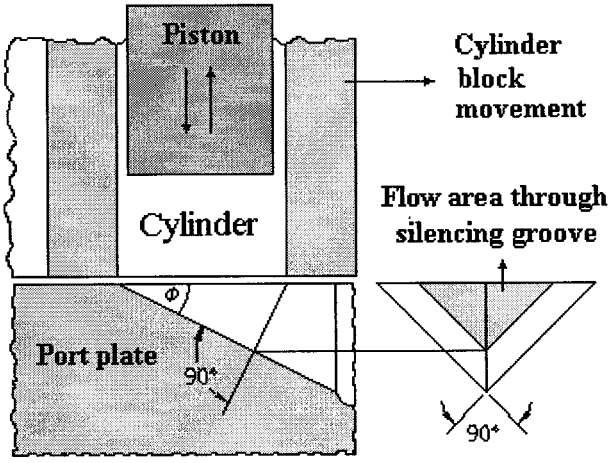

b- Silencing groove sectional view

Fig. 3.1 Port plate configuration

3.2 Effect of the Silencing Groove Angle on the Pump Performance

Simulation of pump performance is carried out first in order to investigate the effect of the silencing groove angle on the cylinder pressure p_k, and total pump flow rate Q. Figure 3.2 shows the simulation results of the cylinder pressure and pump delivery flow rate with θ_k for the first three trials, in which the groove angle equals 5^o, 10^o and 15^o, respectively. The transition period and groove length are considered constant and equivalent to 15° and 20°, respectively.

During the delivery stroke, where θ_k is between 0^o and 180^o, the figure shows that the cylinder pressure increases with the pump angle of rotation and overshoots delivery pressure, then it decreases to the value of the delivery pressure. This is because at the beginning of the delivery stroke, the cylinder is isolated from both the suction and delivery ports. During this stage, the piston advances in its chamber and compresses the fluid causing its pressure to rise at a rate depending upon the piston velocity, piston area, chamber volume, oil bulk modulus and leakage flow rate. After a certain angle of rotation, the cylinder communicates with the delivery port through the silencing groove. Fluid flows from the cylinder into the delivery port if the chamber pressure is higher than the delivery pressure at this moment. Fluid could also flow reversibly in the opposite direction if the delivery pressure is higher than the chamber pressure. In either case, the flow rate depends upon the groove dimensions and the differential pressure. The chamber pressure during this stage can be controlled by the proper choice of groove dimensions and the angle through which this pre-compression period, namely $\theta = \theta_{1d} - \theta_p$, occurs.

When the cylinder is fully connected to the delivery port, the chamber pressure and delivery pressures are equal. When the piston approaches the end of the delivery stroke, the chamber pressure is seen to rise again above delivery pressure. At this point, the silencing groove cross sectional area through which oil flows from the cylinder to the delivery port, A_{dk}, is decreasing rapidly with cylinder block rotation until it becomes zero, while the piston is still moving forward into the chamber compressing the oil inside. Due to the sudden closure of delivery port, fluid hammer effect increases the cylinder pressure p_k above the pump delivery pressure p_d. This explains the presence of pressure overshooting at the exit of the delivery port. Maximum chamber pressure occurs when $\theta_k = 180^\circ$. It is to be noted that the chamber pressure overshoot is high when the groove is narrow and shallow, and it is low when the groove is wide and deep.

During the suction stroke, where θ_k is between 180° and 360°, the piston starts to retract and draws oil from the suction port. Early in the suction stroke, the chamber pressure is seen to decrease based on the restricted area through which the flow is drawn into the cylinder, and it may become even less than zero indicating an occurrence of cavitation. Cavitation develops when the flow rate into the cylinder cannot cope with the flow rate demand dictated by the piston retracting velocity taking into account fluid compressibility. The occurrence of cavitation clearly depends on the silencing groove angle ϕ, as well as the angles at which the silencing grooves start and terminate on the port plate. As shown in Fig. 3.2, cavitation is recorded for the three-selected combination of the silencing groove dimensions.

Increasing ϕ from 5° to 15° is seen to improve variations in the cylinder pressure. It

also improves the fluctuations in the pump delivery flow rate and hence acts positively on pump performance and quietness. Increasing ϕ beyond 15^{o} did not result in avoiding cavitation or improving the chamber pressure overshooting. It is to be noted that the simulation process is automatically terminated when the chamber pressure p_k is less than zero, since cavitation would then develop within the cylinder and the mathematical model would not be valid. In what follows, the effect of the other silencing groove dimensions on cylinder pressure is investigated.

3.3 Effect of the Port Plate Transition Period on the Pump Performance

The change in cylinder pressure and pump flow rate, along transition zone between the suction and delivery ports on the valve plate, was investigated for a groove angle ϕ of 15^{o} and the groove length equal to an arc length subtended by angle of 20^{o}. The transition periods between the suction and delivery ports on the valve plate as shown in Fig.3.1a, are determined by the angles θ_{1d}, θ_{1s}, θ_{4d}, and θ_{4s} respectively. Three other consecutive cases (4, 5 and 6) are considered where the transition periods are equal to 10^{o}, 15^{o} and 20^{o}, respectively. Figure 3.4 shows that increasing θ_{1d} and θ_{1s}, while keeping the valve port plate symmetry, is seen to have a detrimental effect on cylinder pressure and the pump delivery flow rate. The figure shows that decreasing the transition periods yields a better performance. Decreasing transition periods is limited by the value of the cylinder diameter, such that the proper sealing between the delivery and suction ports is respected. The figure reveals that in spite of having less chamber pressure overshooting, cavitation still developed in the three cases presented.

3.4 Effect of the Silencing Groove Length on the Pump Performance

Further simulation runs were carried out to investigate the effect of the length of the silencing grooves on pump performance. At the delivery port, the lengths of the two grooves are proportional to (θ_{2d} - θ_{1d}) and (θ_{4d} - θ_{3d}), while for the suction port, they are proportional to (θ_{2s} - θ_{1s}) and (θ_{4s} - θ_{3s}), respectively. The port plate is kept symmetrical with only the θ_{2d}, θ_{3d}, θ_{2s} and θ_{3s} values changed. The other angles on the port plate were chosen in view of the previously presented results: $\phi = 15^{\circ}$, $\theta_{1d} = \theta_{1s} = 10^{\circ}$ and $\theta_{4d} = \theta_{4s} = 170^{\circ}$. The simulation results are presented in Fig.3.4 for the three cases 7, 8 and 9 in which the groove lengths are proportional to 10°, 15° and 20°, respectively. Results show that the pressure overshoot disappears in these three cases, and in case 7 where the groove length is equal to 10°, cavitation in the cylinder was avoided.

3.5 Effect of the Pump Delivery Pressure on the Pump Performance

The value of the pump delivery pressure is dictated by the system load, and the most commonly met range of working pressure for these pumps is 10 to 30 MPa. Adopting the dimensions of the port plate as given in case 7, in which the system pressure was 10 MPa, further simulation runs were carried out with a pump delivery pressure of 20 MPa and 30 MPa, subsequently. The simulation results are shown in Fig. 3.5 and they illustrate how cavitation was completely avoided in these simulation runs. On the other hand, fluctuations in the pump delivery flow rate increased with the increase of delivery pressure.

3.6 Desirable Valve Plate Configuration

As shown in Fig. 3.5, cavitation is avoided while the port plate's symmetric configuration is maintained. However, the fluctuation in the pump's flow rate needs further discussion. Maintaining the rise in the cylinder pressure without overshooting during the beginning of the delivery stroke leads to a higher pump flow rate fluctuation, particularly when there is higher system pressure. Having a cylinder pressure with precisely tuned overshooting leads to a reasonable flow rate fluctuation along the whole range of the system operating pressure.

Hence, additional computational run were carried out with non-symmetrical delivery and suction silencing grooves to obtain the best flow rate fluctuation while still avoiding cavitation. In these last trials the transition period and the notch length of the delivery stroke entrance are increased. This change allows a little overshooting in the cylinder pressure, which reflects on the pump flow rate fluctuation. The desirable values of the silencing groove dimensions that satisfy both cavitation avoidance and reasonable flow fluctuation were found to be as follows: $\phi = 15^{\circ}$, $\theta_{1d} = 20^{\circ}$, $\theta_{2d} = 30^{\circ}$, $\theta_{1s} = 10^{\circ}$, and $\theta_{2s} = 19^{\circ}$, $\theta_{3d} = \theta_{4d} = 165^{\circ}$ and $\theta_{3s} = \theta_{4s} = 169^{\circ}$.

The pump performance while using such dimensions are illustrated in Fig. 3.6 and presented in cases 13, 14 and 15, corresponding to system pressures of 10 MPa, 20 MPa and 30 MPa, respectively. By comparing the pump flow rate in both Figs 3.5 and 3.6, one can notice that the pump flow rate has been improved, particularly in case of

higher operating system pressure. Figure 3.7 shows the layout of the desirable valve plate configuration with the recommended silencing groove dimensions.

From this study, a recommended port plate configuration was determined. The desirable valve plate configuration renders a gradual rise and drop in the cylinder pressure while avoiding cavitation, for the whole range of the pump delivery pressure, while keeping the pump delivery flow rate fluctuations within reasonable limits. Pump noise is then reduced, thus extending the service life of the pump.

A desirable valve plate configuration is a significant contribution to this thesis since it represents useful information to the manufacturers of such pumps. This study is carried out for a swash plate pump with specific geometrical volume. However, it introduces an example that can easily be translated into similar studies that can be conducted on swash plate pumps of any size using the developed model and software.

In the following chapter, the model will be used again in order to analyze the force and vibration of the pump mechanism.

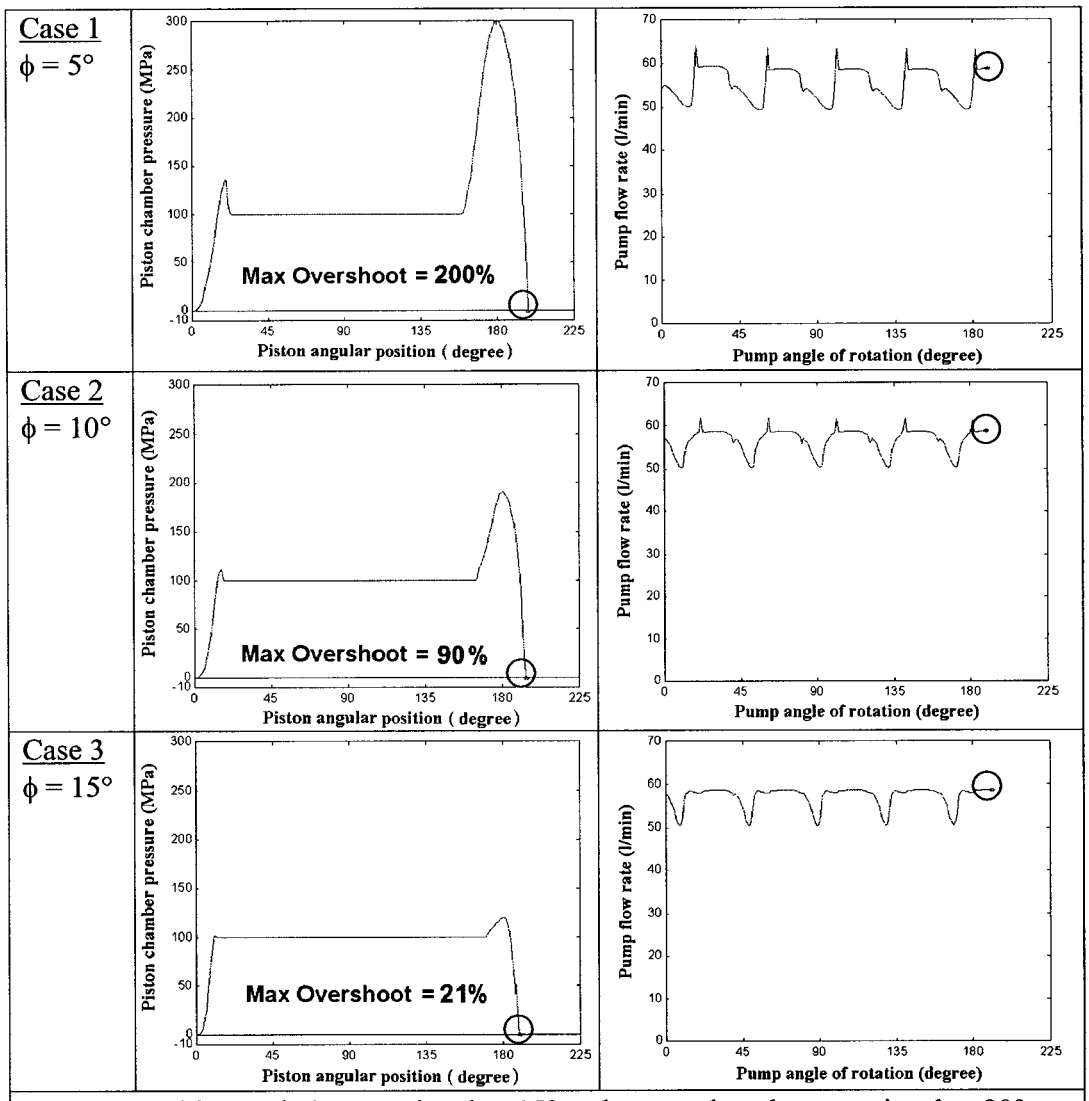

For transition period proportional to 15° and groove length proportional to 20°

where $\theta_{1d} = \theta_{1s} = 15°$, $\theta_{2d} = \theta_{2s} = 35°$, $\theta_{3d} = \theta_{3s} = 145°$ and $\theta_{4d} = \theta_{4s} = 165°$

Fig.3.2 Effect of the groove angle ϕ on the cylinder pressure and pump flow rate

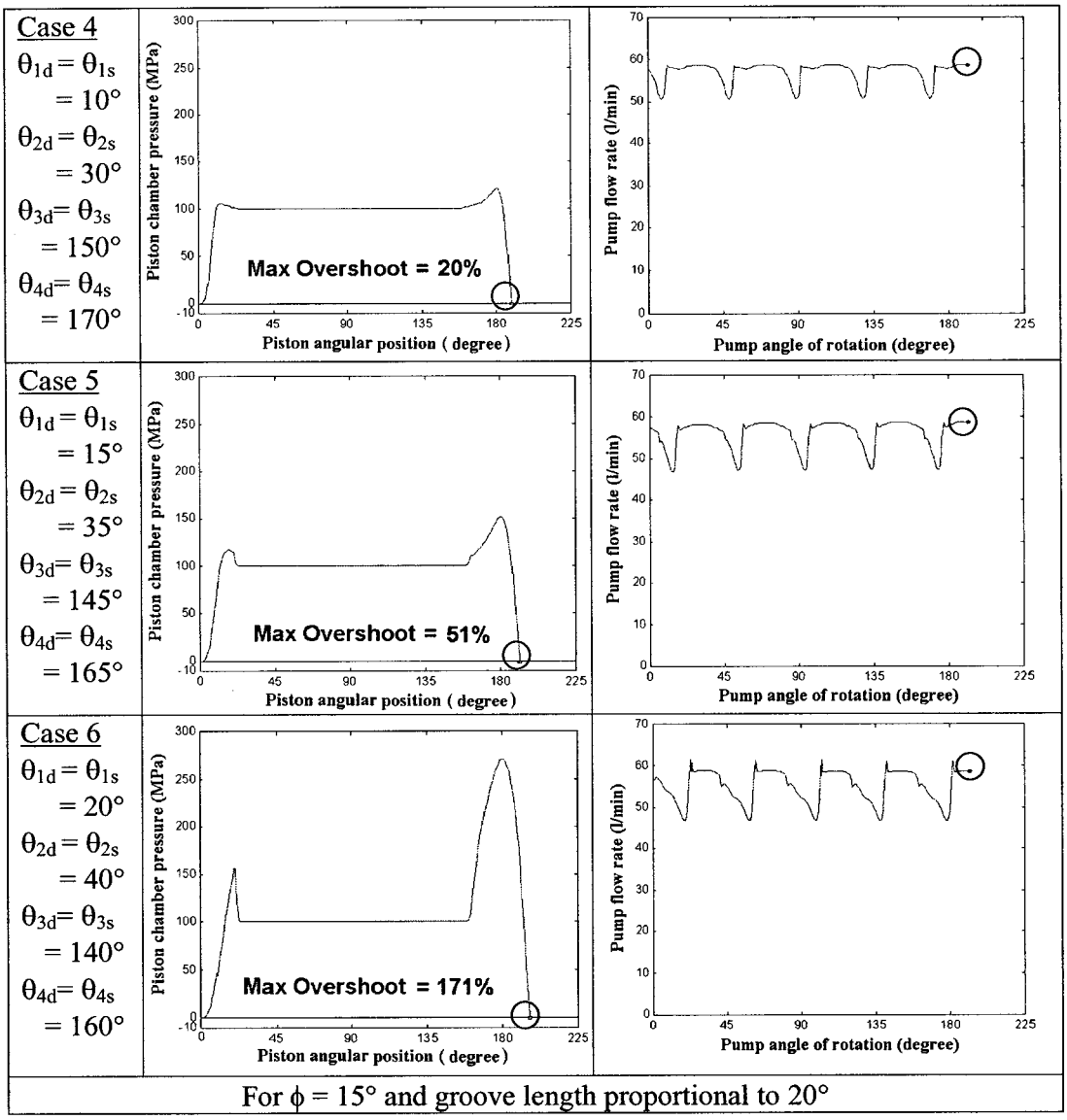

Fig.3.3 Effect of transition periods between suction and delivery port on cylinder pressure and pump flow rate

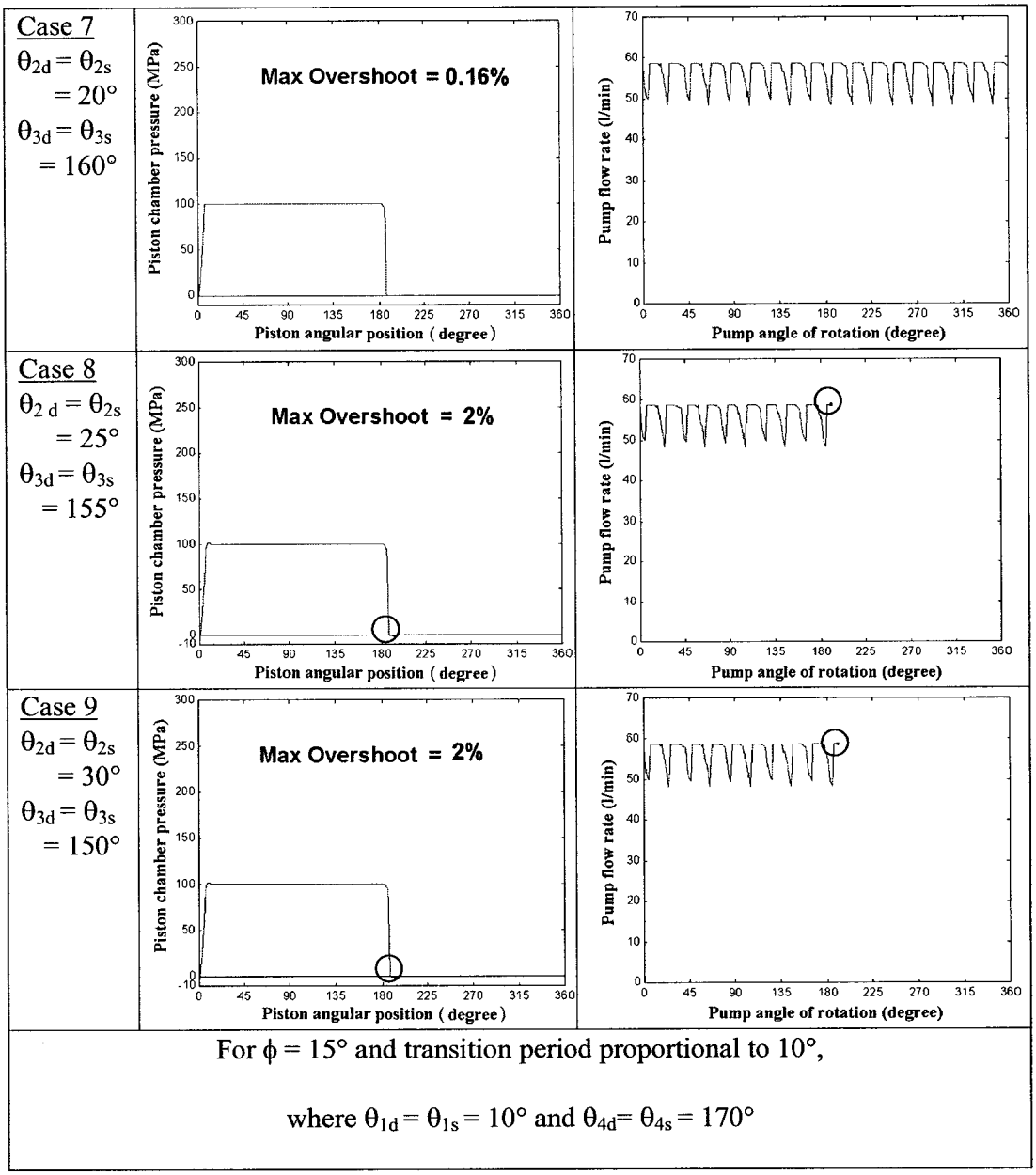

Fig.3.4 Effect of silencing groove length on cylinder pressure and pump delivery flow rate

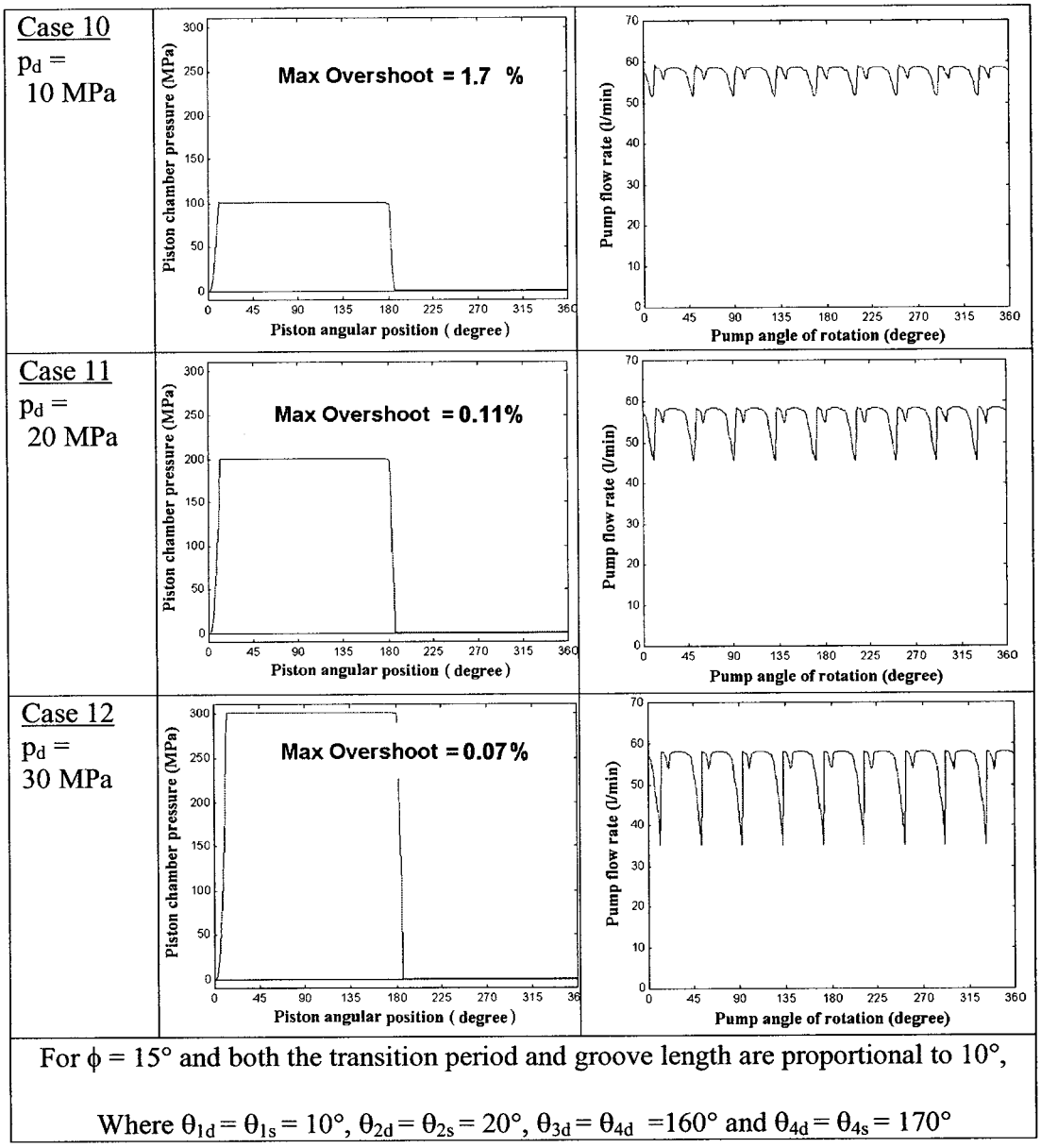

Fig.3.5 Effect of the pump delivery pressure on cylinder pressure and pump delivery flow rate

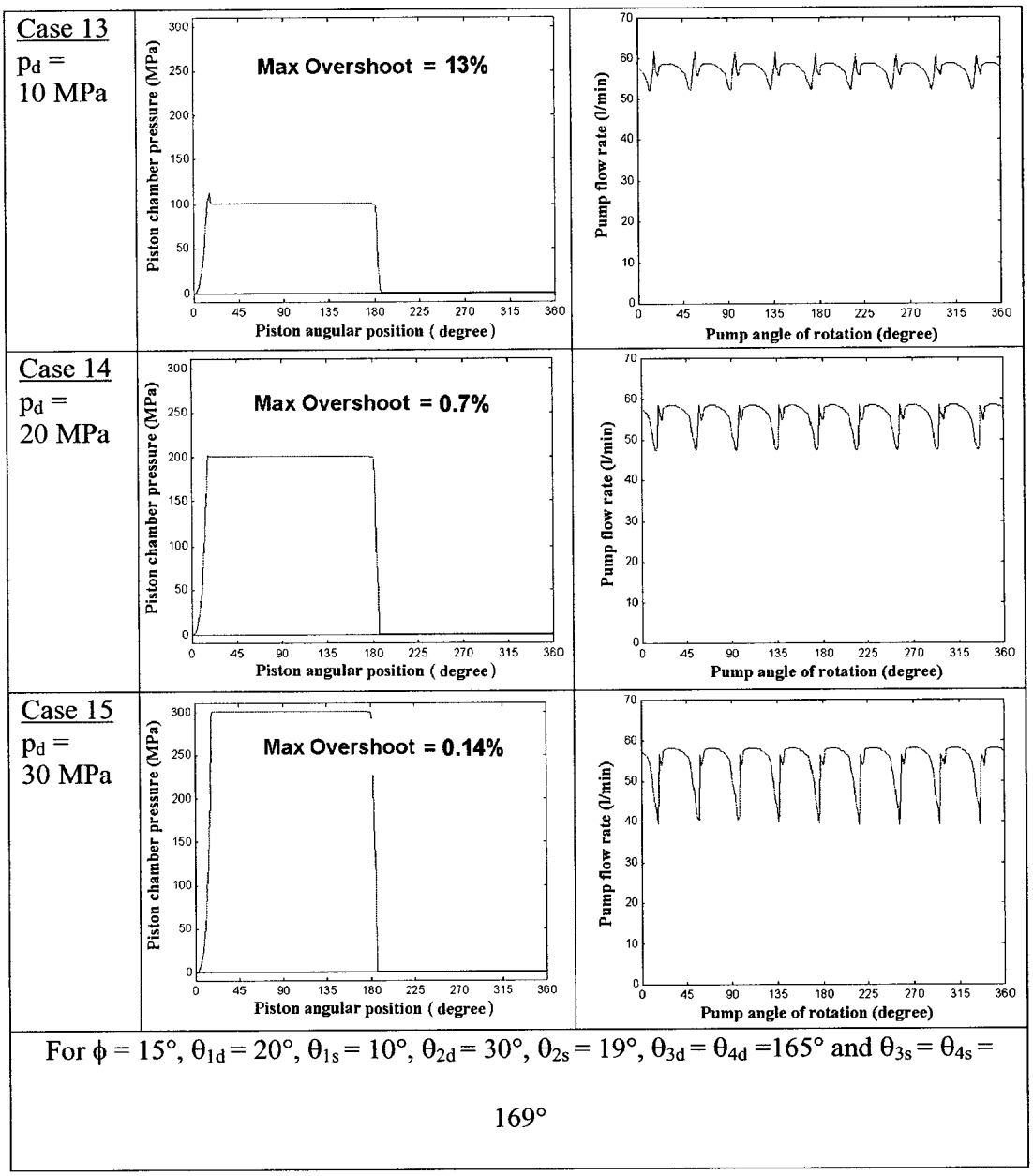

Fig.3.6 Variation of cylinder pressure and pump delivery flow rate using the desirable valve plate configuration

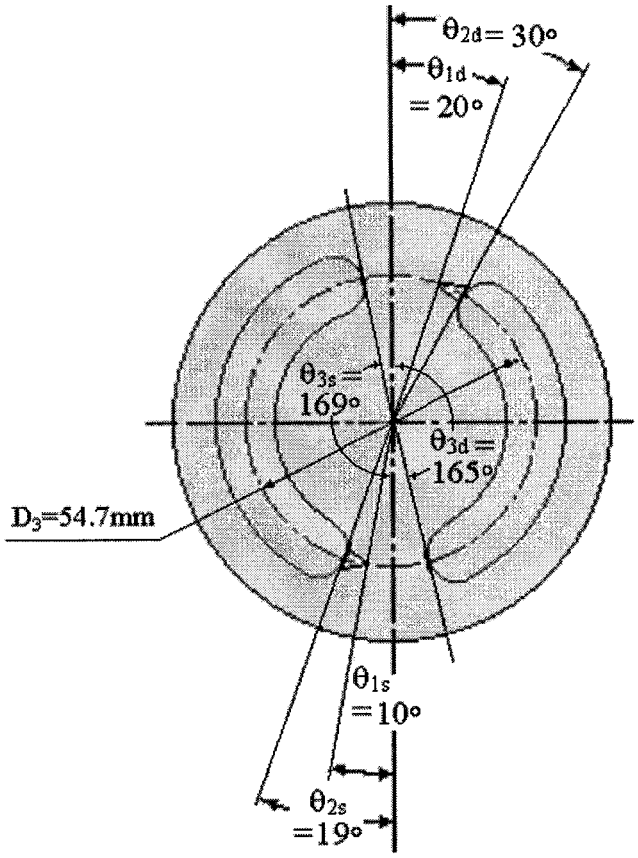

Fig. 3.7 Layout of the desirable port plate for a swash plate pump of geometric volume of 40 cc/rev

CHAPTER 4

FORCE AND VIBRATION ANALYSIS OF THE PUMPING MECHANISM

The swash plate axial piston pumps with conical cylinder blocks possess some desirable static and dynamic characteristics. In this chapter, the advantages of the conical cylinder block arrangement are discussed. The moments acting on the swash plate and the dynamic loads transmitted to the drive shaft bearings are also analyzed.

4.1 Advantages of the Conical Cylinder Block

During the suction stroke, the piston inertia is trying to detach the piston from the slipper pad and/or the slipper pad from the swash plate. Piston detachment force limits the maximum pump driving speed. In case of cylindrical cylinder block, as shown in Fig. 4.1.a, the piston centrifugal force, acting upwards, has no effect on the detachment force. Using conical cylinder block, as shown in Fig. 4.1.b, a component of the piston centrifugal force is generated and acts axially and opposite to the piston inertia. This component reduces the piston detachment, hence increases the maximum pump driving speed and specific power. Detachment force is calculated as the difference between the piston inertia and the axial component of its centrifugal force.

$$F_{dt} = \left|m_p \ddot{s}_k\right| - \left|m_p \omega^2 r_{ck} \sin\beta\right| \tag{4.1}$$

where $r_{ck} = \{[R_1+(L_1-L_2)\tan\beta]-0.5L_p\sin\beta + s_k \sin\beta\}$ and represents the perpendicular distance between the piston center of mass and the drive shaft axes.

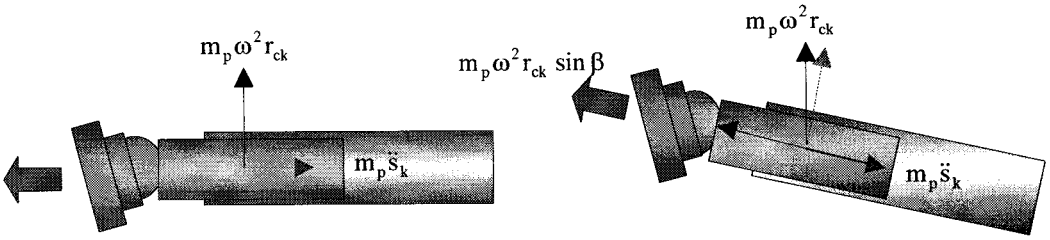

a- In a circular cylinder block b- In a conical cylinder block

Fig. 4.1 Line of action of a piston during suction stroke

Since s_k is function of cylinder block angular displacement θ, the piston detachment force varies with θ during one complete revolution of the cylinder block that has certain cone angle β. Maximum value of the detachment force is only considered in this investigation. From analytical point of view, in order to calculate the maximum detachment force during one complete rotation of the cylinder block, the value of θ at which the detachment force reaches its maximum value should be calculated first. We have $dF_{td}/d\theta = 0$ and from this relation it is possible to solve for the value of θ where F_{td} is maximum. Substituting this value of θ in equation 4.1 results in a direct relation between the maximum detachment force and the cylinder block cone angle β.

Alternatively, due to the complex relation between the detachment force and the cylinder block angular displacement θ and the cone angle β, numerical solution using the developed model and simulation software could be used to calculate the detachment force for one complete revolution of the cylinder block for certain cone angle and rotational speed. Maximum value of the detachment force in each simulation run is recorded. Several runs were carried out in order to plot the

maximum detachment force versus various cone angles and rotational speeds.

Results are presented in Fig. 4.2. The piston maximum detachment force is seen to decrease nearly linearly with an increase in the cone angle β at any rotational speed, while it increases with an increase in the pump driving speed. This result could also be deduced since $F_{dt} = \left|m_p \ddot{s}_k\right| - \left|m_p \omega^2 r_{ck} \sin\beta\right|$ and for small β $dF_{dt} / d\beta \approx -\left|m_p \omega^2 r_{ck} \beta\right|$ that agrees with the Fig.4.2.

The reduction percentage of the piston maximum detachment force is calculated by considering the ration between the reduction in the maximum detachment force at specific β and the maximum detachment force when $\beta = 0$, for the same running speed. Results are shown in Fig. 4.3. The reduction percentage of the piston detachment force is seen to increase almost linearly with β, while it does not depend on the pump rotational speed. Therefore, an increase of β to the value allowed by design considerations is recommended. A decrease in the detachment force with the increase of the cylinder block cone angle helps to drive the pump at higher speeds which results in an increase in pump specific power.

An added advantage of the conical cylinder block arrangement is the relatively larger geometric volume for the same piston diameter. A study of the pump geometry shows that for a cylinder block cone angle equal to 5°, the piston stroke increased by 4% for the circular arrangement of the cylinder block.

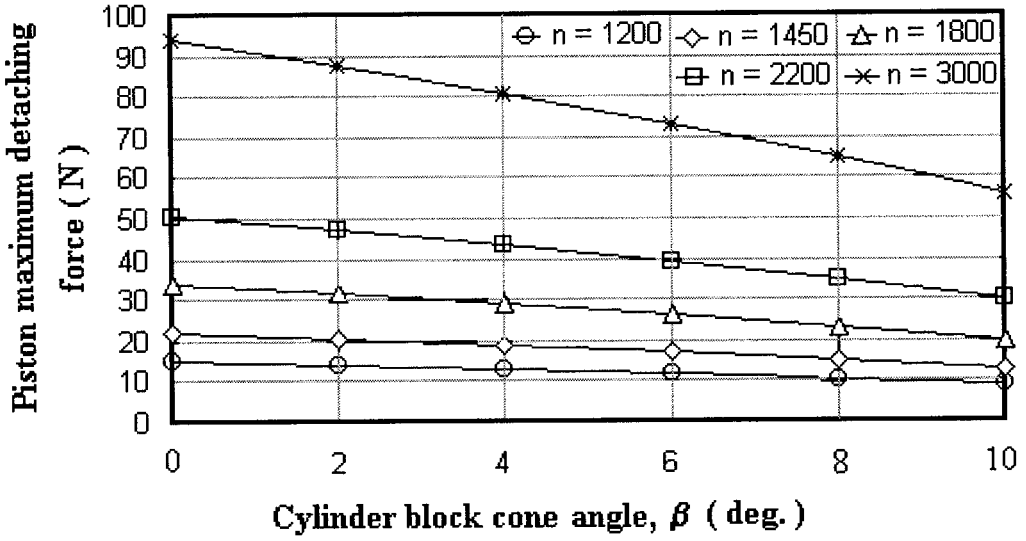

Fig. 4.2 Effect of cylinder block cone angle on the piston maximum detachment force

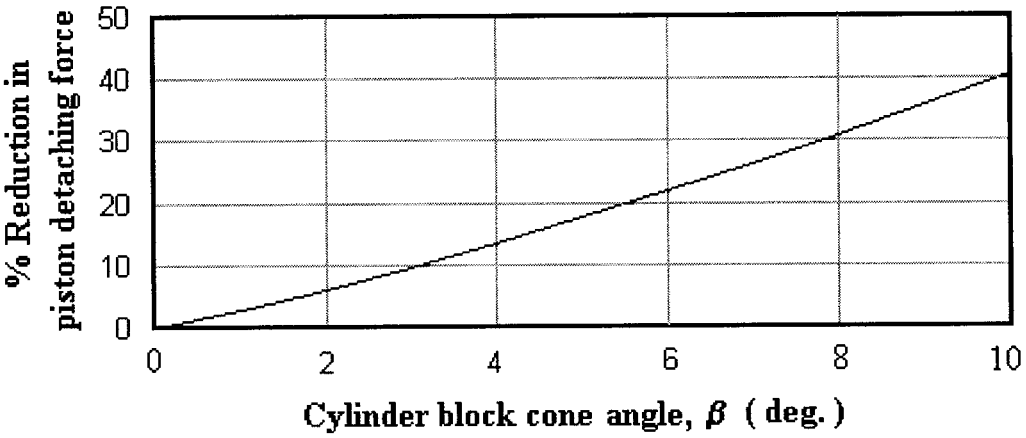

4.3 Effect of cylinder block cone angle on percentage reduction of the detachment force for all running speeds

4.2 Analysis of the Moment Acting on the Swash Plate

The three components of the moment acting on the swash plate during one complete rotation of the pump driving shaft can be calculated by simultaneously solving equations (2.1) to (2.21). The software package based on the Matlab-Simulink program mentioned in Chapter 3 is further developed and used to calculate these moments for a pump of a geometric volume of 40 cc/rev and running at 1450 rpm. It is assumed that the pump is equipped with the recommended port plate shown in Fig. 3.8. The moment components were calculated for pump delivery pressures of 10 MPa, 20 MPa and 30 MPa, and the results are shown in Figs. 4.4, 4.5 and 4.6, respectively.

The simulation results reveal that the three components of the moment are of periodic nature and do not change their signs except for the component M_y that alternates between positive and negative values with a higher maximum negative value. The two components M_z and M_b are nearly constant compared to M_y, which must be overcome by the pump control system in variable geometric volume pumps.

The moment component M_y disturb the swash plate during its transient and steady state conditions. Therefore, from the design point of view, it is important to know the frequency content of M_y in order to supress the swash plate steady state vibration that results due to M_y. The moment wave M_y for one complete revolution of the driving shaft is digitized into certain number of points (nop). Based on Fourier analysis, the periodic wave M_y is found to have an average value plus cosine and sine terms and could be rewritten as follows:

$$M_y = M_{yo} + \sum_{i=1}^{nof} [a_i \sin(iT) + b_i \cos(iT)] \qquad (4.2)$$

$$\text{where } M_{yo} = \frac{1}{nop} \sum_{k=1}^{nop} M_k, \quad a_i = \frac{2}{nop} \sum_{k=1}^{nop} M_k \sin(iT) \text{ and } b_i = \frac{2}{nop} \sum_{k=1}^{nop} M_k \cos(iT)$$

Figure 4.7 shows the simulation results of the moment M_y as compared with that one resulted from the harmonic analysis when the load pressure is 10 MPa. Results show that the Fourier series expansion with 27 terms can represent the original periodic wave reasonably well. The frequency of the first harmonic was equal to the pump rotational speed, and the others are multiples of the first harmonic. This was found true for different delivery pressures, running speeds and swash plate inclination angles. It is also seen that the average value M_{yo} is negative, i.e. it tends to decrease the swash plate inclination angle with a magnitude equal to 10 N.m., 35 N.m and 62 N.m for the three system pressure values of 10MPa, 20MPa and 30MPa, respectively.

The average value of the moment M_y has been found to increase with an increase in delivery pressure and decrease with swash plate inclination angle as shown in Fig. 4.8. The average value of the moment M_z, which equals the pump driving torque, is seen to increase with the increase of the pump delivery pressure and/or flow rate as shown in Fig. 4.9. The moment M_b acting on the swash plate bearing system is seen to increase with an increase in delivery pressure while it is not much influenced by the swash plate inclination angle as depicted in Fig. 4.10.

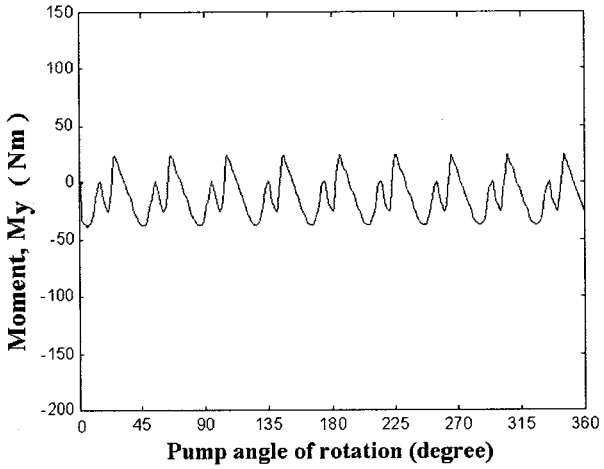

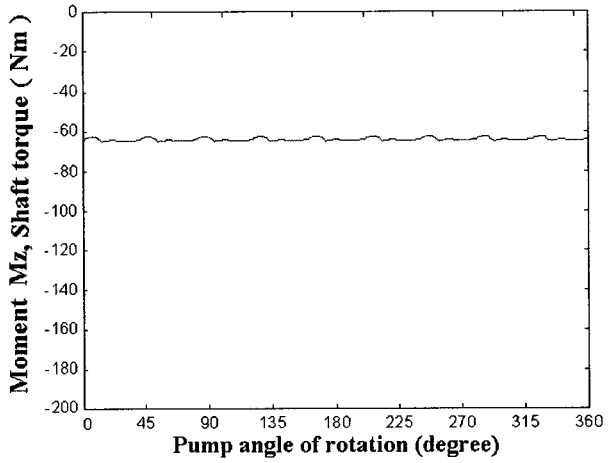

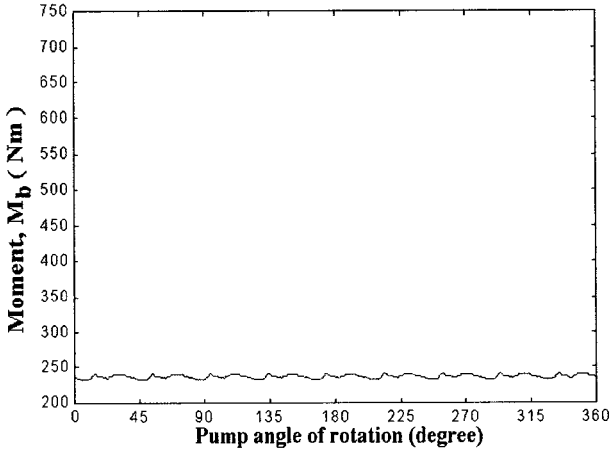

Fig 4.4 Moments acting on the swash plate at 10 MPa delivery pressure

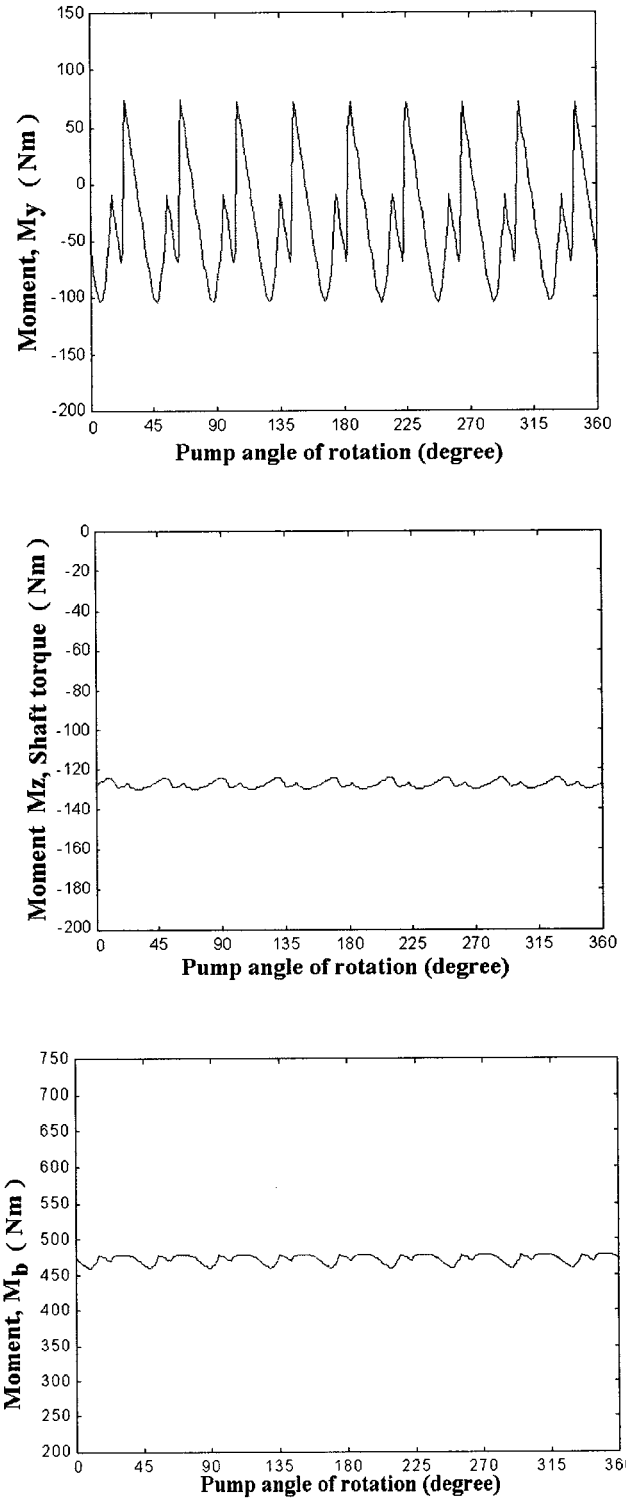

Fig 4.5 Moments acting on the swash plate at 20 MPa delivery pressure

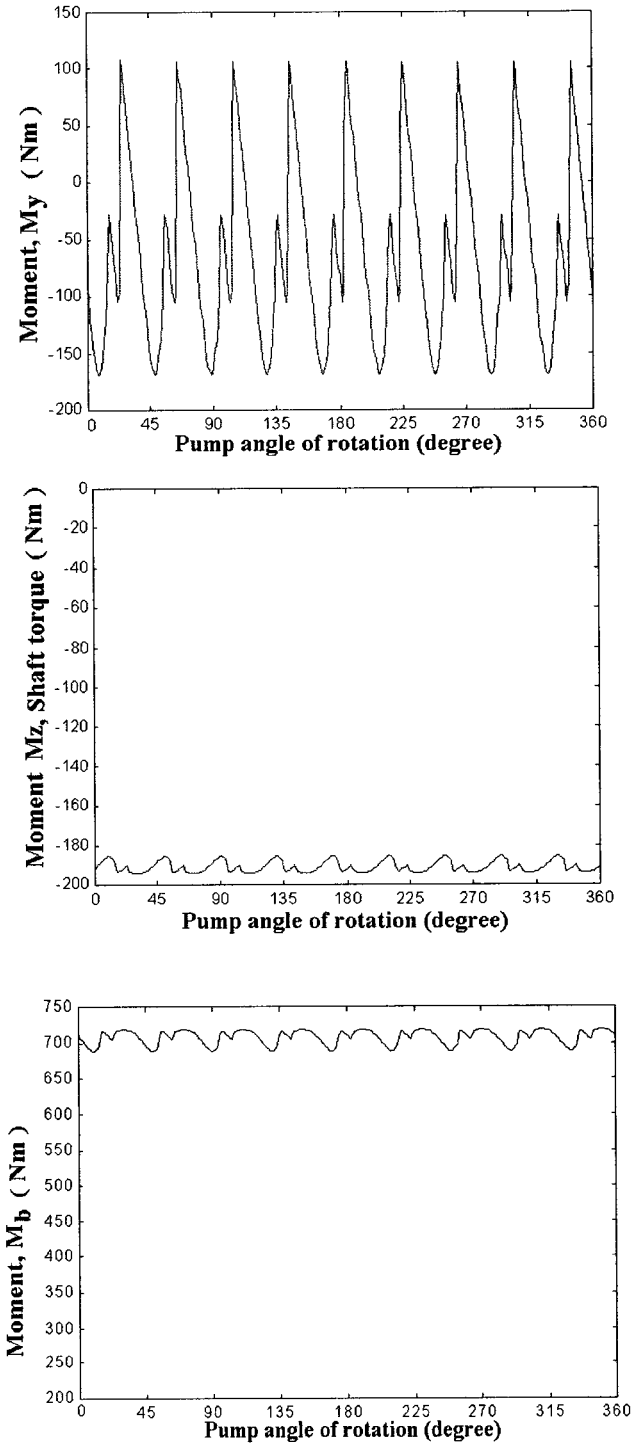

Fig 4.6 Moments acting on the swash plate at 30 MPa delivery pressure

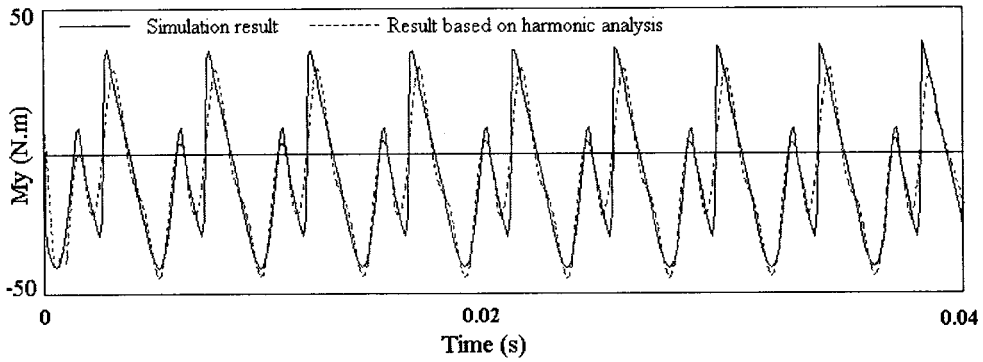

Fig 4.7 Simulation results of the moments M_y and the Fourier series representation with 27 terms

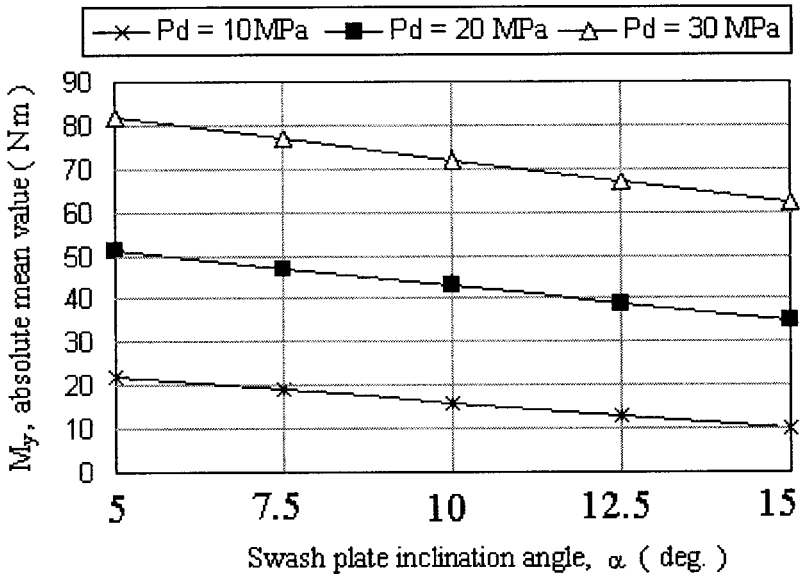

Fig 4.8 Effect of swash plate inclination angle on the average M_y.

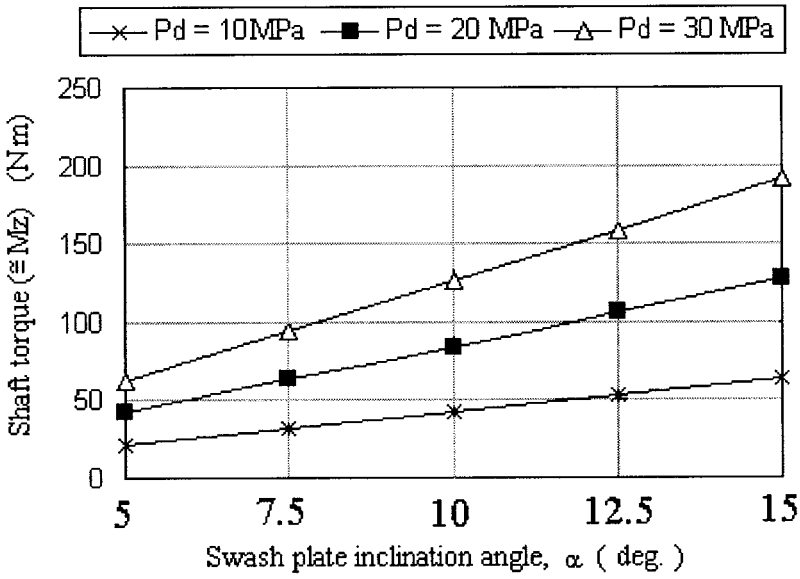

Fig 4.9 Effect of swash plate inclination angle on the average M_z

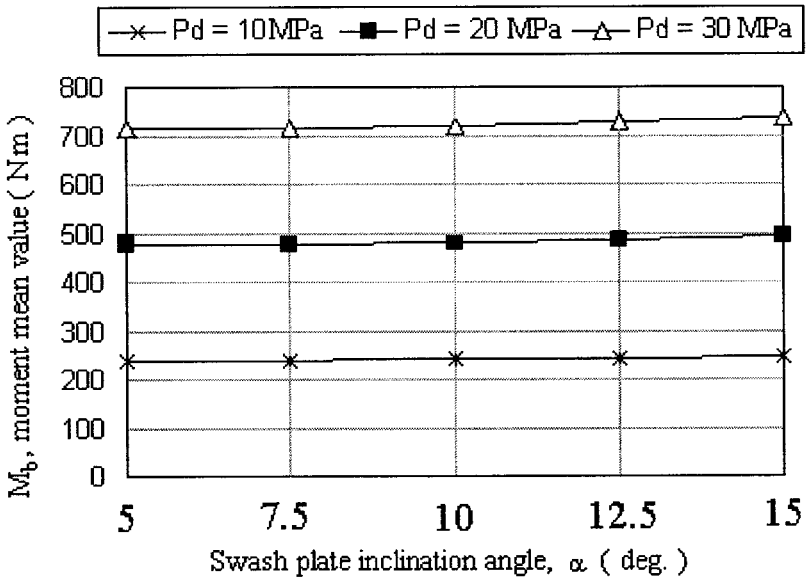

Fig 4.10 Effect of swash plate inclination angle on the average M_b.

4.3 Swash Plate Vibration due to Lateral Moment

Figure 2.8 demonstrates how the swash plate may be kept at any inclination angle as a result of a nearly zero pressure difference p_c across the control piston. During pump rotation, the control piston spring force and the negative mean value of the lateral moment are acting on the swash plate and tending to push it towards the zero inclination angle position. Therefore, the control pressure p_{c1} in the left side chamber of the control piston is found slightly higher than p_{c2}. In the absence of the pump control unit, the swash plate is highly affected by the lateral moment fluctuation. Next, the swash plate vibration due to the lateral moment in an open loop is evaluated for different design and off-design parameters as presented in [58].

The swash plate is assumed held in a steady inclination angle of $7.5^?$ angle, which is 50% of its maximum inclination angle as a result of zero pressure difference across the control piston, which is mechanically attached to the swash plate. For the pump with the constructional parameters shown in Appendix 2, the software package based on the Matlab-Simulink program is further developed to calculate the swash plate movement under the assumed conditions by solving equations (2.29) and (2.30). As illustrated in Fig. 4.11, in the absence of a pump control valve, the swash plate is shown to fluctuate under the exciting moment M_y. Evidently, the swash plate inclination angle fluctuates periodically around 50% of its maximum value with the amplitude increasing proportionally to load pressure. The amplitude of the swash plate fluctuation is found to be nearly equal to 3%, 6% and 9% corresponding to the load pressure values of 10 MPa, 20 MPa and 30 MPa, and are presented in Figs 11a, 11b and 11c, respectively.

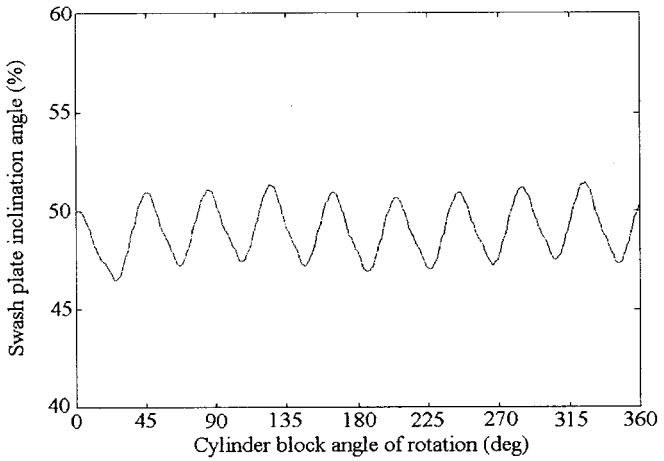

a- $p_d = 10\ MP_a$

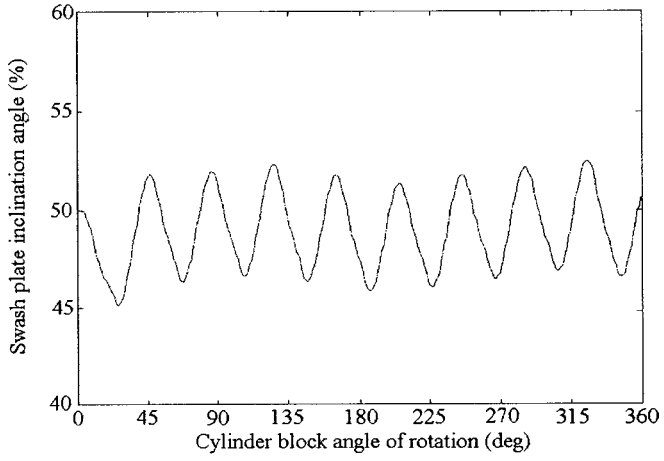

b- $p_d = 20\ MP_a$

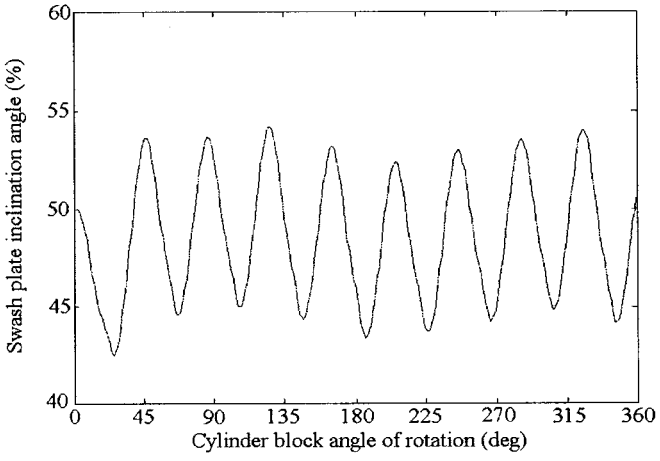

c- $p_d = 30\ MP_a$

Fig. 4.11 Swash plate forced vibration under the effect of the lateral moment

A theoretical study was carried out to investigate the influence of the damping coefficient and the spring stiffness of the control piston, as well as the effects of the oil bulk modulus on the swash plate vibration. Simulation results shows that variation of these parameters between 50% and 150% of the design values did not significantly affect the swash plate response.

4.4 Dynamic Loads on the Drive Shaft Bearings due to Pressure Forces Transmitted by the Cylinder Block

As shown in Figs. 1.2 and 1.3, the cylinder block and pump-driving shaft could be considered one single system. The pump driving shaft carrying the cylinder block is supported within the pump case by one front and one rear bearing. Evidently, the pistons are not rigidly connected to the cylinder block and they are free to slide within the cylinders. Pistons are connected to the slipper pads that are held against the swash plate, which is held at an arbitrary position by means of the control system. Each cylinder ends in an annulus area on which the cylinder pressure acts on during the delivery stroke. The pressure force exerted on this annulus area expected to be transmitted from the cylinder block to the driving shaft bearings. In the following, the dynamic loads on the drive shaft bearings due to pressure forces transmitted by the cylinder block are evaluated, as presented in [59]. This analysis is helpful in the future designs of the pump in sizing the bearings or when the effect of the bearing parameters on the pump performance is to be studied.

In Chapter 2, the variation of the k^{th} cylinder pressure was calculated by solving equation (2.7). The resulting pressure force F_{pk} that acts on the piston along its line of action is simply the product of the piston cross-section area and the cylinder pressure. Equation (2.12) calculates the three components of the cylinder pressure force in the main directions of the inertial frame of reference. Similarly, cylinder pressure force that is transmitted to the cylinder block F_{kc}, is calculated as follows:

$$[F_{kc}]_0 = A_a p_k \begin{bmatrix} -\cos\theta_k \sin\beta \\ -\sin\theta_k \sin\beta \\ \cos\beta \end{bmatrix} \tag{4.3}$$

where the effective area in this case is the projected annulus area A_a at the cylinder exit; the components of this force in the main directions are F_{kcx}, F_{kcy} and F_{kcz}, respectively. As shown in Fig. 4.12, relative to the point of application of the force, the front and rear bearings are located on the left at a distance of d_{fb} and on the right at a distance of d_{rb}.

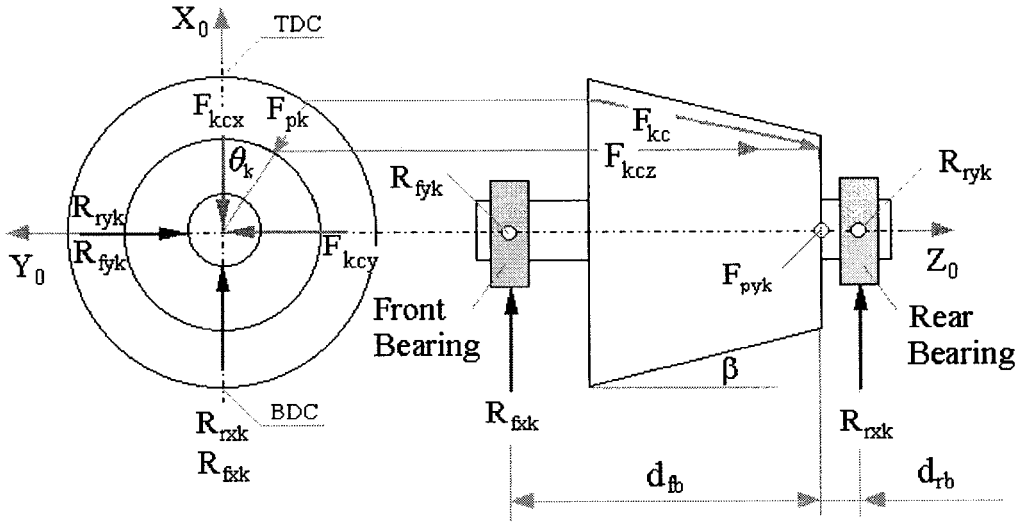

Fig. 4.12 Forces transmitted into the shaft bearing due to k^{th} cylinder pressure

Reaction forces transmitted by the cylinder block due to the single piston are then calculated as follows:

$$R_{fxk} = F_{kcx} \times d_{rb}/(d_{fb} + d_{rb}) \tag{4.4}$$

$$R_{fyk} = -F_{kcy} \times d_{rb}/(d_{fb} + d_{rb}) \tag{4.5}$$

$$R_{rxk} = F_{kcx} \times d_{fb}/(d_{fb} + d_{rb}) \tag{4.6}$$

$$R_{ryk} = -F_{kcy} \times d_{fb}/(d_{fb} + d_{rb}) \tag{4.7}$$

$$R_{zk} = -F_{kcz} \tag{4.8}$$

where R_{fxk} and R_{fyk} are the reactions on the driving shaft front bearing along X_0 and Y_0 directions, respectively. Similarly, R_{rxk} and R_{ryk} are the reactions for the rear bearing. R_{zk} is the axial reaction to the force F_{kzc}, which is transmitted by the cylinder block in the direction of the driving shaft axis Z_0 towards the valve plate. In view of equations 4.4 through 4.8, each bearing experiences combined loading. Conical bearings are used in such cases to take care of the radial and axial loads.

The Matlab-Simulink simulation program was further developed to calculate the bearing reaction forces. Bearing reactions due to the single piston in X_0, Y_0 and Z_0 directions are shown in Figs. 4.13, 4.14 and 4.15, respectively. These figures demonstrate that at the middle of the delivery stroke, where θ_k equals 90°, the bearing reactions in the direction of X_0 switch from positive to negative, while the reactions in the direction of Y_0 and Z_0 stay negative. During the suction stroke, all reactions are nearly zero. It must be noted that in the initial stage of the delivery stroke, the

reactions in direction of X_0 increase gradually with the cylinder pressure p_k, which also gradually increases until it reaches system pressure after a certain delay. The gradual increase of that reaction leads to a negative mean value over the whole period of the delivery stroke.

The reaction forces along the main directions due to the whole piston group are then calculated by superimposing the reaction forces due to single pistons as follows:

$$R_{fx} = \sum_{k=0}^{N} R_{fxk} \tag{4.9}$$

$$R_{fy} = \sum_{k=0}^{N} R_{fyk} \tag{4.10}$$

$$R_{rx} = \sum_{k=0}^{N} R_{rxk} \tag{4.11}$$

$$R_{ry} = \sum_{k=0}^{N} R_{ryk} \tag{4.12}$$

$$R_{z} = \sum_{k=0}^{N} R_{zk} \tag{4.13}$$

Figures 4.16, 4.17 and 4.18 show the reaction forces due to the whole piston group in the X_0, Y_0 and Z_0 directions. These figures show that each of the reaction forces fluctuate around a mean value in a periodic fashion during one complete revolution of the cylinder block. In order of magnitude, it is evident that the absolute mean value of the rear bearing reactions are higher than those of the front bearing due to bearing displacement distribution. The absolute mean value of the reactions in X_0 directions are less because the reaction forces in other directions do not change their signs and accumulate when they are superimposed on the whole piston group. From the fluctuation point of view, the bearing reaction forces along Y_0 show less fluctuation.

As bearing reactions in both directions X_0 and Y_0 have negative mean values, the bearing wear is expected in the region where θ_k is between 270^o and 360^o. Reaction in the direction of Z_0 shows a higher degree of fluctuation but with content of less frequency. This moment reaction acts on the bearing surface of the port plate and is helpful in tightening the clearance between the cylinder block and the valve plate that consequently decreases the leakage between them and maintains a higher system pressure.

In this chapter, the mathematical model of the pump derived earlier is employed in investigating some design aspects of the pump. The novelty of using the conical cylinder block in the swash plate pump is justified. The vibration of the swash plate, due to the lateral moment acting on it, is analyzed. Dynamic loads transmitted to the drive shaft bearings are evaluated. In the following chapter, pump performance with different control schemes will be simulated and investigated.

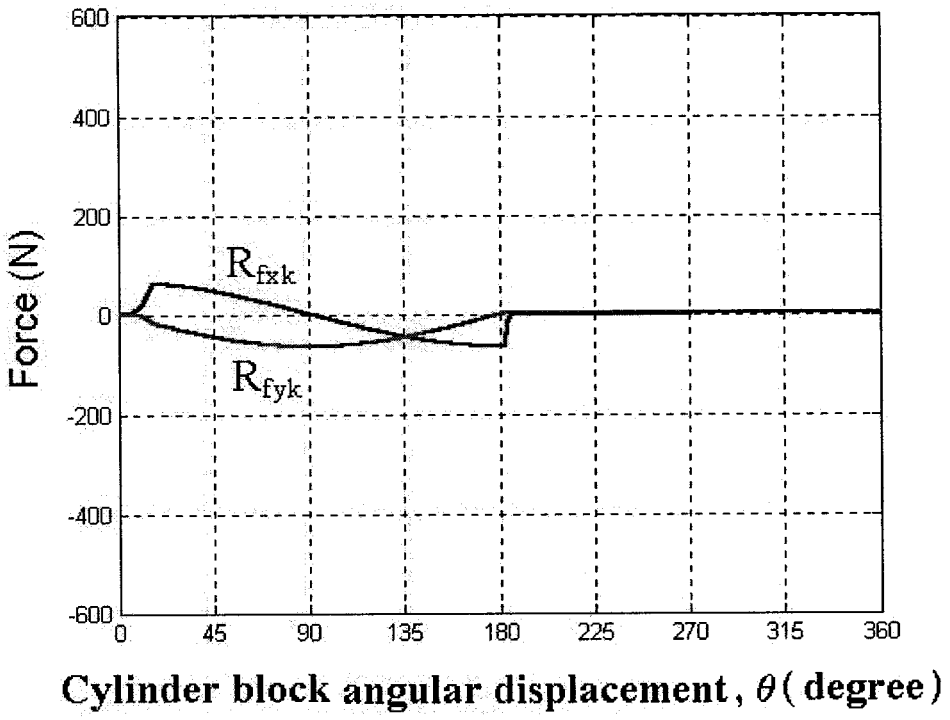

Fig. 4.13 Front bearing radial reactions due to single piston

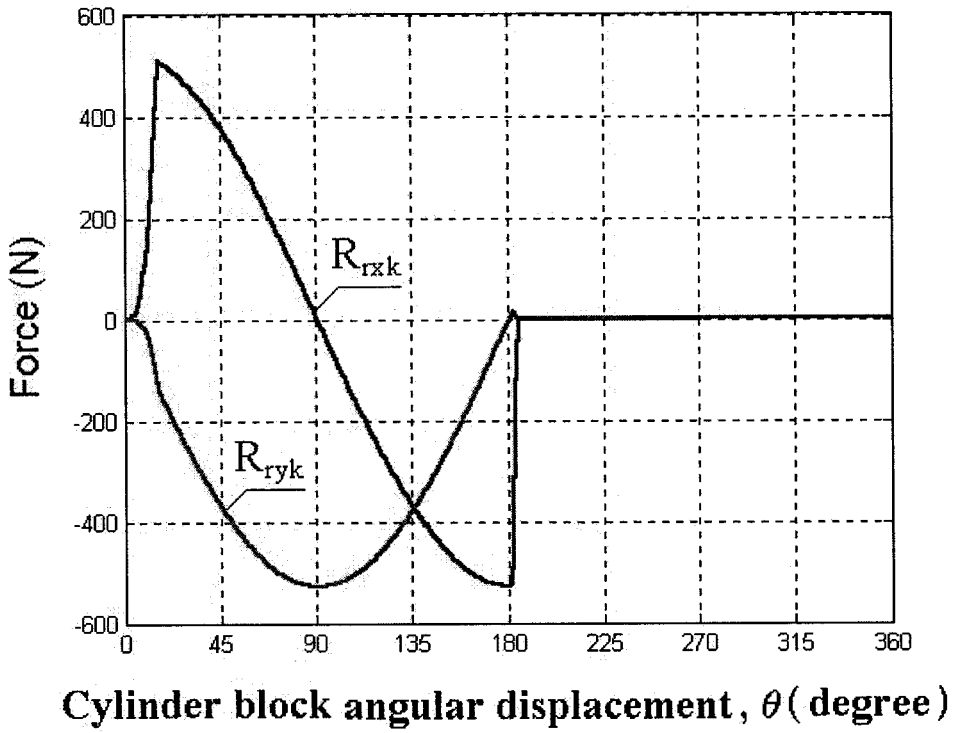

Fig. 4.14 Rear bearing radial reactions due to single piston

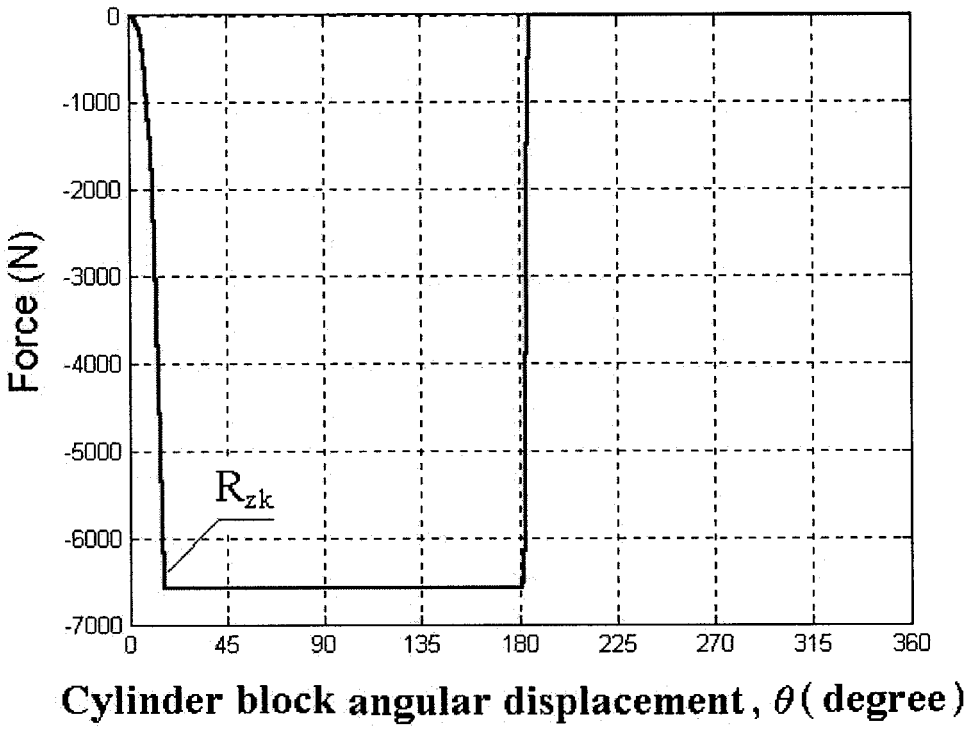

Fig. 4.15 Axial reaction on the valve plate due to single piston

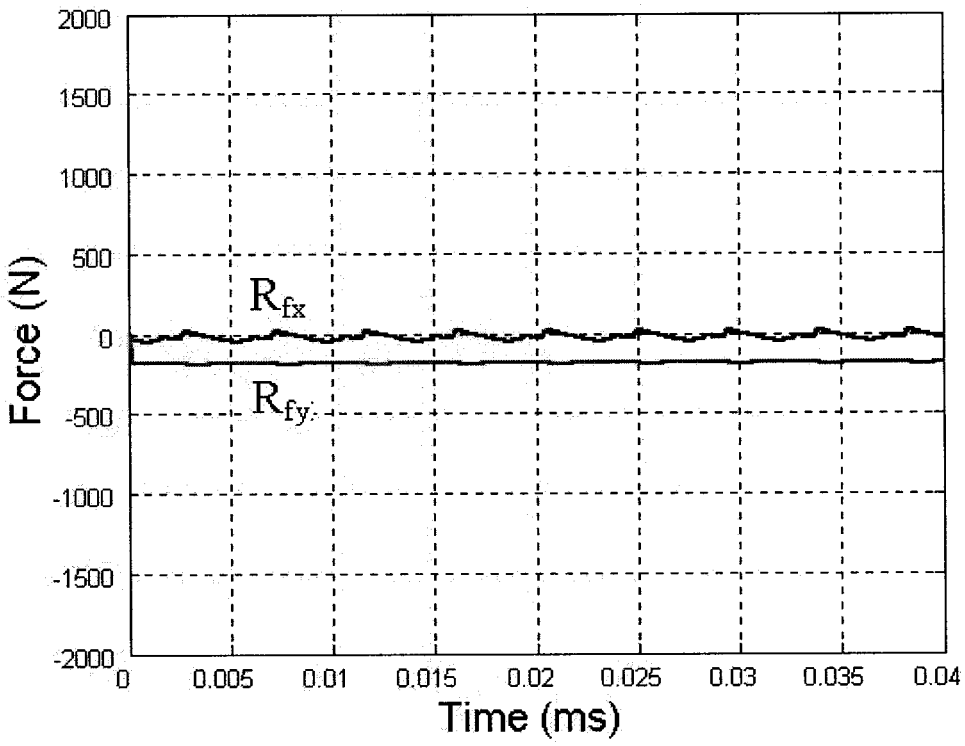

Fig. 4.16 Front bearing radial reactions due to the whole piston group

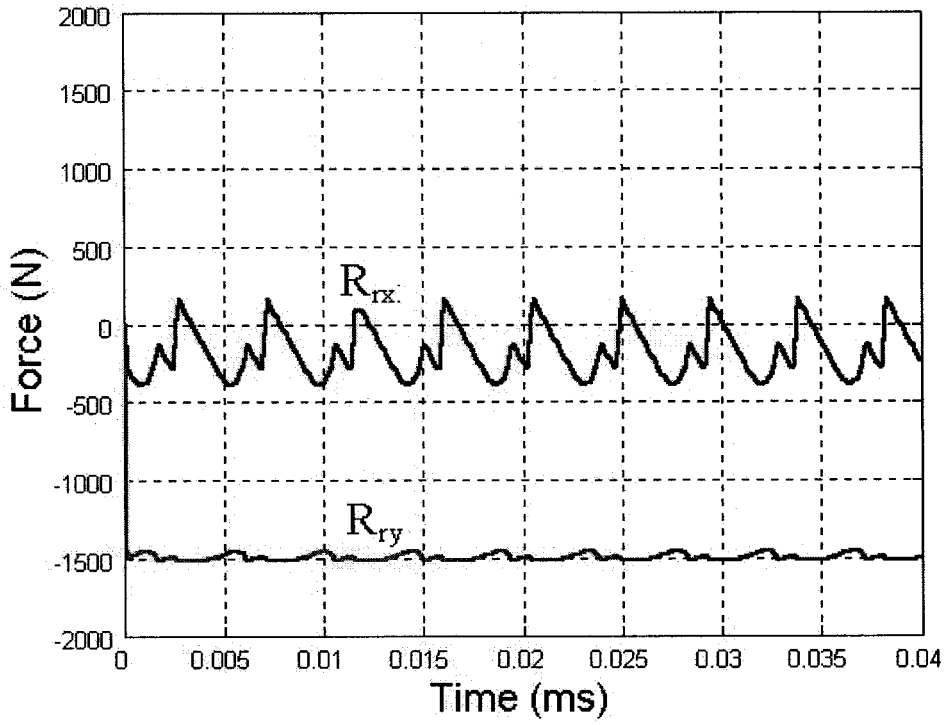

Fig. 4.17 Rear bearing radial reactions due to the whole piston group

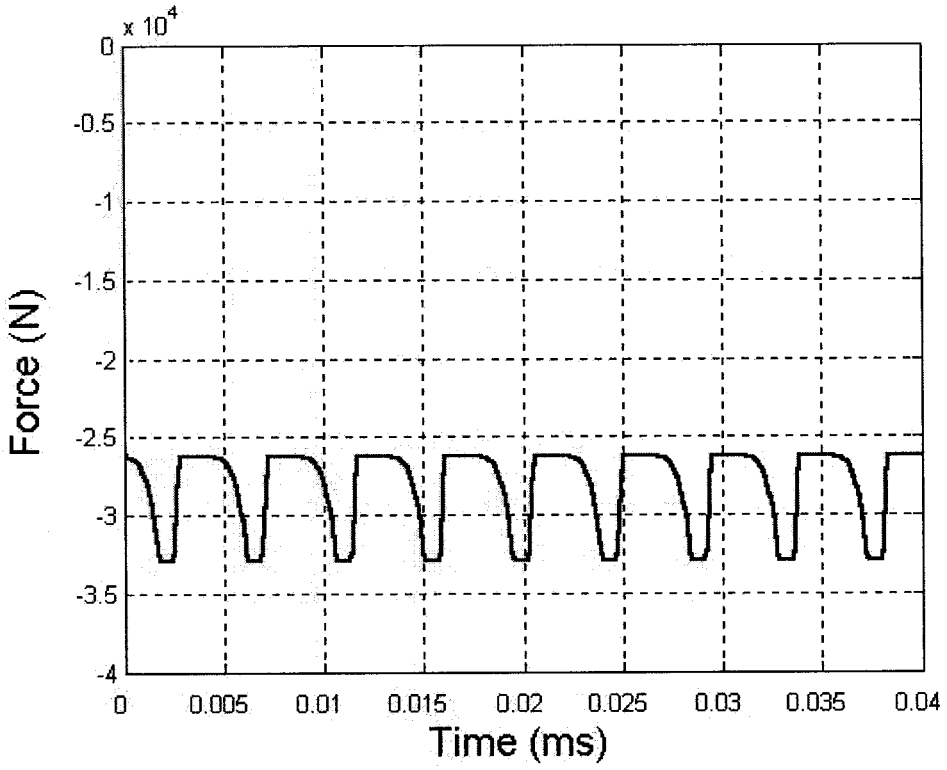

Fig. 4.18 Axial reaction on the valve plate due to the whole piston group

CHAPTER 5

INTRODUCTORY STUDY OF THE PUMP PERFORMANCE WITH DIFFERENT CONTROL SCHEMES

In the previous chapter, a mathematical model was used to evaluate the advantages of conical cylinder blocks, to study the vibrations of the swash plate and to calculate the dynamic loads transmitted to the drive shaft bearings. Such information is helpful for pump designers. In this chapter, an introductory study of the pump performance with different control schemes is conducted. Three alternative control schemes are proposed where each of them has reasons to use and leads to a pump performance with features that suit certain application.

5.1 Proposed Control Schemes

The pump performance will first be simulated using double negative feedback control loops as shown in Fig. 5.1. The inner loop controls the proportional valve spool position using a PID controller. The outer loop controls the swash plate swiveling angle. As shown in Figs. 2.6 and 2.7, pump control unit is composed of a proportional valve and a symmetric hydraulic cylinder attached mechanically to the swash plate. The motion of the cylinder described in equations 2.27 to 2.31, is as a result of flow integration. Therefore the cylinder acts as a physical integrator and PD controller is used without the need of the integral part in the controller.

Some uncertainties in the pump working conditions are mainly due to the change in the fluid properties. For example, hydraulic oil aging and/or aeration reduce both oil bulk modulus and system stiffness, which would result in swash plate position error. Therefore, a second control scheme is proposed that is similar to the first one but with a fuzzy logic controller replacing the PD controller. Construction of a fuzzy controller is discussed in the next section and will consider the change in the oil bulk modulus. The control action is then expected to be more robust to that change.

A single negative feedback control loop is proposed [57] as the third control scheme and is shown in Fig. 5.2. In this scheme, only the outer control loop is considered based on the acceptable open loop characteristics of the proportional valve. The reason behind this is to make the system less responsive and consequently to get rid of the swash plate vibration under steadies state conditions. At the same time, the control scheme and its electronic hardware are simplified and there is a reduction in the cost of the pump production.

The dynamic performance of the proportional valve will be separately investigated in both open and closed loop conditions. Its performance will then be evaluated within the entire system performance.

The Matlab-Simulink simulation program was further developed to simulate the pump and its valve dynamics with the different control schemes proposed.

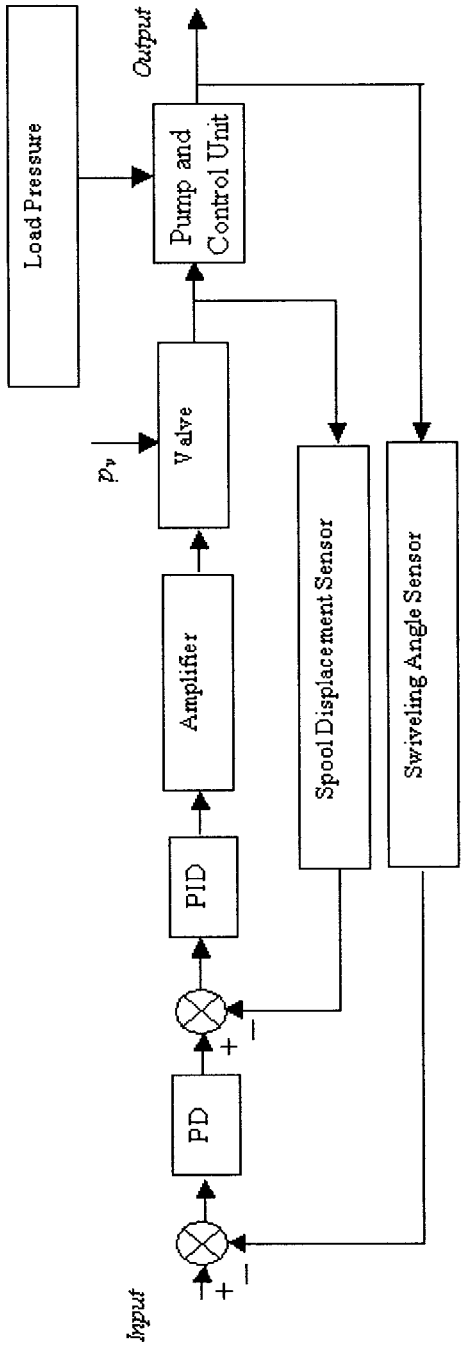

Fig. 5.1 Pump controlling using double feedback loop and PD controller

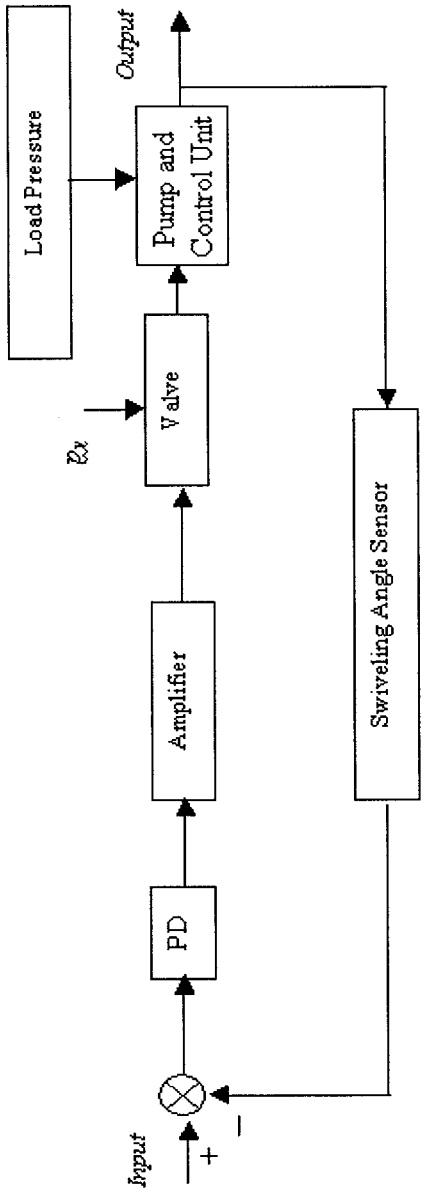

Fig. 5.2 Pump controlling using single feedback loop and PD controller

5.2 Design of Fuzzy Logic Controller

The fuzzy logic control scheme, shown in Fig. 5.3, is known as a rule–based control system in which a set of fuzzy rules represents a skilled human operator. The fuzzy logic control mechanism is independent of a deterministic mathematical model; it thereby overcomes the system uncertainties. The flexibility in constructing the rule base and the membership functions could act as a substitute for the shortage in system knowledge. Five sequential steps explain how is the fuzzy control mechanism works, as introduced in [62], is presented in Appendix 5.

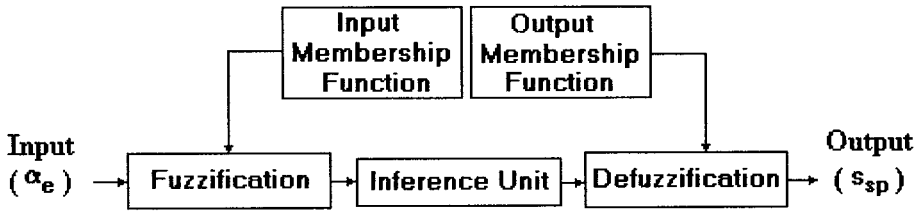

Fig.5.3 Fuzzy logic controller structure

5.3 Simulation of the Proportional Valve Performance

Figures 5.4 and 5.5 demonstrate that the proportional valve consists of a moving part, called a spool, which is fitted inside the valve casing, called a sleeve. The sleeve has four ports designated by standard code as P, T, A and B. Port P is connected to the source of the control pressure p_v. Port T is connected to the oil reservoir as a return line. Ports A and B are connected to the two side chambers of the control piston that is mechanically attached to the swash plate. The valve performs an internal connection between those four ports by virtue of the relative position between the valve spool and

sleeve. The spool is moved by the effect of the electromagnetic force generated when the proportional solenoid receives the control signal i_v.

The figures show that the valve spool has two extreme positions. When the control signal i_v equals zero, the spool is pushed by the spring to the extreme right position at which the control pressure is fully connected to side A of the control piston, while side B is fully connected to the oil reservoir. The swash plate is then held at the lowest possible inclination angle and is adjusted by means of a mechanical stopper in order to keep the flow rate at just enough to satisfy the pump self-lubrication requirements. The alternative extreme spool position occurs when the control signal i_v equals the maximum, and where the spool is pushed to the extreme left against the spring by the effect of the electromagnetic force. At that position, the control pressure is fully connected to side B of the control piston, while side A is fully connected to the oil reservoir. The swash plate is then held at the maximum possible inclination angle allowing the maximum pump flow to be discharged.

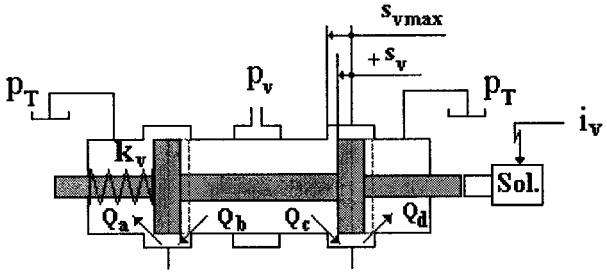

Fig.5.4 Schematic of the proportional valve

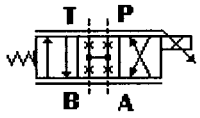

Fig.5.5 Symbolic representation of the proportional valve

Between those extreme positions there is a continuum of spool positions proportional to the strength of the control signal. At any of those positions the swash plate is found to decrease or increase its inclination angle depending on the spool position. The speed of the change of the swash plate inclination angle depends on how far the spool position is from the middle.

Among these positions there is a special position in which the proportional solenoid receives a control signal equal to nearly the mid of the maximum value. This position is reached at steady state conditions where the swash plate must be fixed at the current position by distributing the control pressure equally on the sides of the control piston. In fact, at steady state conditions, the spool is slightly biased in connecting the control pressure to port B more than to port A to withstand the control piston spring effect and the average lateral moment that tend to push the swash plate to the minimum inclination angle position.

The proportional valve characteristics must be investigated first before implementing them within the entire control scheme. In view of the above discussion, the proportional valve dynamics could be simply represented by a single second order linear differential equation that represents spring-mass dynamics as shown in equation (2.22). For simplicity, an equivalent viscous friction coefficient is considered to represent both the viscous and spool seal friction. With the assumption that the electromagnetic force is linearly proportional to the control signal, the open loop characteristics of the valve are expected to be linear.

The Matlab-Simulink simulation program is further developed to include valve dynamics. In an open loop, the valve is assumed to receive a control signal ranging from zero to 100%. Several runs were carried out to calculate the corresponding steady state normalized spool displacement. The theoretical open loop static characteristic of the spool displacement, shown in Fig. 5.6, is found to be perfectly linear as expected.

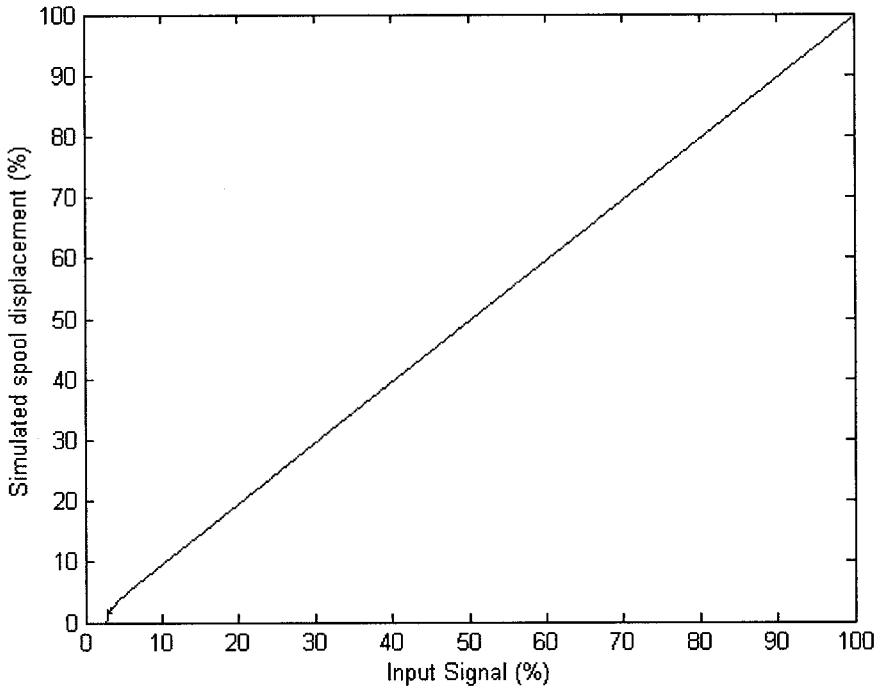

Fig.5.6 Open loop static characteristics of the proportional valve

A negative feedback closed control loop as shown in Fig. 5.7, is constructed using the Matlab-Simulink simulation program in order to investigate the dynamics of the proportional valve. The reason for developing this control loop is to establish the valve dynamics before inserting the inner closed control loop in the entire control scheme shown in Fig.5.1.

The empirical-analytical method known as "Ultimate Sensitivity" introduced by Ziegler–Nichols [63] is used to parameterize the PID valve controller. This method is applied as follows. The proportional gain is increased until the system becomes marginally stable and continuous oscillation just begins with the amplitude limited by the proportional valve saturation. The corresponding gain is defined as K_u (called ultimate gain) and the oscillation period is P_u (called ultimate period). The PID parameters are then calculated as follows: the Control Signal(s)= $K_p[1+1/T_iS+T_dS]$, where $K_p=0.6K_u$, $T_i=0.5P_u$ and $T_d=0.125P_u$. Some further fine tuning was found necessary to make the simulation results closer to the experimental measurements of the valve dynamic performance reported in [69] and to compensate the error in the estimation of the valve design parameter. Eventually, following such approach, the valve PID controller was found as follows $K_p=1$, $T_i=0.01$and $T_d=0.001$. The valve design parameters such as spring stiffness, damping coefficient and spool mass are estimated within the reasonable limits that suit the valve dynamics.

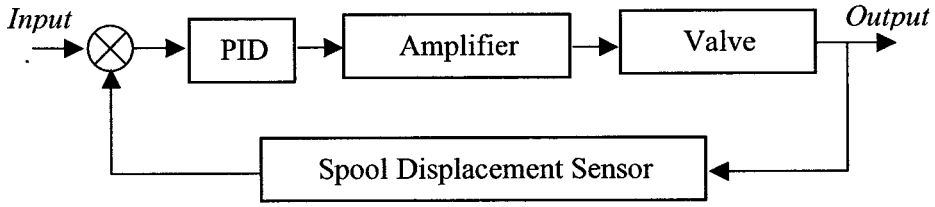

Fig.5.7 Closed loop negative feedback control of the proportional valve

The response of the valve to step inputs is then simulated. The simulation program is provided with successive step input command signals equal to 25%, 50%, 75% and 100% of the full range of the spool displacement. After reaching the steady state, each command signal is assumed to reduce stepwise manner. Figure 5.8 shows the

normalized simulated response of the valve along a 9 second time span. The valve response experiences a little overshooting when the command signal is more than 25% of the full range. Spool displacement overshooting does not occur when the signal is 100% because of valve saturation, or in other words, due to the physical end of the spool displacement. Note that the spool is subjected to impact if it reaches one of its physical ends with a speed above zero. The spool in this case carries kinetic energy proportional to the square of the contact speed.

Figures 5.9 and 5.10 show a zoomed view of the valve step response when the spool moves from the zero position to a certain percentage of its full stroke and vise versa. In view of the simulated results, the PID controller is parameterized to allow nearly 60 ms of settling time for the spool full stroke with 5 ms of delay time, and nearly zero contact speed at the end of the stroke.

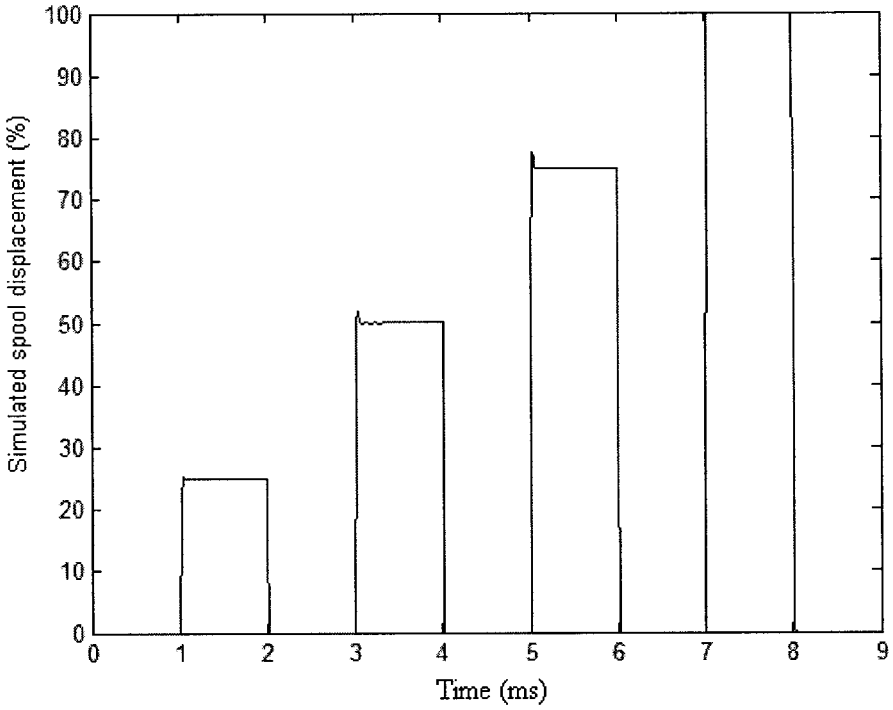

Fig.5.8 Step response of the proportional valve

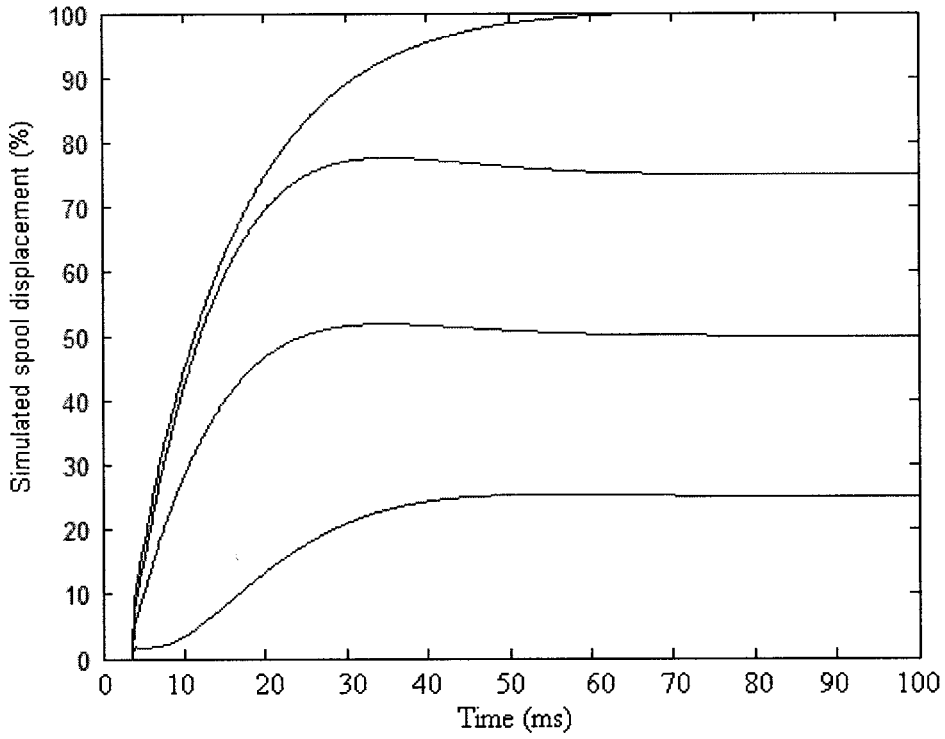

Fig.5.9 Step response of the valve when the spool moves from zero position to a different percentage of its full stroke

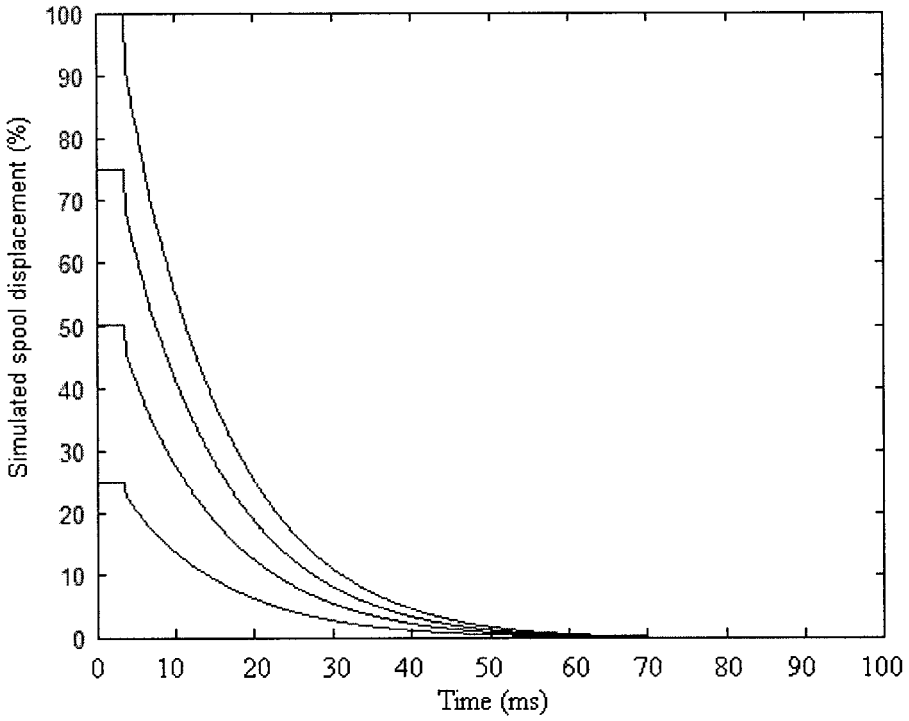

Fig.5.10 Step response of the valve when the spool moves from different percentage of its full stroke to the zero position

5.4 Simulation of the Pump Step Response at Constant Load

The Matlab-Simulink simulation program is now ready to simulate the pump static and dynamic characteristics with the three proposed control schemes shown in Figs 5.1 and 5.2. Simulation runs were carried out to study the static and dynamic performance of the 9-piston pump with a 40cc/rev geometric volume that has the design parameters presented in Appendix 2.

Using successive step input command signals equaling 25%, 50%, 75% and 100% of the maximum swash plate swiveling angle, simulations were carried out at constant load pressure equal to 10MPa. When the pump step response to the previous signals reach the steady state, the command signals are assumed to be reduced to zero in a stepwise manner also. The simulations are repeated three times; once for each proposed control scheme.

The first control scheme considered in the simulation is that which is shown in Fig. 5.1, where the double feedback control loops are used with a PD pump controller. The same approach is used with the control loop of the proportional valve. An ultimate sensitivity method is used to begin to parameterize the PD pump controller, which ended up having a relatively large settling time. Considering the future constant power operation of the pump, a short settling time is recommended in order to protect the prime mover against power shocks during the transient periods in which the loading pressure increases. Therefore, the PD parameters were then tuned a little more, and were found to be K_p=1 and T_d= 0.02.

With these parameters and this control scheme, Fig. 5.11 illustrates the response of the pump to successive step inputs at a constant load pressure during a 9 second time span. Figures 5.12 and 5.13 show a zoomed view of the transient periods of pump response when the swiveling angle increases from the zero position to different percentages of its maximum value and vise versa. Considering this control scheme and the selected PD parameters, the transient periods have a nearly 80 ms settling time when the swiveling angle is increasing, and 60 ms when the swiveling angle is decreasing, as shown in Figs 5.12 and 5.13, respectively. Both cases experience a 10ms delay time. The figures demonstrate that the settling time is reduced on account of having a steady state swiveling angle vibration. The magnitude of the steady state vibration is reduced to 1% instead of the 3% that was recorded earlier in Fig.4.11a in the case of an absence of the control action. This vibration is justified by selecting a reduced settling time, and by regarding the effect of the periodic lateral moment acting on the swash plate M_y.

The behavior of the proportional valve spool is monitored while the pump step response is simulated. Figure 5.14 shows that the spool impacts with the ends of its stroke when the swiveling angle is commanded to increase or decrease to more than 25% of its maximum value.

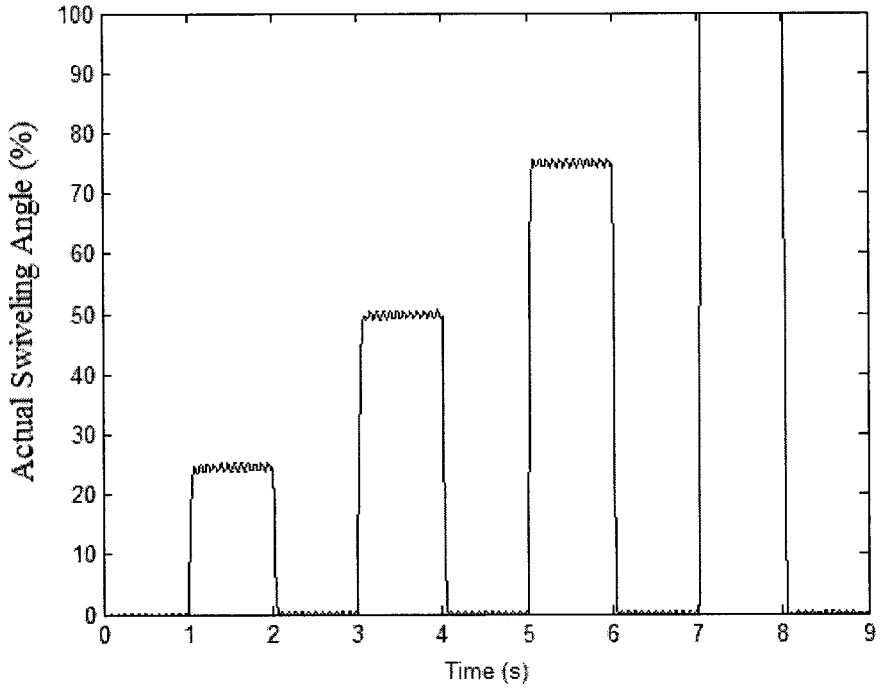

Fig. 5.11 Pump step response at constant load pressure using double feedback control loop with PD controller

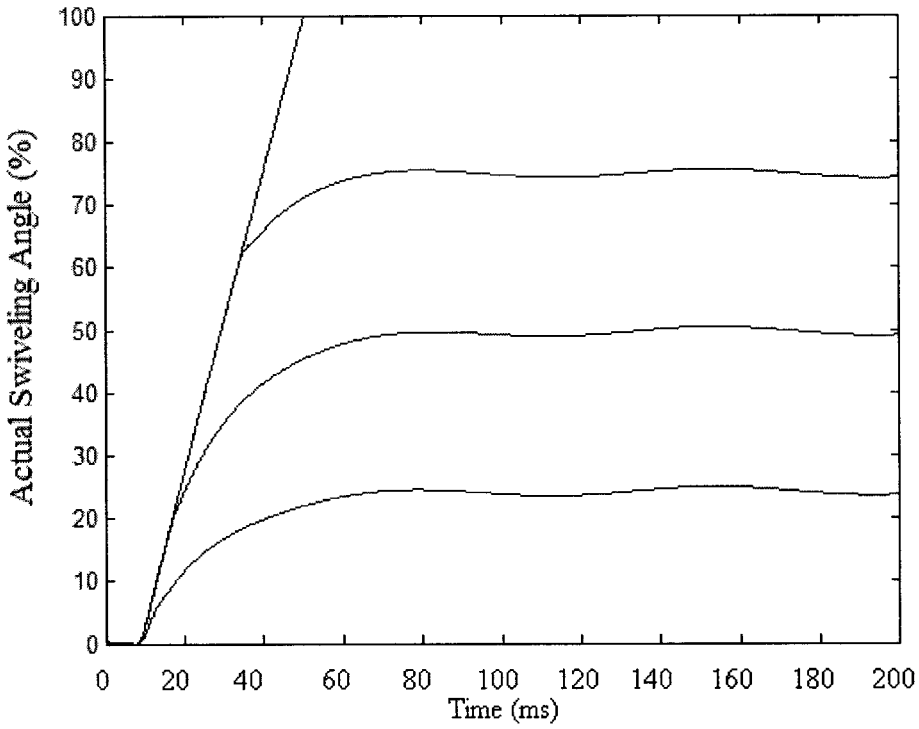

Fig. 5.12 Swiveling angle increases from zero position to different percentages of its maximum value using double feedback control loop with PD controller

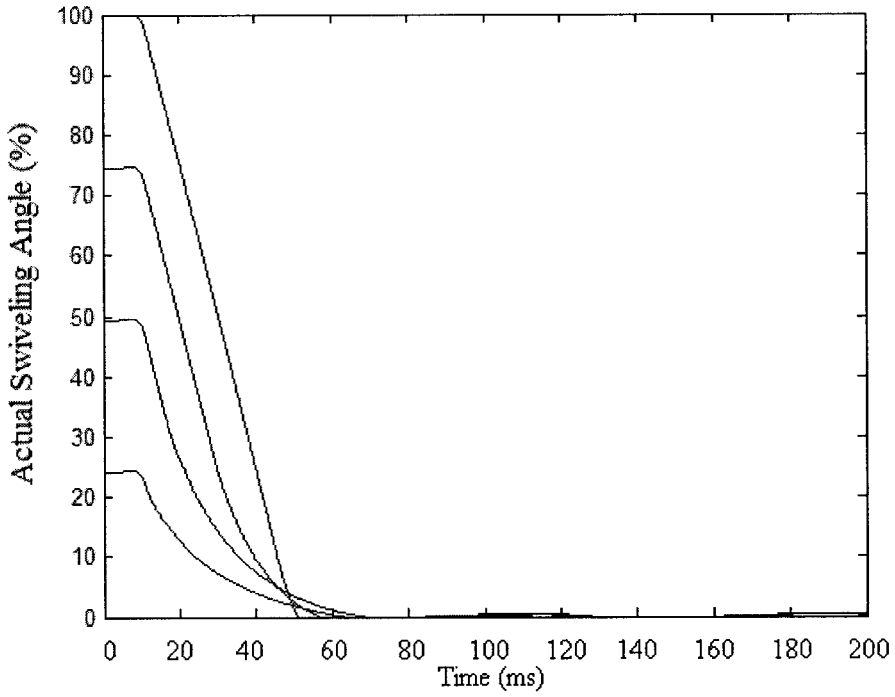

Fig. 5.13 Swiveling angle reduces from a position of different percentages of its maximum value to zero position using double feedback control loop with PD controller

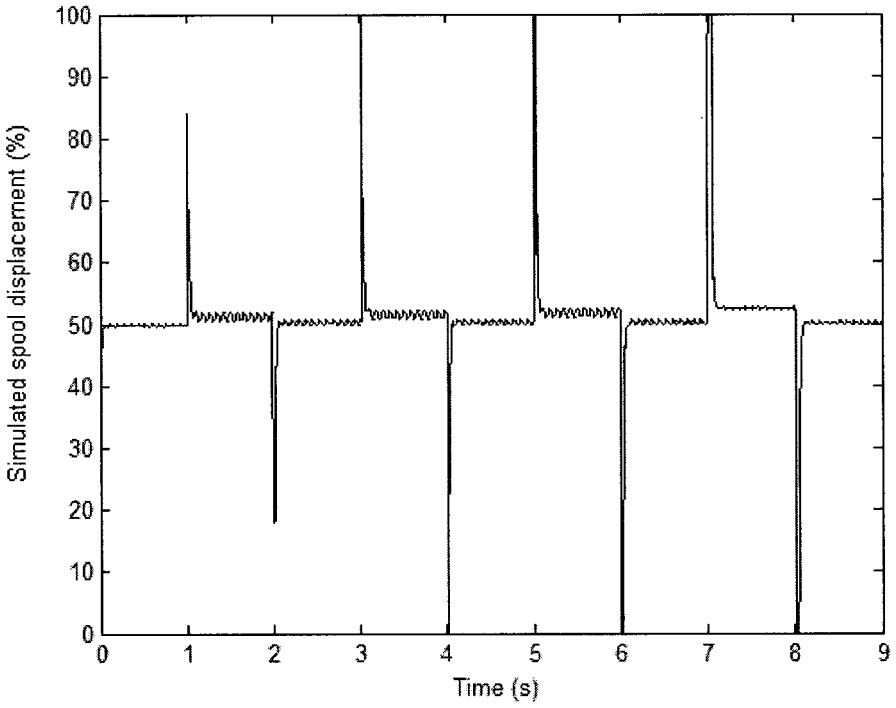

Fig. 5.14 Proportional valve behavior when the pump responses to step inputs at constant load pressure using double feedback control loop with PD controller

The second control scheme is that one in which the PD controller is replaced by fuzzy logic controller in double negative feedback control loops. The first simulation run took into consideration normal operating conditions in which the oil bulk modulus is high. In this run, the focus is to check the suitability of the fuzzy controller for such pumps from a basic control action point of view. Results are presented in Figs 5.15 to 5.18. An overshooting is noticed in Fig. 5.15, which shows the response of the pump to successive step inputs at a constant load pressure during a 9 second time span. Transient periods, shown in Figs 5.16 and 5.17, experience little increase in settling time as compared to the settling time with the PD controller. Figure 5.18 shows the spool does not come into contact with the side ends of its stroke, which means a more gentle behavior and a longer service life. It can be concluded that the fuzzy controller can reasonably replace the PD controller and perform the same basic control action.

The focus of the second simulation run is to check the robustness of the fuzzy controller in relation to the PD controller. In this simulation, the oil bulk modulus assumed to be reduced, a case that might be encountered in many practical applications. The assumed value of the oil bulk modulus is 0.7×10^9 Pa, which means of L fuzzy value. Simulation results show that the swash plate response is not affected considerably in either case. Figure 5.19 shows that the fuzzy controller compensates for the effect of the change in the oil bulk modulus on the valve response, while some valve instability is recorded around its steady state when the PD controller is used. Although the swash plate response is more important, the control valve response has a direct impact on its service life and the whole system reliability.

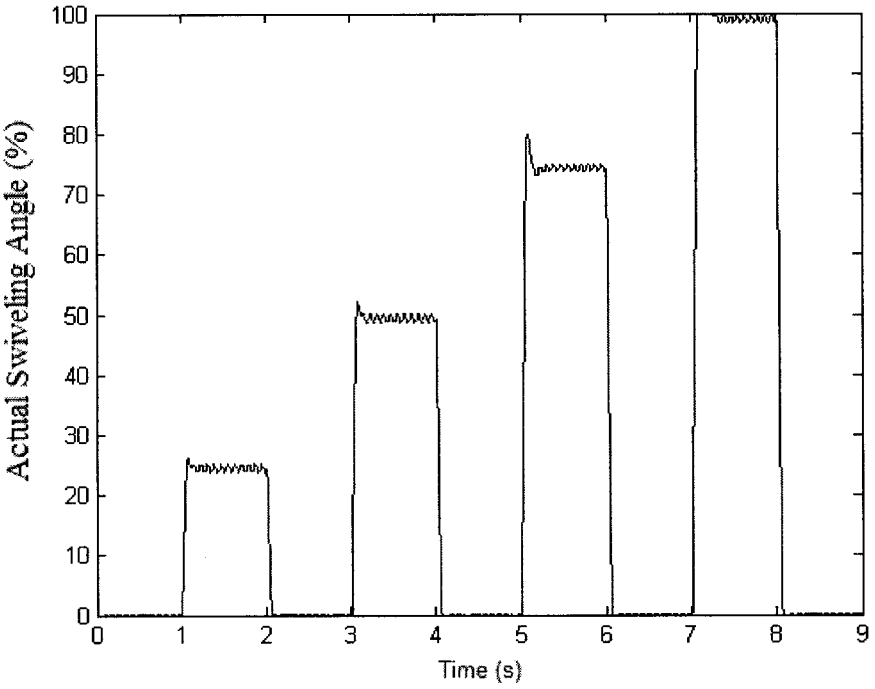

Fig. 5.15 Pump step response at constant load pressure using double feedback control loop with fuzzy controller

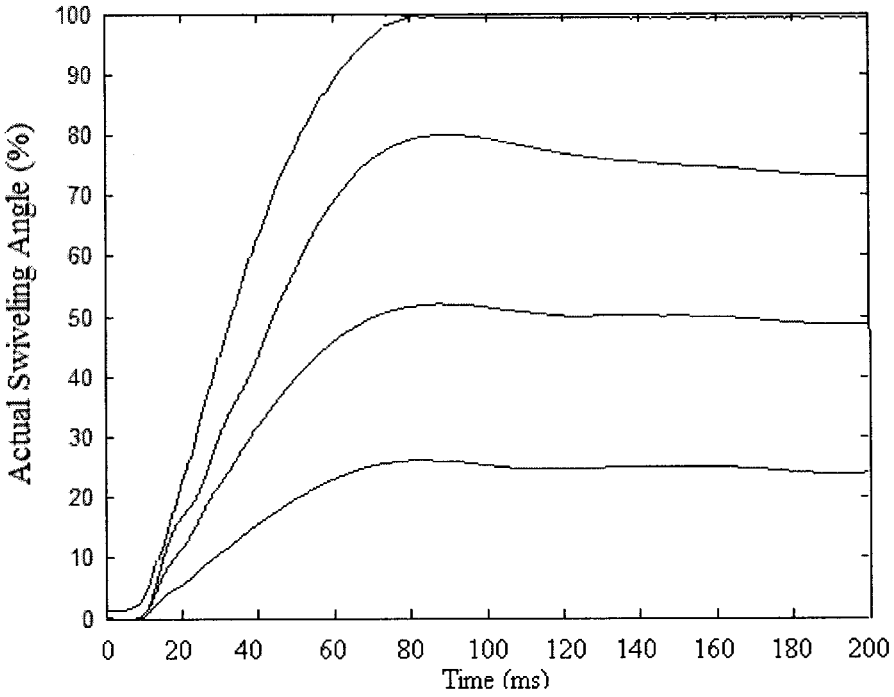

Fig. 5.16 Swiveling angle increases from zero position to different percentages of its maximum value using double feedback control loop with fuzzy controller

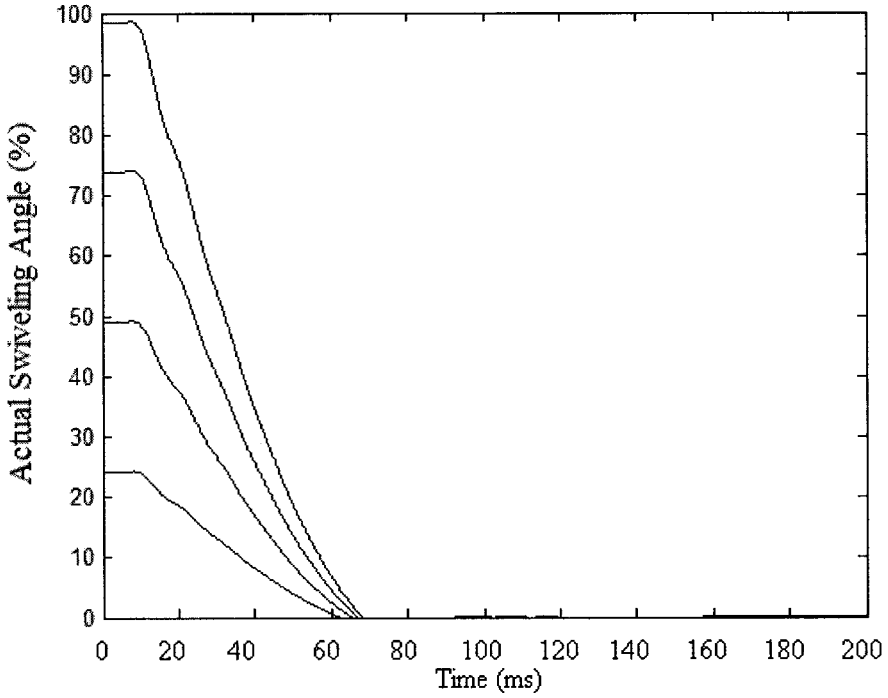

Fig. 5.17 Swiveling angle reduces from a position of different percentages of its maximum value to zero position using double feedback control loop with fuzzy controller

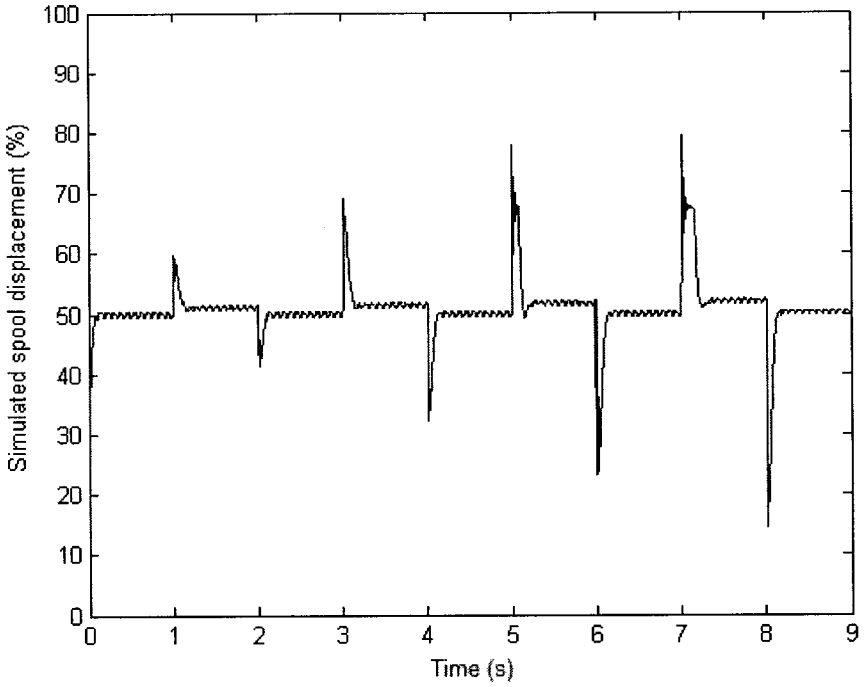

Fig. 5.18 Proportional valve behavior when the pump responses to step inputs at constant load pressure using double feedback control loop with fuzzy controller

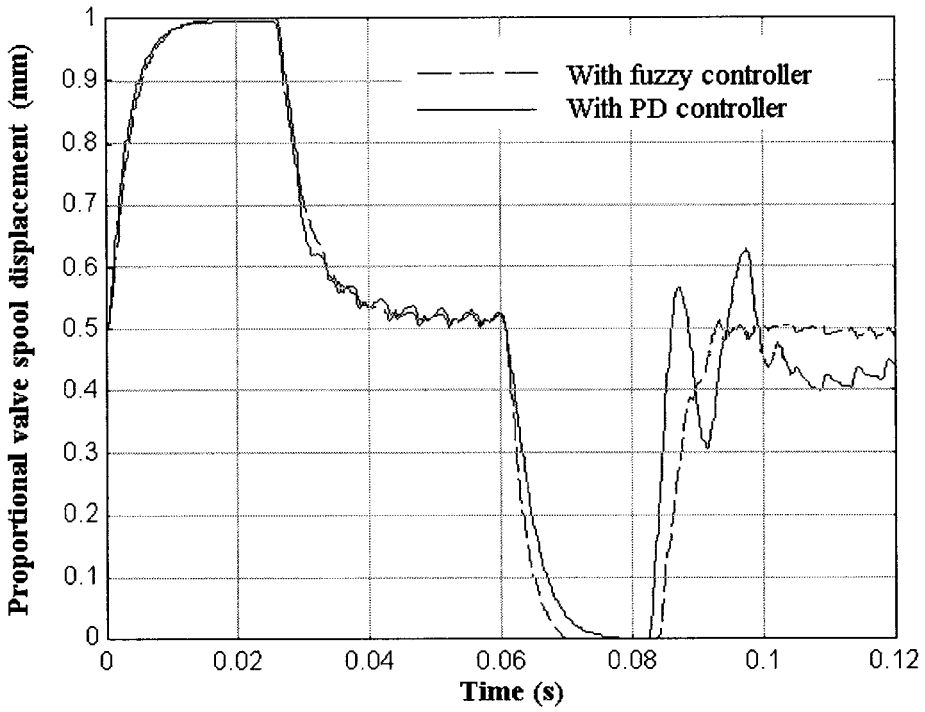

Fig. 5.19 Proportional valve behavior in case of low oil bulk modulus

Based on the simulated linear open loop characteristics of the proportional valve shown in Fig. 5.6, the third control scheme with a single feedback control loop with PD pump controller is considered for simulation. There are two motives for considering such a control system. The first is to make the system less responsive in order to suppress the swash plate steady state vibration and hence the pump flow rate will be smoothened as much as possible. The second is to reduce in cost of manufacturing the pump by removing the electronic circuit of the proportional valve as well as the spool displacement sensor. The parameter of the PD controller is tuned following the same approach used previously with the double loop. The trial for decreasing the settling time with the single feedback loop in order to keep the convenience of the pump constant power operation leads to an unstable system. The controller parameters that fit the requirements of the system stability were found to be K_p=1 and T_d= 0.01.

As shown in Fig. 5.20, the result was a less responsive system that avoided the swiveling angle steady state vibration. Figures 5.21 and 5.22 show a more gradual change of the swiveling angle in the transient periods and the settling time increases to 200 ms, which is inconvenient to the constant power operation of the pump. On the other hand, this can be considered an advantage when the control piston arrives at the end of its stroke with a nearly zero velocity, which reduces the impact on it. The proportional valve performance shown in Fig.5.23 shows the same result of having no impact on its side end as in the case of using a fuzzy controller.

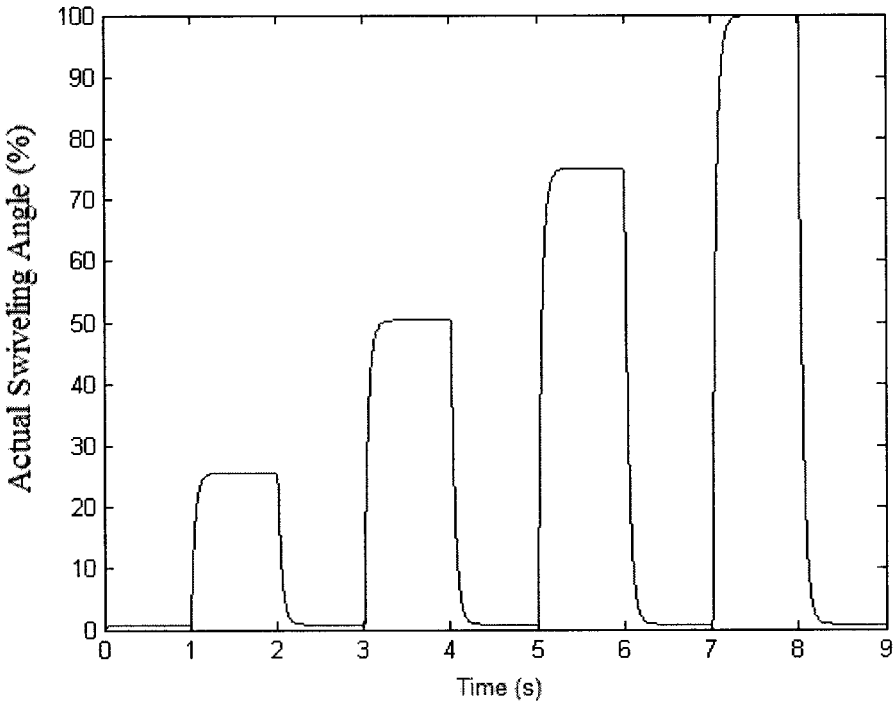

Fig. 5.20 Pump step response at constant load pressure using single feedback control loop with PD controller

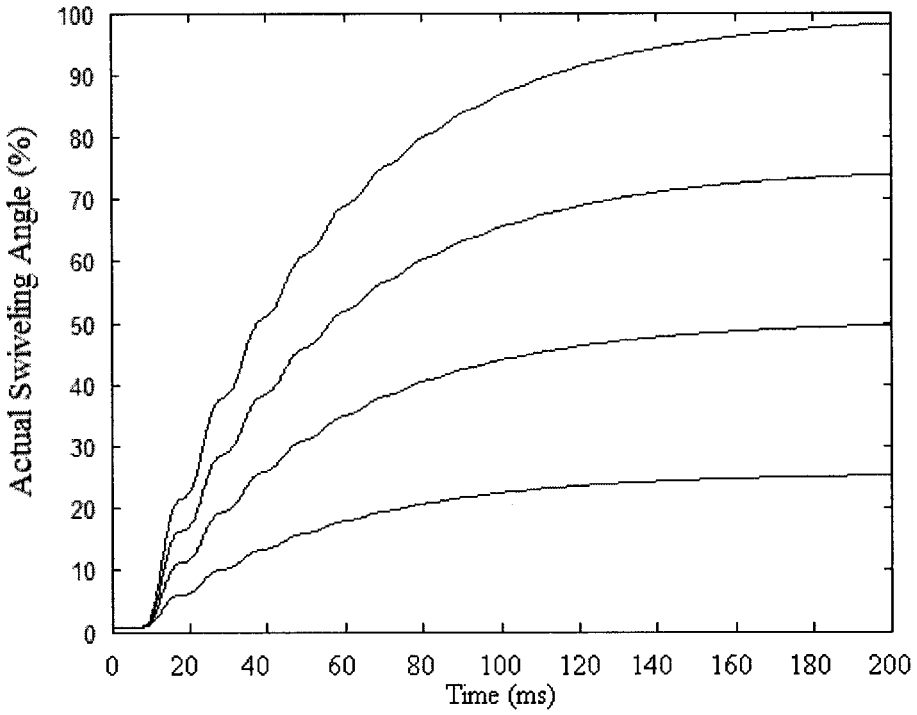

Fig. 5.21 Swiveling angle increase from zero position to different percentages of its maximum value using single feedback control loop with PD controller

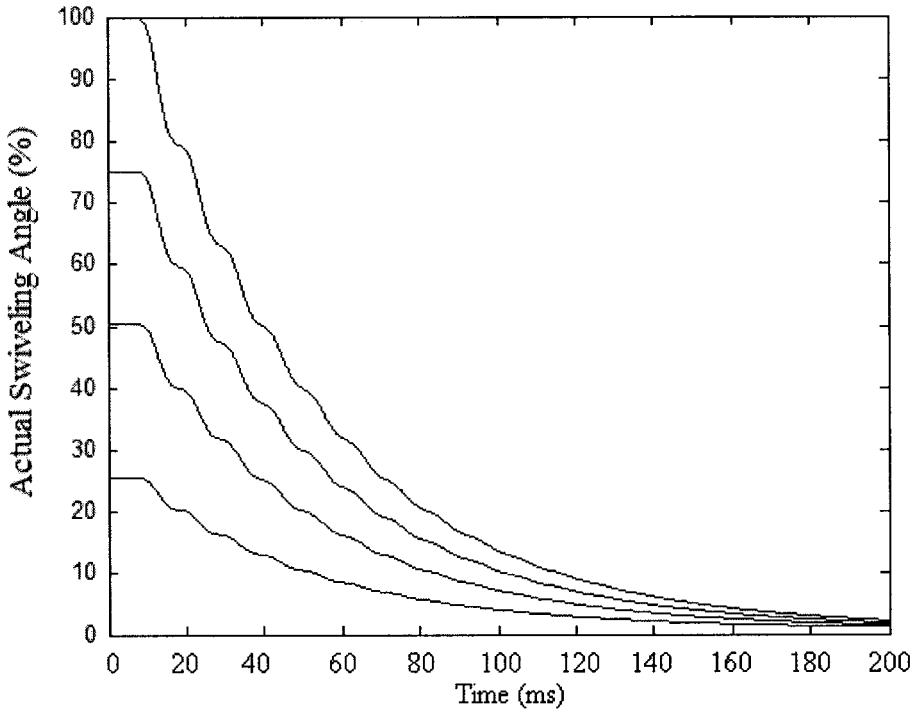

Fig. 5.22 Swiveling angle reduction from a position of different percentages of its maximum value to zero position using single feedback control loop with PD controller

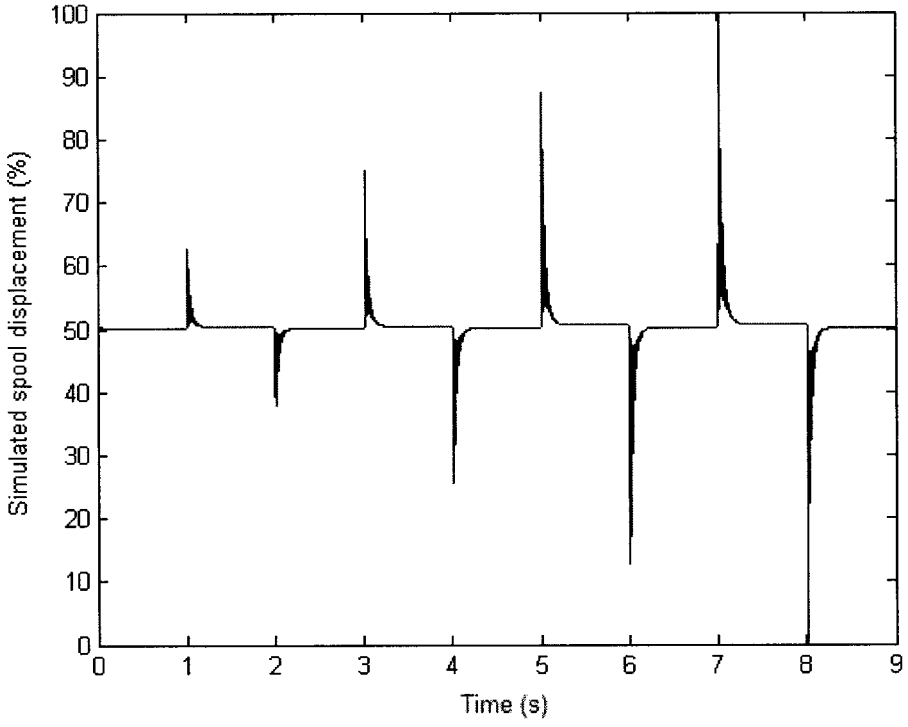

Fig. 5.23 Proportional valve behavior when the pump responds to step inputs at constant load pressure using single feedback control loop with PD controller

5.5 Simulation of the Pump Static Characteristics at Constant Load

After establishing the control schemes and discussing the pump step response, the pump static characteristic is simulated. The simulation program is fed by a command signal that is assumed to change slowly and gradually from zero to 100%, while the corresponding normalized change in the swash plate swiveling angle is recorded. The simulated pump static characteristics confirm the presence of the steady state vibration when the double negative feedback control loop is considered, either with a PD or fuzzy logic controller as shown in Figs 5.24 and 5.25. Using the single feedback loop eleminates the swiveling angle steady state vibration as shown in Fig. 5.26. In all three considered control schemes, the simulation results show linear characteristics of the pump along the full range of the command signal.

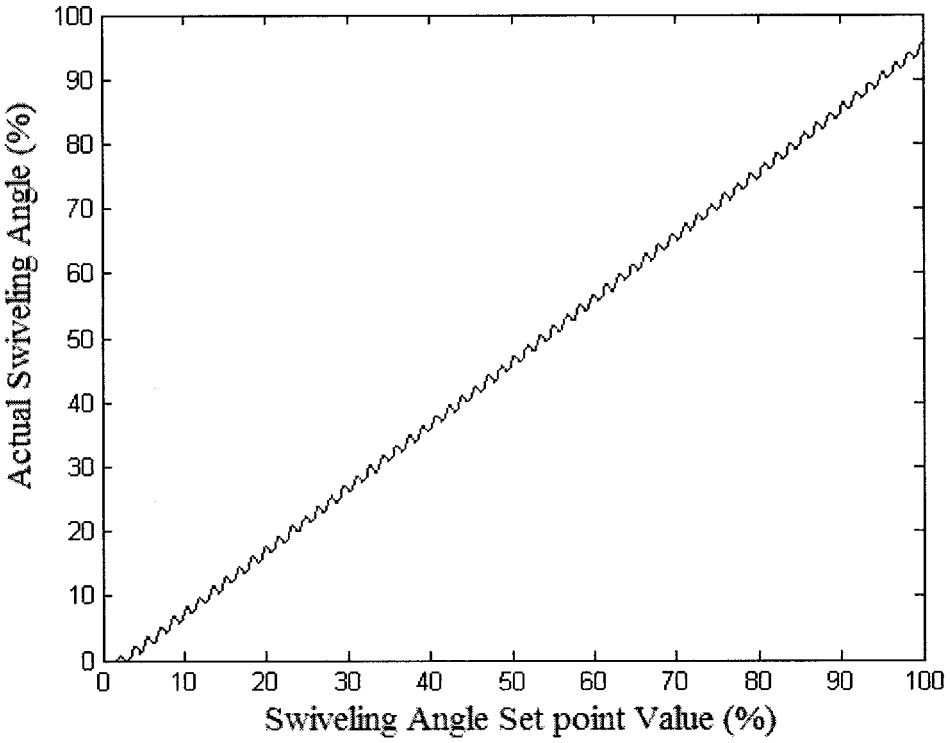

Fig. 5.24 Pump static characteristics at constant load pressure using double feedback control loop with PD controller

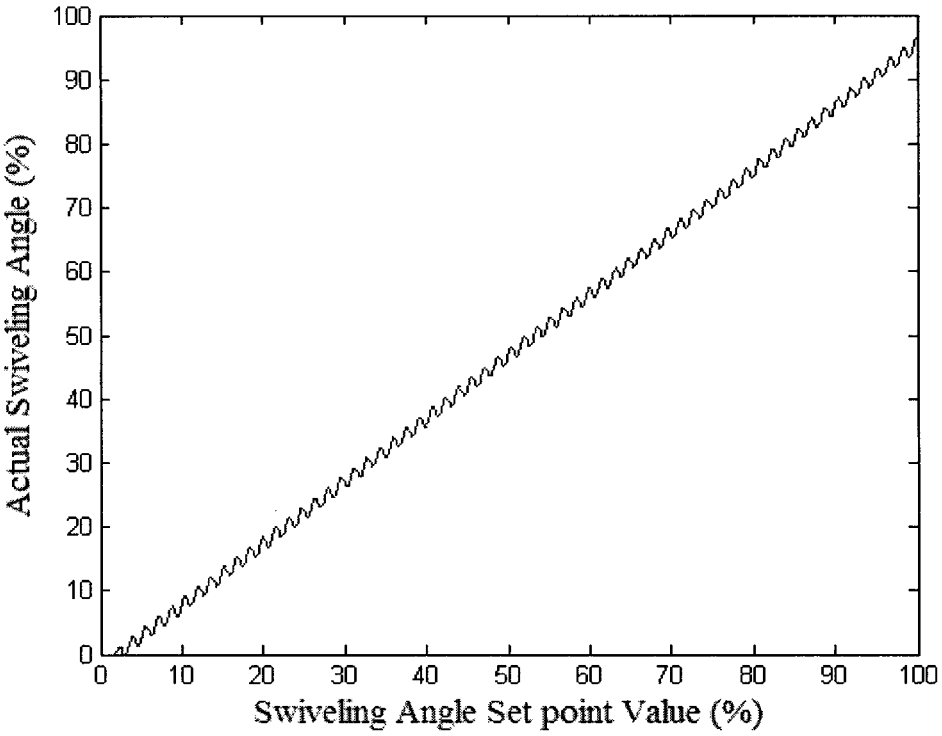

Fig. 5.25 Pump static characteristics at constant load pressure using double feedback control loop with fuzzy controller

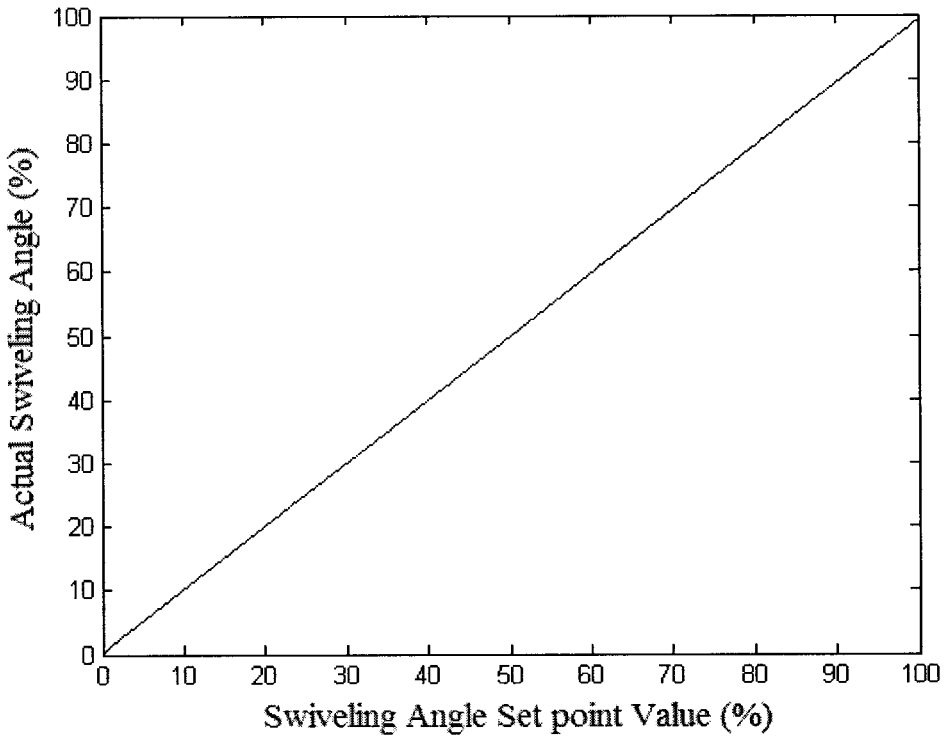

Fig. 5.26 Pump static characteristics at constant load pressure using single feedback control loop with PD controller

5.6 Simulation of the Pump Performance at Constant Power Operation

The simulation program is further developed to simulate the constant power operation of the pump. An arithmetic unit is added as input to the simulation programs as shown in Fig. 5.27. The unit receives the knowledge about the load pressure from the pressure sensor, and then generates the corresponding set point value for the swash plate swiveling angle for the pump constant power operation. The arithmetic unit is designed to logically respect the static characteristic limits; namely maximum power, maximum flow rate and maximum pressure.

Simulation runs were carried out with the pump flow rate monitored in accordance with system pressure, which is assumed to change gradually from zero to a maximum value of 14 MPa. The steady state vibration is still recorded when using a double feedback control loop with the outer one having the PD or the fuzzy controller, as shown in Figs. 5.28 and 5.29, respectively. Fig. 5.30 shows a single feedback loop in constant power operation releasing the swiveling angle steady state vibration. Figures 5.28, 5.29 and 5.30 show that each of the three proposed control schemes respect the constant power operation that results in a perfect hyperbolic relation between the pump flow rate and system pressure.

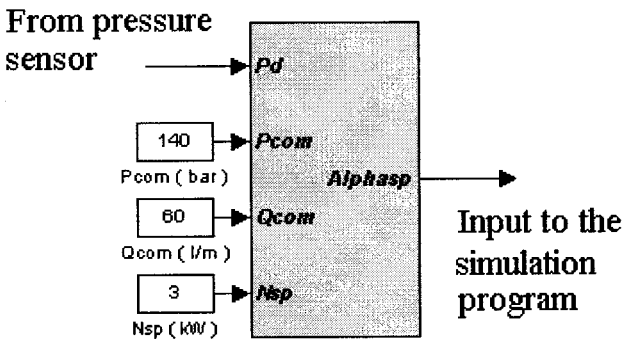

Fig. 5.27 Arithmetic unit added as input to the simulation programs to achieve pump constant power operation

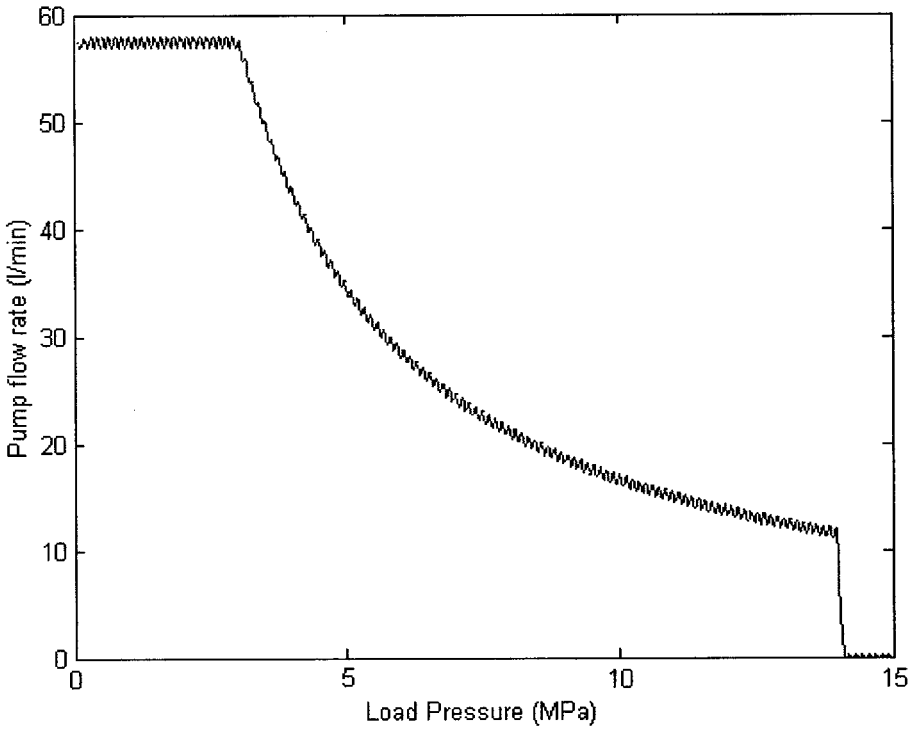

Fig. 5.28 Pump constant power operation using double feedback control loop with PD controller

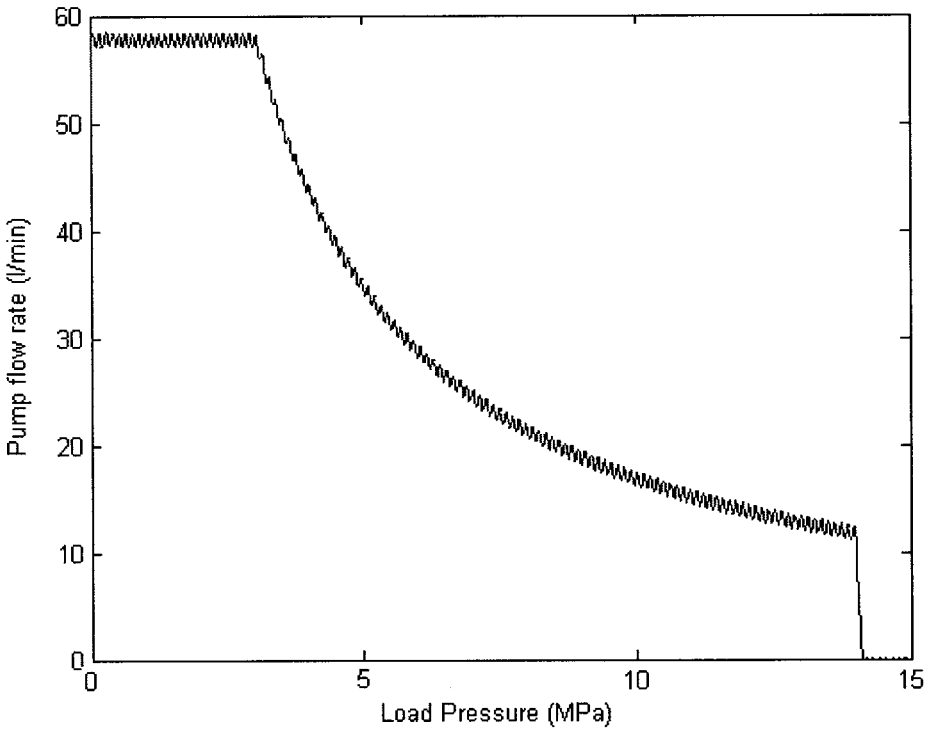

Fig. 5.29 Pump constant power operation using double feedback control loop with fuzzy controller

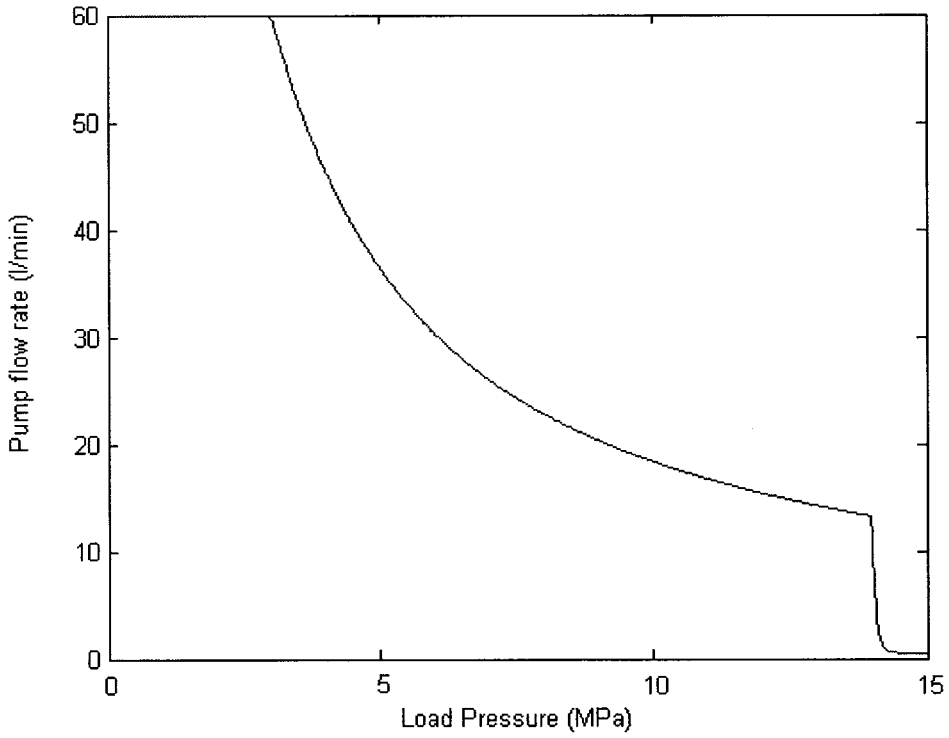

Fig. 5.30 Pump constant power operation using single feedback control loop with PD controller

5.7 Simulation of the Pump Frequency Response in Constant Power Operation

A harmonic variation in the load pressure is quite frequent in practical applications. Therefore, it is important to study the pump response to harmonic input. As shown in [61], the swash plate was assumed to have an initial position equal to 50% of its maximum inclination angle. The pump is then subjected to a sinusoidal change in load pressure. The change in load pressure is sensed by the pressure sensor and fed back to the arithmetic unit. The latter generates the sinusoidal swash plate inclination angle set point value α_{sp} in accordance with the load pressure change to achieve constant power operation. The value of α_{sp} is fed to the main process controller in one of the three proposed control schemes. The actual swash plate inclination angle α is then monitored.

Successive simulation runs were carried out with the input frequency increased in steps of 5 Hz to cover a range of 30 Hz. Simulation runs were carried out three times, once for each control scheme. The simulation results presented in Fig. 5.31 show that, in the case of using double feedback loop, the swash plate responds with a sinusoidal fluctuation that has nearly the same input amplitude up to a 15 Hz input frequency. Considerable attenuation in the amplitude of the swash plate frequency response is found above 15 Hz. The frequency responses when using a fuzzy control are found to be slightly lower and closely follow the response of the PD controller. Using a single feedback control loop is found to greatly decrease the pump frequency response time from the beginning due to a larger settling time.

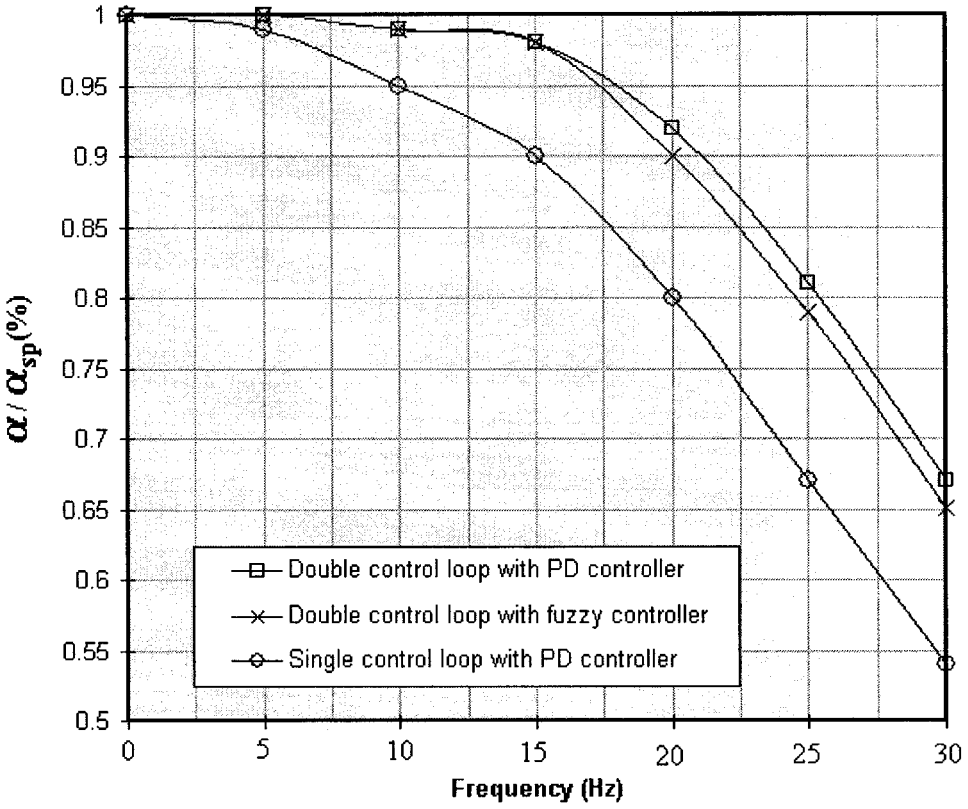

Fig. 5.31 Pump frequency response in constant operation

In this chapter, the pump performance was investigated with different control schemes. The proposed control schemes show significant advantages relative to each other depending upon the application. In the next chapter, the proposed control schemes are prototyped using a real time control scheme, the pump model is validated, and the pump performance with the different control schemes is verified experimentally. A full description for the test setup is presented.

CHAPTER 6

EXPERIMENTAL INVESTIGATIONS OF THE PUMP PERFORMANCE

In the previous chapter, a simulation of the pump performance with different control schemes was presented. In this chapter, pump model validation is conducted and the static and dynamic performance of the pump with those control schemes is experimentally investigated. Experimental setup consists of a hydraulic test bed interfaced with real time control software and data acquisition system has been built for measuring the pump performance. The experimental setup is initially used to measure the step response of the pump, which is equipped with a conventional PD controller in double negative feedback control loop, at a constant load pressure. The theoretical results are compared with the experimental results in order to validate the pump model. The experimental results for the static and dynamic pump characteristics are then obtained in the same sequence used in the analytical investigation presented in Chapter 5. The experimental results are presented, compared with the analytical findings, and then discussed.

6.1 Description of the Hydraulic Test Bed

As shown in Fig. 6.1, the hydraulic test bed consists of four main units; the hydraulic pump, the control pressure supply unit, the load disturbance unit and the oil-conditioning unit.

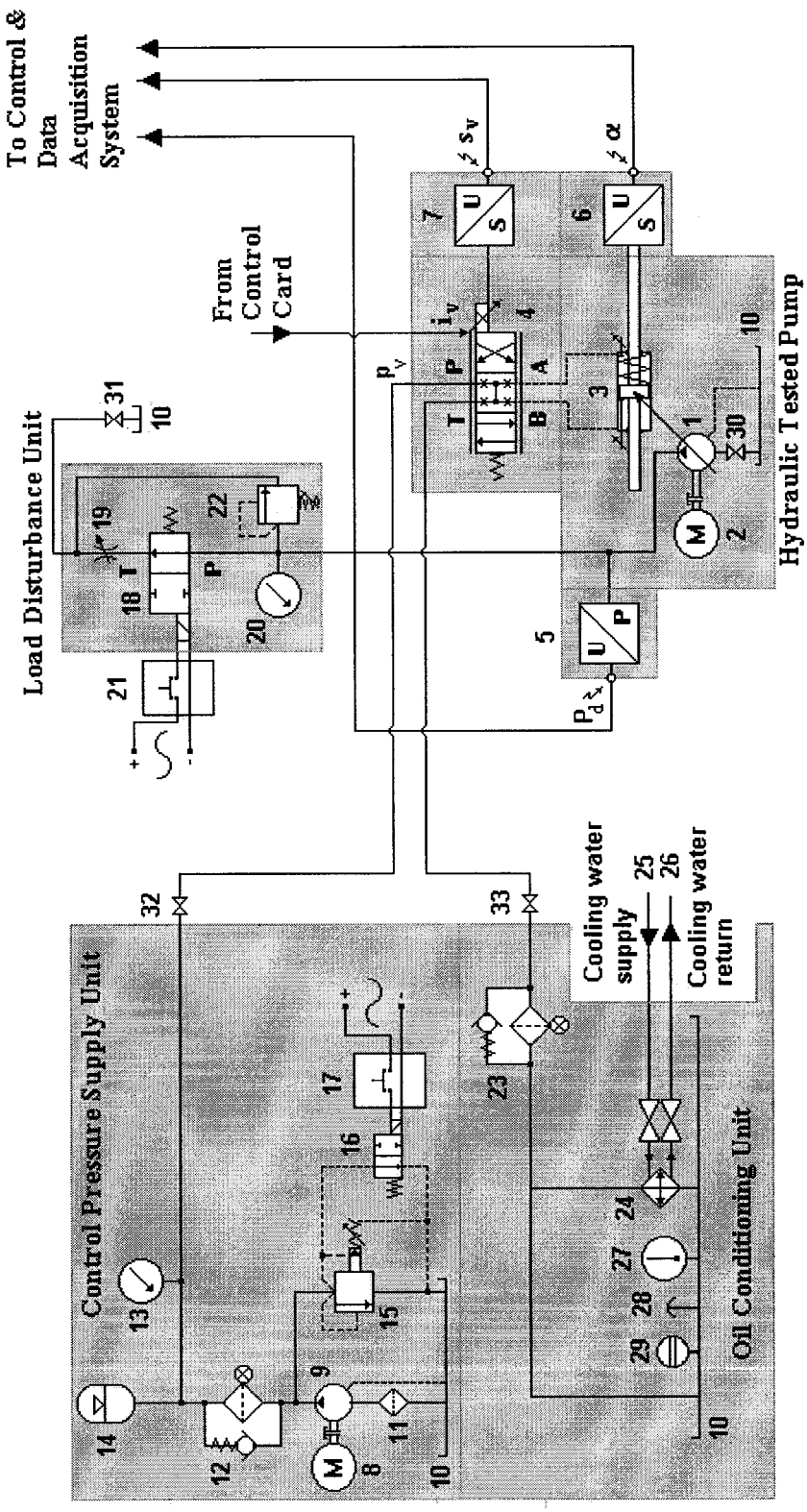

Fig.6.1 Hydraulic test bed

6.1.1 Hydraulic Pump Unit

As shown in Fig.6.1, the hydraulic pump unit consists mainly of the test pump (1); a 9 piston pump of a 40cc/rev geometrical size that has a conical cylinder block. The construction and design parameters of the pump are presented in Appendix 2. The test pump is shown in Fig. 6.2 [69].

The test pump is coupled to 7.5 kW electric motor (2) and uses a flexible coupling to absorb any axial and/or lateral vibration between the connected shafts. The swash plate is rigidly connected to a built in symmetrical hydraulic cylinder (3), which drives the swash plate to change its inclination angle. The position of the symmetrical hydraulic cylinder piston (3) is controlled by means of a hydraulic proportional valve (4) integrated with the pump.

The hydraulic proportional valve is supplied with control pressure p_v from the control pressure supply unit. The hydraulic proportional valve also receives the actuating electrical signal i_v from the control and data acquisition system. The tested pump is equipped with three transducers; a pressure transducer (5) that senses the pump delivery pressure, and LVDT position transducers (6) and (7) that sense the swash plate position and the proportional valve spool displacement. These transducers produce voltage signals proportional to the measured variables. The output signals are fed back into the control and data acquisition system.

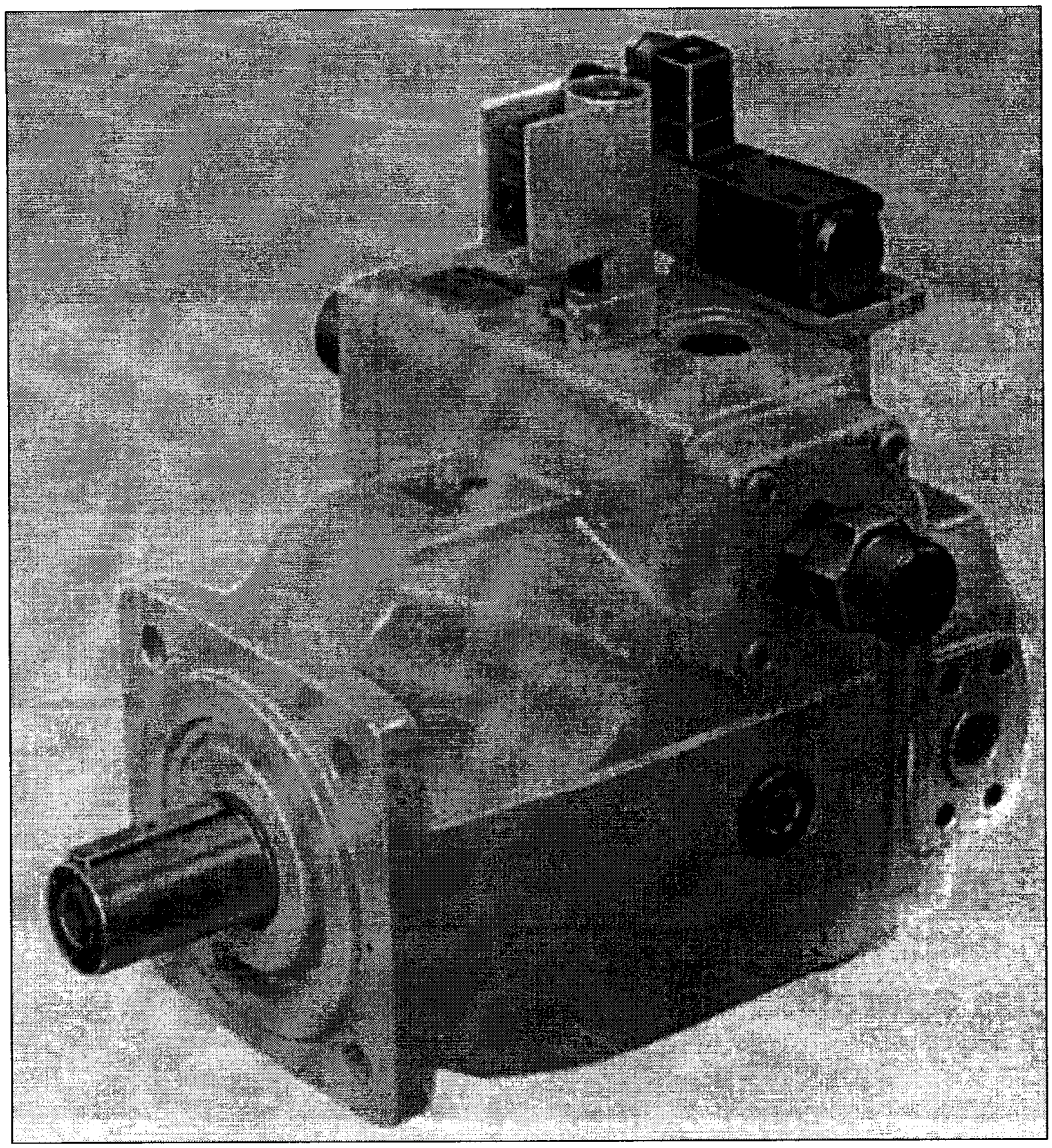

Fig.6.2 Outer shape of the test pump [69]

6.1.2 Control Pressure Supply Unit

The control pressure unit supplies the control pressure to the hydraulic proportional valve. In earlier designs, the control pressure was taken as a branch from the pump delivery pressure. However, a separate constant control pressure supply would help to avoid the frequent changes in the pump delivery pressure on the control process, particularly when using reduced system loads. The external control pressure supply unit consists of an electric motor (8) of suitable output power coupled with the control pressure pump (9) that allows for a pressure of up to 15 MP_a. The control pressure pump draws fluid from the main reservoir (10) via a 100 μm mesh size strainer (11). In view of the high sensitivity of the test pump to contamination of hydraulic fluid, the control pressure pump is equipped with a pressure line filter (12) of a proper flow capacity and a 5 μm size mesh. Control pressure is measured using the dial pressure gauge (13). The control pressure supply line is connected parallel to an accumulator (14) in order to absorb the possible variation of pressure and to keep it constant. The control pressure pump is protected against overload by a pilot operated pressure relief valve (15), which should be connected parallel to the main supply line as close to the pump exit as possible. The pressure relief valve is integrated with an unloading valve (16) in order to remotely apply or release control pressure. The unloading valve initially connects the pilot line to the tank so that the control pressure pump is initially unloaded. When the push button (17) is down, the spool of the unloading valve moves against the side spring to close the pilot line and apply the control pressure. When the push button is released, the spring returns the unloading valve to its initially open position and consequently the control pressure pump is once again unloaded.

6.1.3 Load Disturbance Unit

The load disturbance unit is built to simulate different modes of change in external load pressure. The unit consists of a 2/2 hydraulic directional loading valve (18) that initially connects the test pump supply line to the tank via a throttle valve (19). The throttle valve is used to adjust the test pump loading pressure p_d to a certain value that can be measured by the dial gauge (20).

When the push button (21) is down, the spool of the loading valve moves against the side spring, thereby closing the current connection of the pump with the tank line. Consequently, the tested pump is suddenly subjected to maximum pressure adjusted by the pressure relief valve (22), while the swash plate is driven from its current position to the position of the minimum inclination angle. When the push button is released, the spring returns the loading valve to its initial position. As a result, the loading pressure is reduced to the value that was adjusted to before by the throttle valve. The swash plate inclination angle is then suddenly returned to its previous values. Such a mode of the load disturbance simulates the stepwise change in the load pressure.

Measuring a pump performance while it is in constant power operation requires a gradual change of load pressure. For this purpose, the hydraulic directional loading valve (18) is left in its initial position connecting the test pump with the tank via the throttle valve (19). The throttle valve in this case could be used manually to change the load pressure gradually.

6.1.4 Oil Conditioning Unit

The oil-conditioning unit maintains the hydraulic fluid conditions as recommended by the pump specifications. The important oil conditions, monitored in most hydraulic control systems, are the class of oil cleanliness and the oil temperature. The oil is kept clean by using an online return filter (23) in the direction of the control pressure return line. A water oil cooler (24) is connected parallel to the main return line after the return filter in order to partially cool the return oil and keep its temperature within a 55° to 60°C range as recommended. The oil cooler is positioned in the direction of the return oil after the filter, primarily for the following two reasons: (i) filtration and capturing the contaminants from hot oil is easier than capturing from cold oil (ii) clean oil inside the filter ensures an efficient cooling process. The cooler is connected to the cooling water supply and returned via the shutoff valves (25) and (26)

The oil tank (10) has a significant role in performing oil conditioning. In order to have better heat radiation, some design aspects for the oil tank internal space should be considered and the outside dimensions should be properly calculated. The oil tank is equipped with some necessary accessories. A thermometer (27) is used for measuring oil temperature, an air breather (28) works to guarantee clean breathing, and an oil level indicator (29) is used to measure the quantity of oil in the tank. The test pump suction and return lines are connected to the oil tank via shutoff valves (30) and (31), respectively. Also, the control pressure supply and return lines are connected to the oil tank via shutoff valves (32) and (33), respectively. These valves are considered in the hydraulic circuit design in order to facilitate disconnection of the different units from the tank without the need to empty the tank.

6.2 Description of the Control and Data Acquisition System

The pump is currently supplied with an electronic control card denoted in the text by card (A). Fig. 6.3 shows how the pump is connected to card (A).

Figure 6.3 also shows the basic contents of the amplifier card (A). It contains the arithmetic logic unit, the swash plate controller of the PD type, and the proportional valve spool displacement controller of the PID type; all are physically built onto the card. The contents of card (A) form the double negative feedback loop for the hybrid control of the pump performance. The card is used physically with an analogue and/or digital setting unit for parameterization of the pump static characteristic limits, which are the maximum pressure, the maximum flow rate and the maximum power. Measuring sockets are found in the front panel of card (A) and they are used for measuring pump pressure and flow rate. Card (A)'s power is supplied by a 24 DC voltage.

For testing purposes, control and data acquisition systems are constructed and are composed of software and hardware parts. During the test, the basic contents of the original amplifier card (A) are not used, and card (A) is used only to transfer the knowledge from the sensors to the I/O card.

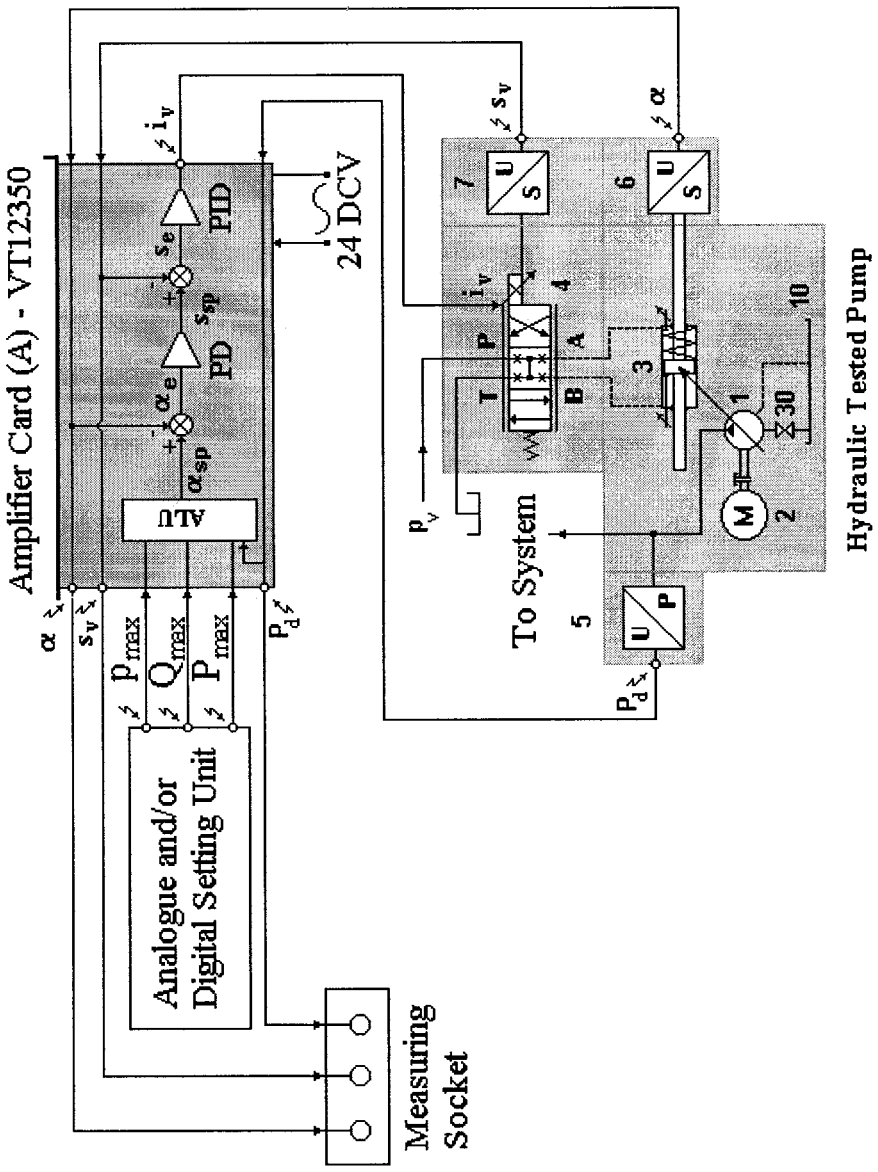

Fig.6.3 The test pump connection configuration with the original amplifier card (A)

6.2.1 Real Time Control and Data Acquisition Software

Real time control software is built based on the Matlab-RT workshop to replace the physical contents built on card (A). Using such real time control software facilitates parameterization of the pump controllers, prototyping the new proposed fuzzy controller, and constructing the newly proposed control schemes.

Figure 6.4 illustrates the double feedback control loop schemes with either a PD or fuzzy controller. The figure shows that the real time control software includes a unit for monitoring and for data acquisition. It also contains an arithmetic logic unit for setting the pump static characteristic limits that should be respected by the control scheme. The first limit is on the power P_{max}, which should not be exceeded by the pump. The second limit is the maximum pressure p_{max} after which the pump controller should drive the pump to the minimum discharge position. The third limit is the maximum pump flow rate Q_{max}. Based on the value of actual pump pressure fed back to the arithmetic logic unit, the latter calculates the corresponding pump flow rate in order to achieve constant power operation with the static characteristic limits respected.

The calculated pump flow rate is then represented by the set point value of the swash plate inclination angle α_{sp}. The swash plate inclination angle set point value is compared to the actual inclination angle. The error value α_e is fed to the swash plate PD or fuzzy controller. Consequently, the swash plate controller produces another set point value s_{sp} for the position of the hydraulic proportional valve spool. The spool position set point value is compared to the actual value of s_v. The resulting error value

s_e is fed to the spool position PID controller that eventually produces the control current signal i_v that is sent to the proportional solenoid. The control scheme is designed to respect the pressure and flow rate preset limits when they are reached, regardless of power.

Figure 6.5 illustrates the control scheme in which a single feedback control loop is implemented. In this scheme, the PD controller receives an error in the swiveling angle α_e and then directly produces the control current in digital form $i_v(D)$ that is submitted to the I/O. The hydraulic proportional valve sensor is kept for monitoring spool displacement during this control process.

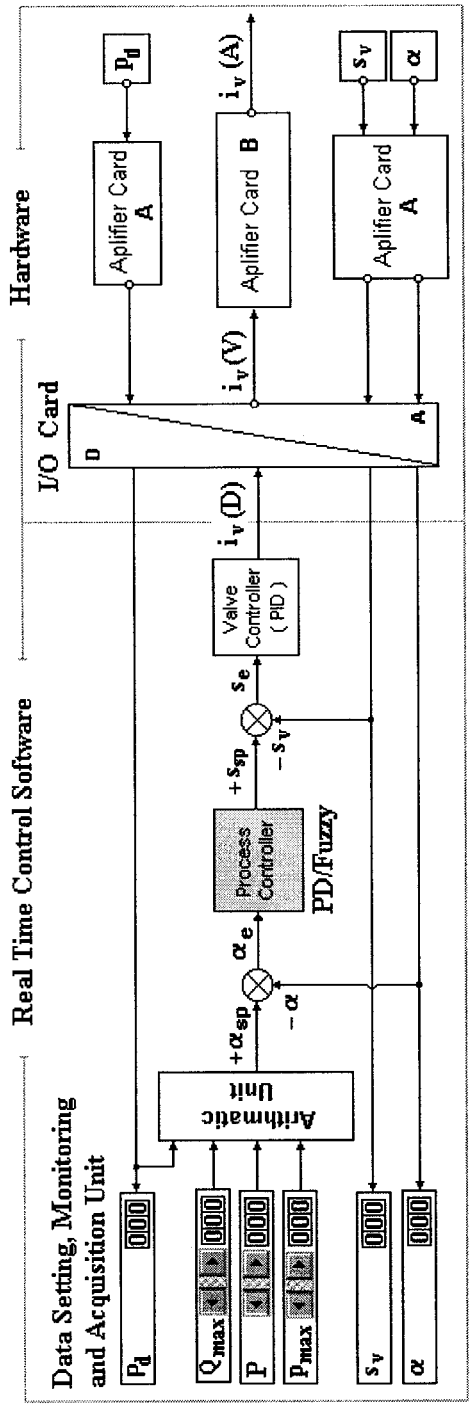

Fig.6.4 Block diagram of control and data acquisition system

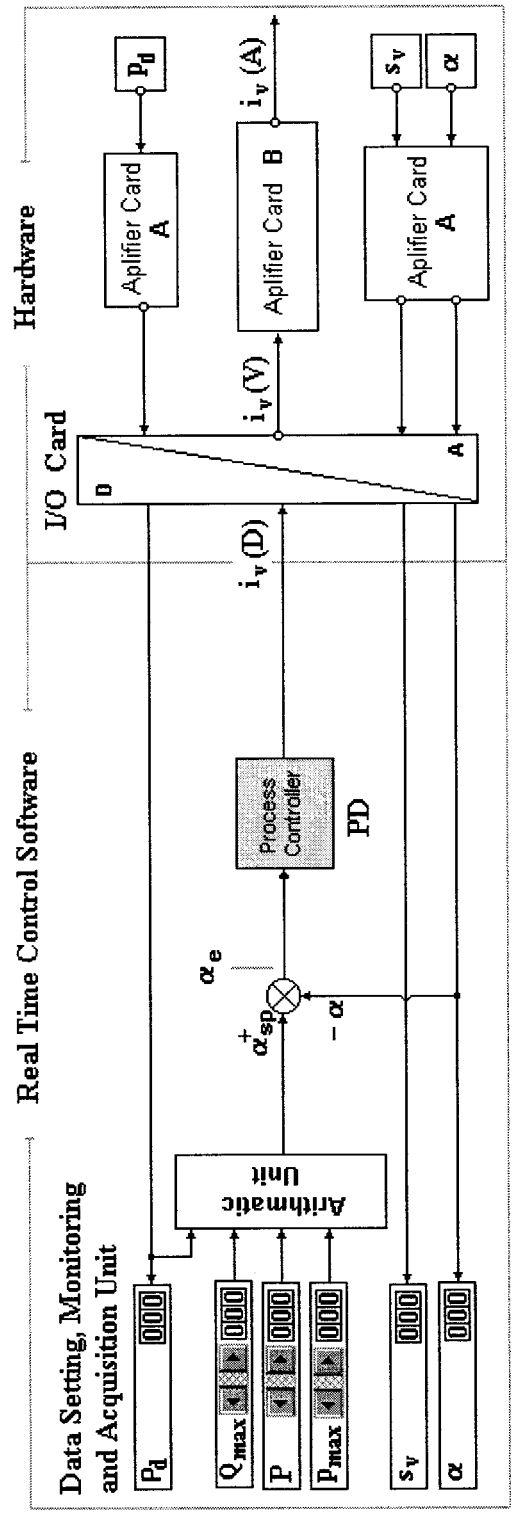

Fig.6.5 Block diagram of control and data acquisition system

6.2.2 Hardware Part of the Control and Data Acquisition System

Figure 6.4 also shows that the hardware is composed of an I/O card and a locally developed amplifier card denoted in the text as amplifier card (B). The I/O card is used to interface the real time control software with the amplifier cards. Only standard I/O interface cards that are adaptable to Matlab-RT can be used. It should have at least three digital input channels and one analogue output channel.

Information from the hydraulic test bed is transmitted to the real time control software through the analogue input channels on the I/O card via the card (A). Consequently, it is converted into digital form and received by the real time control software that generates the corresponding control signal in the digital form $i_v(D)$. The latter is converted into analogue form and transmitted out of the computer in analogue voltage form $i_v(V)$ through the output channel in the I/O card. The amplifier card (B) has no role but to convert the control signal from analogue voltage form into analogue current form $i_v(A)$ with enough power to drive the proportional hydraulic valve solenoid.

Three analogue input channels and one analogue output channels are implemented on the I/O card. The maximum sampling rate available the I/O card used is one sample per millisecond. The dynamic response of the system shows that the pump and control valve time constant, in the most responsive case, is 60 ms. From time domain point of view, sampling rate used is fair enough to track the system dynamics. From frequency point of view, the pump is driven close to 1500 rpm, i.e. 25 Hz. Hence, every one

complete pump cycle is measured by 40 samples. Any periodic change of frequency up to 250 Hz, within one pump complete cycle, could be also fairly represented.

6.3 Test Preparations and Calibrations

In the following, the installation instructions for the setup and the steps that should be taken to integrate its different components are described. Figure 6.6 shows the symbolic presentation of the experimental setup as completely integrated and with the different units connected to each other. The figure illustrates the double feedback control loop. When using a single feedback control loop, it will have the same connection configuration as the rest of the system.

The schematic layout and photographic view of the experimental setup are shown in Figs 6.7 and 6.8, respectively. It must be noted that the component numbering system used in Figs 6.6 and 6.7 are the same. It is important now to check the proper functionality of each part of the setup to facilitate the diagnosis of any malfunctions in the setup. Therefore, in the following sections, a step-by-step explanation for the setup integration, pretests and calibrations are presented.

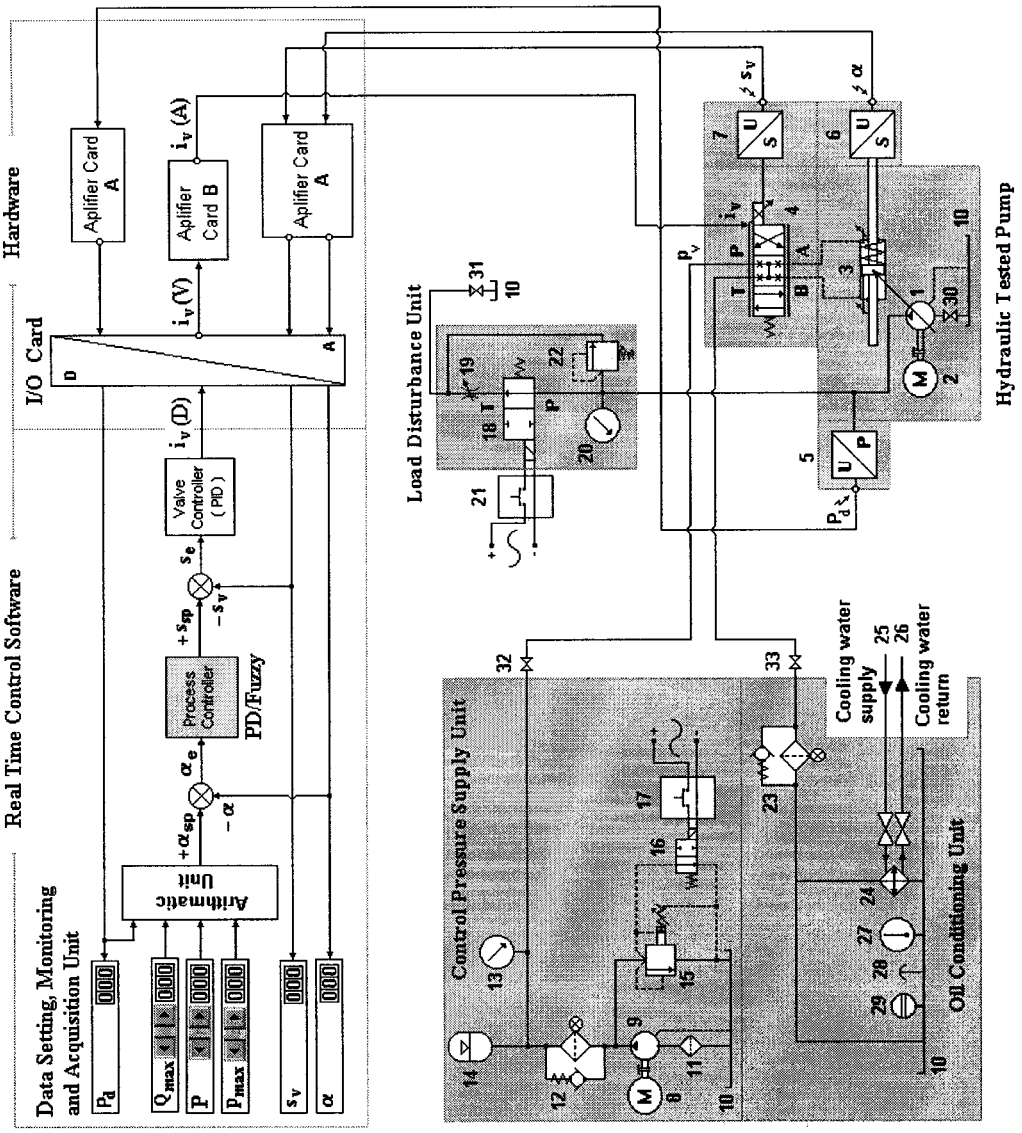

Fig.6.6 Block diagram of the integrated experimental setup

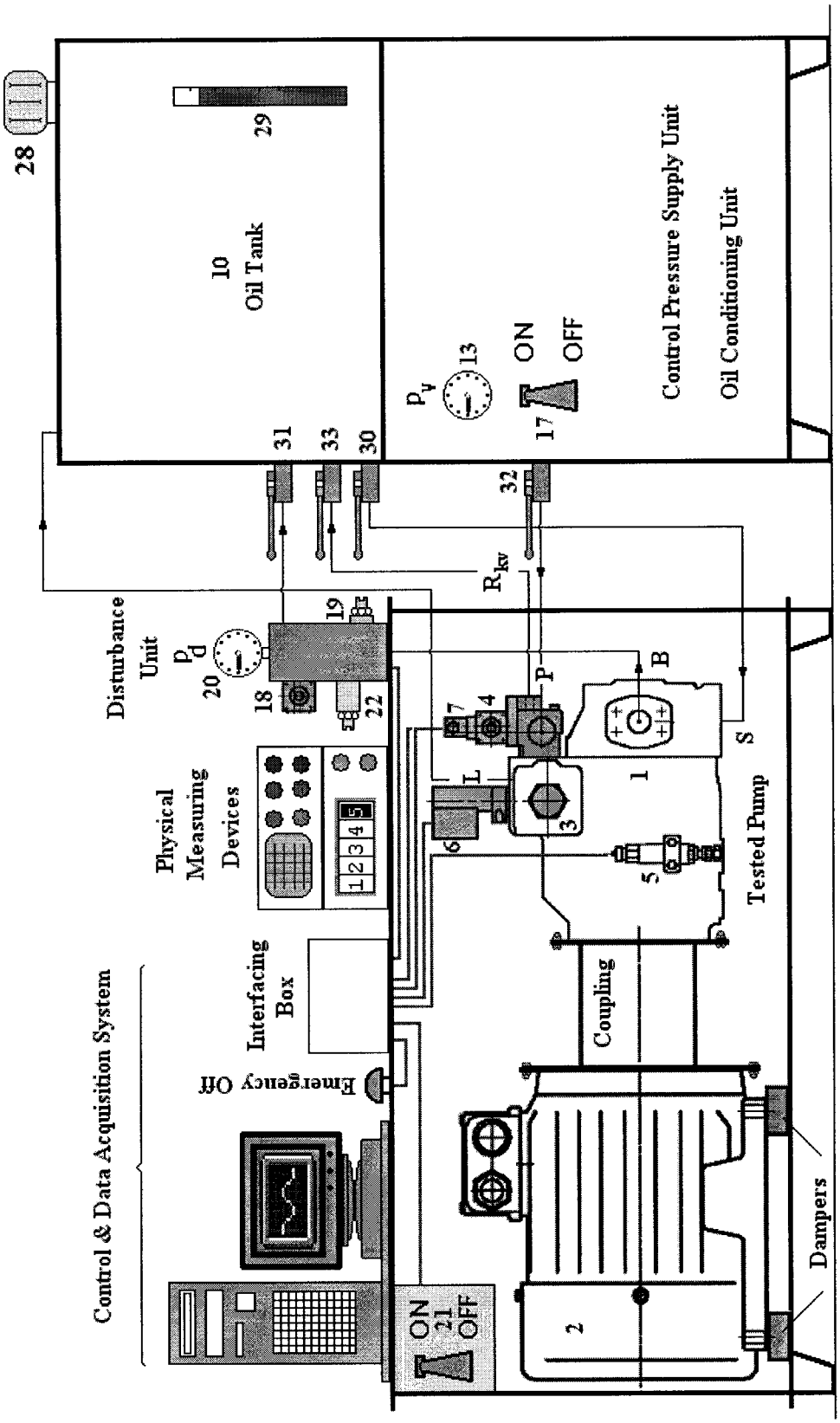

Fig.6.7 Schematic layout of the integrated experimental setup

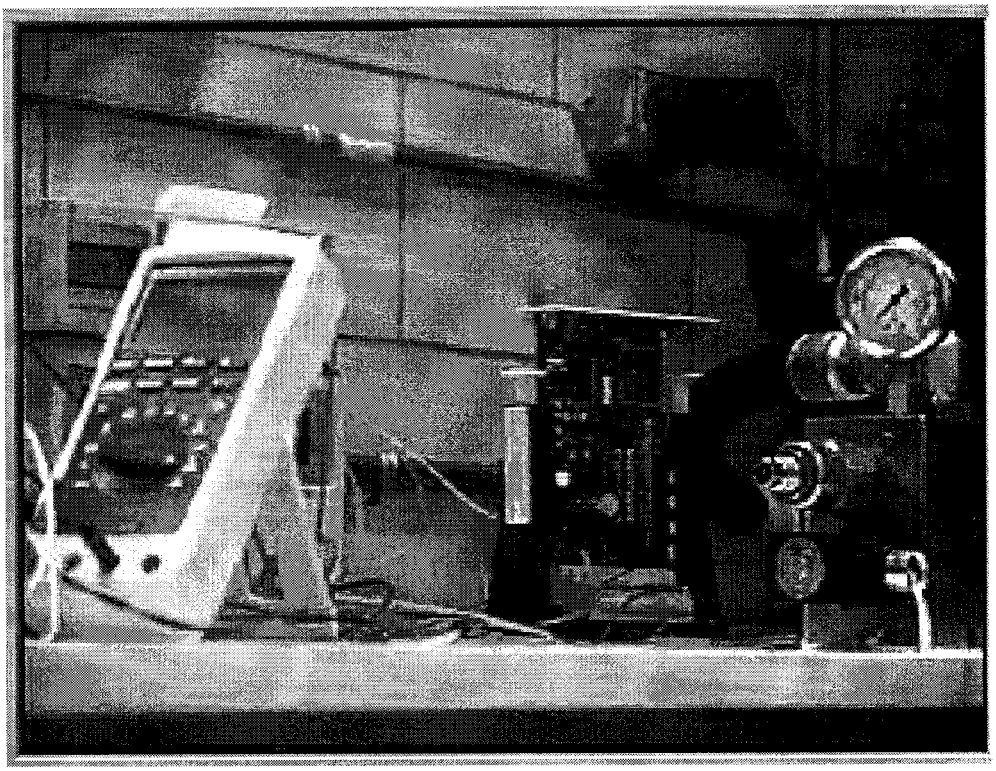

a- A view of the pump loading unit and real time controller interface

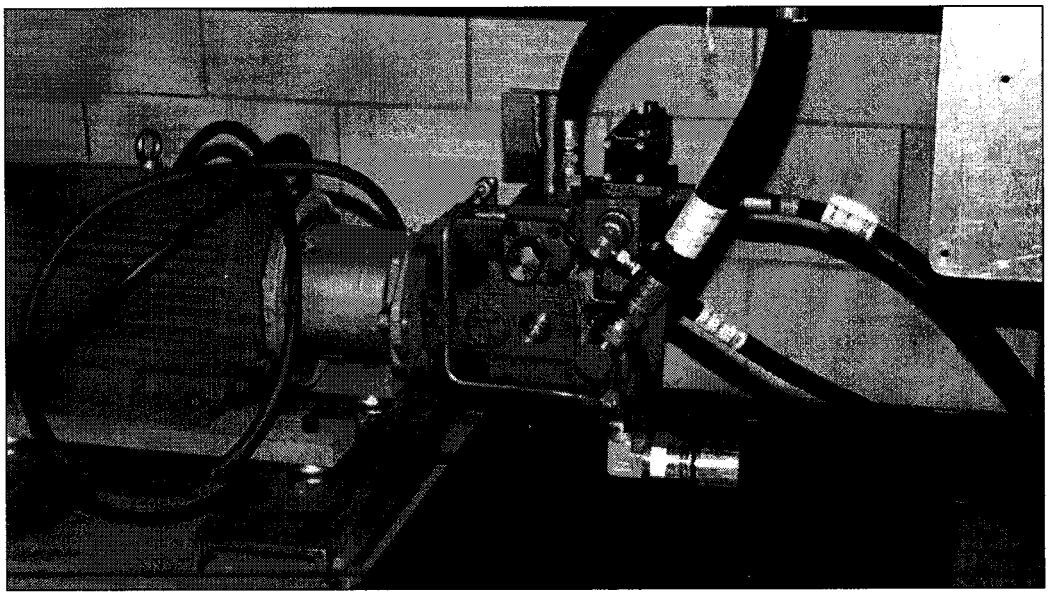

b- A view of the pump with the integrated control unit and set of sensors

Fig.6.8 Photographic views of the experimental setup

6.3.1 Integration of the Hydraulic Test Bed

A well organized presentation for the test ensures accurate and trustworthy results. In the following steps, instructions for the integration of the test setup are given.

(i) Preparing the Hydraulic Fluid Used in the Test: The hydraulic oil cleanliness class must be at an appropriate level. In the case of axial piston pumps, class 6 is fairly acceptable [64, 65]. This class specifies, according to standard code NAS 1638, the upper limit of contamination of the oil used with such pumps and control components. In this regard, samples of the used oil are tested using the electronic particle counter. The oil tank is cleaned and thoroughly flushed, and then filled with the specified oil up to the maximum oil level mark. All types of hydraulic fluid of a petroleum base are suitable for providing the recommended oil viscosity.

(ii) Integrating the Pump with the Drive Motor: As shown in Fig. 6.6, the pump is coupled with the drive motor and mounted on the lower level of a table. The motor is bolted over two pairs of dampers to absorb the vibration coming out of the pump and the motor. A coupling between the drive motor and pump is correctly assembled and aligned.

(iii) Fixing the Disturbance Unit: Elements of the disturbance unit are initially cleaned by compressed air and then integrated in one manifold block which is fixed on the upper level of the table, as shown schematically in Fig. 6.7.

(iv) Pipelines Work: Cleaning the pipes with compressed air is highly recommended. Also, the pipes should be color coded in order to avoid confusion. The diameter of the pipelines should not be less than the corresponding port dimension at the pump. As presented in [69] and shown in Fig. 5.7, the pump ports are defined as follows: "S" for suction port, "B" for pressure port, "L" for case drain port, "P" for the control pressure supply port, and "R_{kv}" for the control pressure return port. The pipelines are then connected and correctly arranged to be free of tension and excessive bending. In open hydraulic circuits, this type of pump can be used with a suction pressure ranging from a –0.8 bar gauge pressure up to a 30 bar posting pressure. As shown in Figs 6.7 and 6.8, the pump is mounted where suction port "S" is lower than the free surface of the oil in the tank by approximately half a meter head, which is considered in the pump mathematical model by 0.5 bar posted suction pressure. Pressure port "B" is connected to the disturbance unit inlet. There are different drain ports "L" in the pump; the selected port in any pump installation position should be the highest one and the others should be plugged. The drain line is connected directly to the oil tank below oil level to avoid generating oil turbulence. Both the control pressure and return line are connected to the pump ports "P" and "R_{kv}", respectively, with the general recommendations observed.

(v) System Air Bleeding: In order to avoid air pockets during the first run of the system, the air in the system must be bled. The pump housing is to be filled with oil. For a pump positioned horizontally as shown schematically in Fig. 6.7, the pump case filling is done from the upper port (drain port "L"). Filters, heat exchangers and suction lines are to be filled with oil also.

(vi) Control Pressure Supply Unit and Oil Conditioning Unit: These units must be prepared to function properly. Accumulator charging pressure is to be reviewed and control pressure is to be adjusted. The cooling water supply and return lines are to be connected as shown in Fig.6.5.

(vii) Electrical Power Connections: Connect the electrical power supply to the drive motor, "Emergency Off" button, directional valve in the disturbance unit and the control pressure supply unit. Before carrying out any functional testing, the "Emergency Off" button must be tested to ensure its proper functioning.

(viii) Testing the Correct Direction of Rotation of the Drive Motor: This is an important step in order to avoid pump cavitation and occasional failure if the motor is improperly rotated. The letter "R" in the ordering code of such pumps designates that the pump direction of rotation is to the right. This conventionally means that when one looks at the pump from the side of the drive shaft, i.e. from the drive motor fan side, the fan should rotate clockwise. Before testing, valves 19, 22, 30 and 31 should be fully open. Switching the pump ON without a load for a very short time verifies the direction of rotation.

6.3.2 Interfacing with the Control and Data Acquisition System

In this step, both the real time control software and I/O card must be tested for proper functioning. In this regard, as shown in Appendix 6, module 1, three physical function generators and one oscilloscope are used. The function generators are connected to the analogue input channels on the I/O card to simulate the information coming from

the sensors. The oscilloscope is connected to the analogue output channels on the I/O card. The function generators are adjusted to generate three different signals. Real time control software is built to read from the function generators through the I/O card, and then outputs one of the incoming signals outside to be read again by the oscilloscope. The proper functionality of the I/O card and the real time control software is tested for an error free connection with the outside world, and proper phase shifting based on the coincidence between the output of the physical devices and the readings of the real time control software.

6.3.3 Calibrations and Pretests

(i) Configuration of Amplifier Card (B): Real time control software, shown in Appendix 6, module 2, is designed to interface with card (B) in order to test its proper functioning and to recognize its static characteristic features before implementing it in pump testing. Card (B) is initially connected to the I/O card. The software is designed to produce a digital signal, from 0 to10 V, simulating the control signal which is converted by the I/O card into an analogue voltage form. Through the I/O card, the digital signal is converted into analogue voltage form and output to card (B), which produces the corresponding current form of the signal from 0 to 3. A physical conditioner is used to convert the output signal of card (B) into voltage form to be read by the I/O card. The accompanying real time software reads the output signal of card (B) through the I/O card again. The input-output relation of card (B) is recorded. As shown in Fig. 6.9, it was found to be perfectly linear which means that the card was properly designed and parameterized to perform its function.

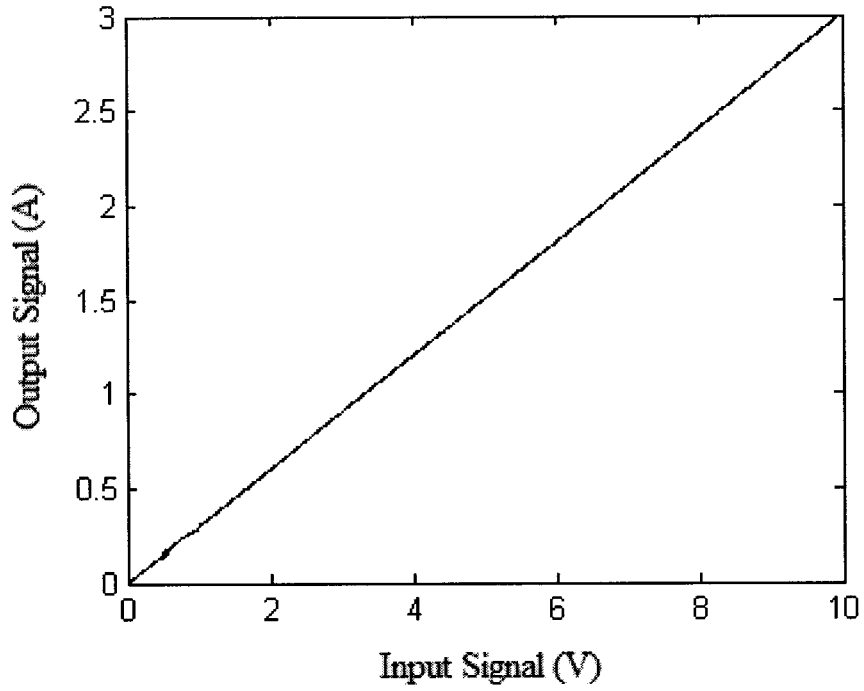

Fig.6.9 Input-Output relation of the card (B)

(ii) Calibration and Conditioning of the Hydraulic Proportional Valve: In this step, the proportional valve spool displacement is to be calibrated in an open loop. A new real time control software module, shown in Appendix 6, module 3, is designed to produce a reference signal from zero to 10 Volts, and to read the corresponding amount of spool displacement. In this step, the output signal of the amplifier card (B) is connected to the proportional solenoid, while the sensor of the proportional valve spool displacement is connected to amplifier card (A), and then this is connected to the I/O. Software conditioning of the input and output signal is being used to remove the saturation parts of the valve response. A normalized Input-Output relation represents the proportional valve static characteristics, which is then measured and compared with the simulated results shown earlier in Fig. 5.11. The results are presented in Fig. 6.10. The maximum deviation was found to be 7%. The non-

linearity arises due to the electro-magnetic characteristics of the proportional solenoid is not considered in the valve modeling.

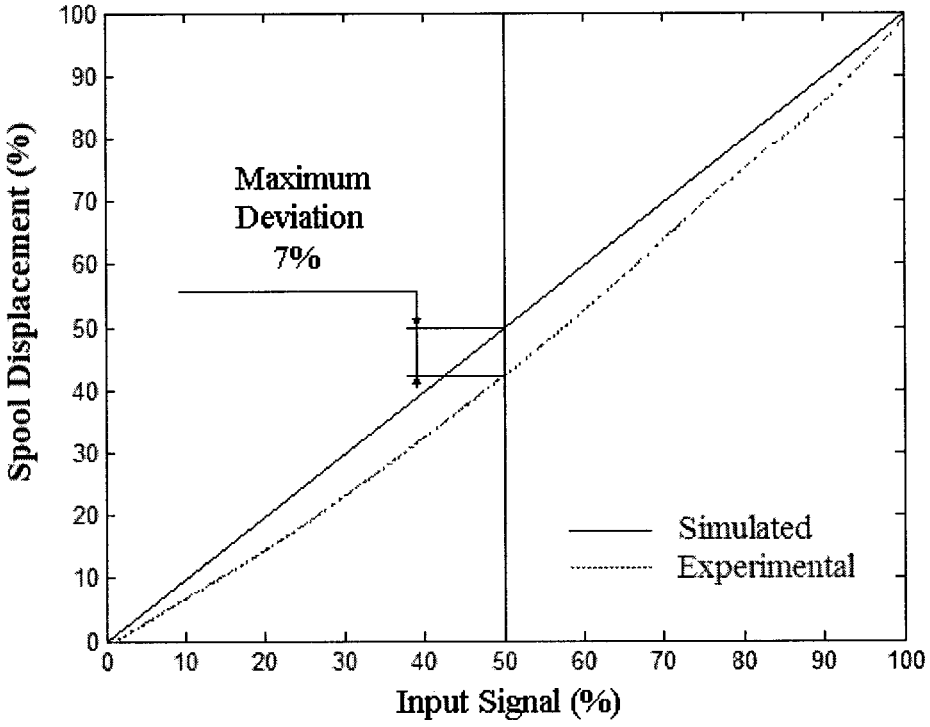

Fig.6.10 Measuring of open loop static characteristics of the proportional valve

(iii) Establishing the Closed Control Loop for the Proportional Valve: In this step, as shown in Appendix 6, module 4, the real time control software is further developed to implement a closed control loop to control the position of the proportional valve spool. The software is designed to produce a step input signal in the same procedure followed in the simulation process discussed in chapter 5, section 5.3. The following test could be done with a dry valve without supplying control pressure. However, it is recommended that control pressure be supplied to the valve in order to include its effect on valve dynamics. Therefore, as shown in Fig.6.7, shuttle valves 32 and 33 should be fully opened before switching button 17 to the ON position to ensure that there is no leakage in the control pressure lines. The valve response to step inputs is then measured and recorded. Figure 6.11 shows global agreement between the simulated and measured step response of the valve during a 9 second time span. Figures 6.12 and 6.13 show an enlarged view of the measured valve step responses as compared with the simulation results when the spool moves from the zero position to a certain percentage of its full stroke and vise versa. A comparison of the results with those obtained from the simplified valve model shows qualitative agreement in the transient response period and good agreement in the steady state based on nearly equal settling time.

The same module is used for measuring the closed loop static characteristics of the proportional valve. Step inputs are replaced by a normalized reference input signal that changes slowly and gradually from zero to 100%. The corresponding normalized spool displacement is recorded. Figure 6.14 shows acceptable agreement between the results and exhibits perfect linearity along the whole range of the input signal.

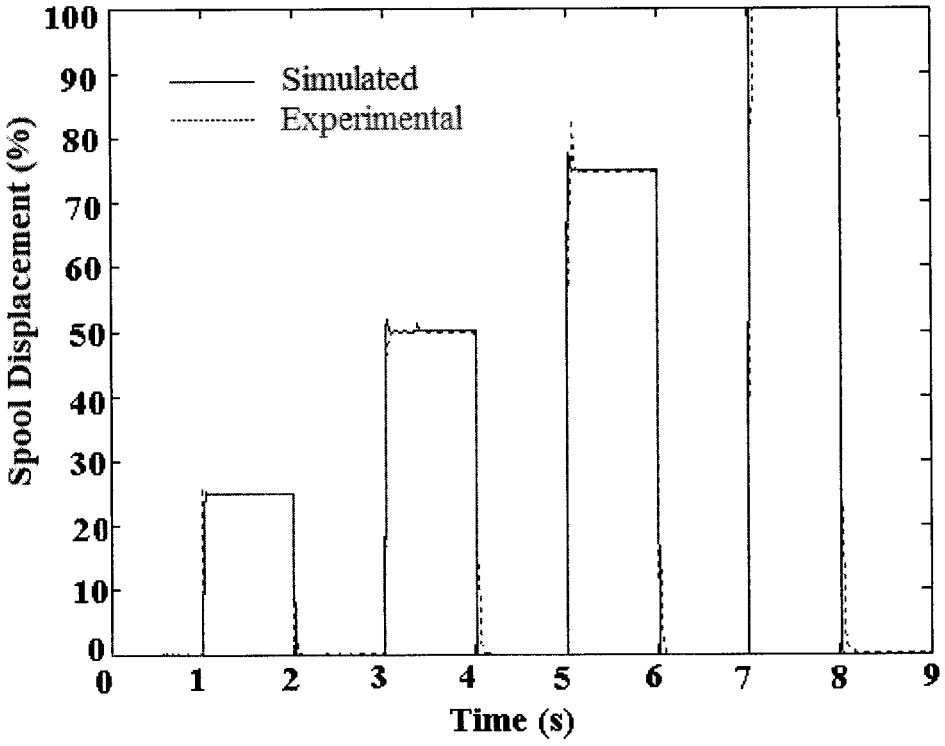

Fig.6.11 Measurement of the step response of the proportional valve

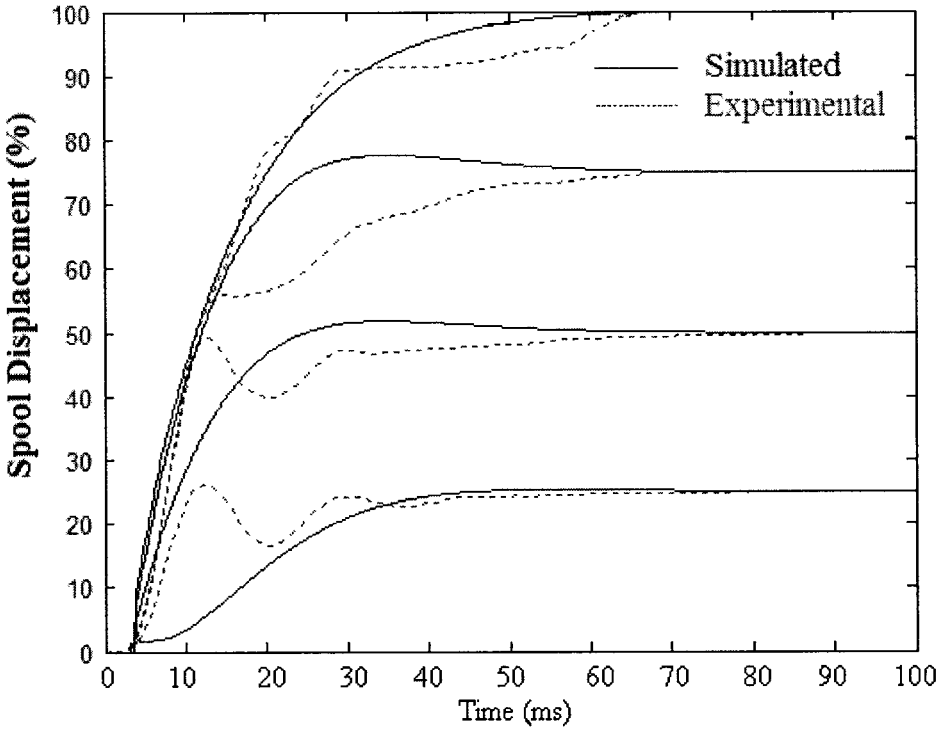

Fig.6.12 Measurement of the step response of the valve when the spool moves from zero position to a different percentage of its full stroke

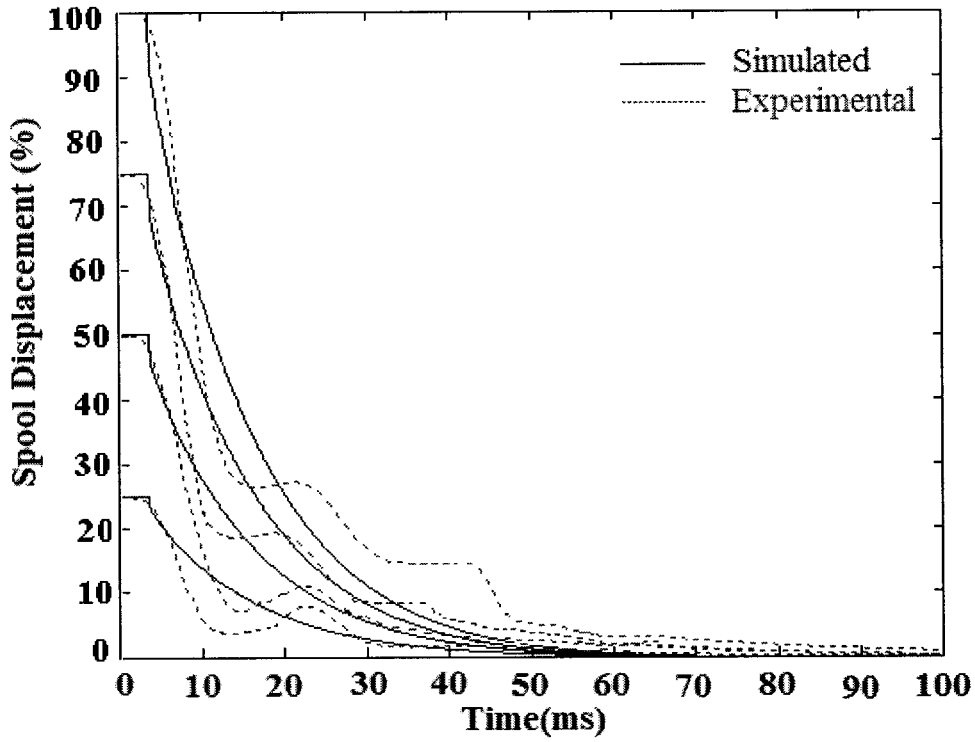

Fig.6.13 Measurement of the step response of the valve when the spool moves from different percentage of its full stroke to the zero position

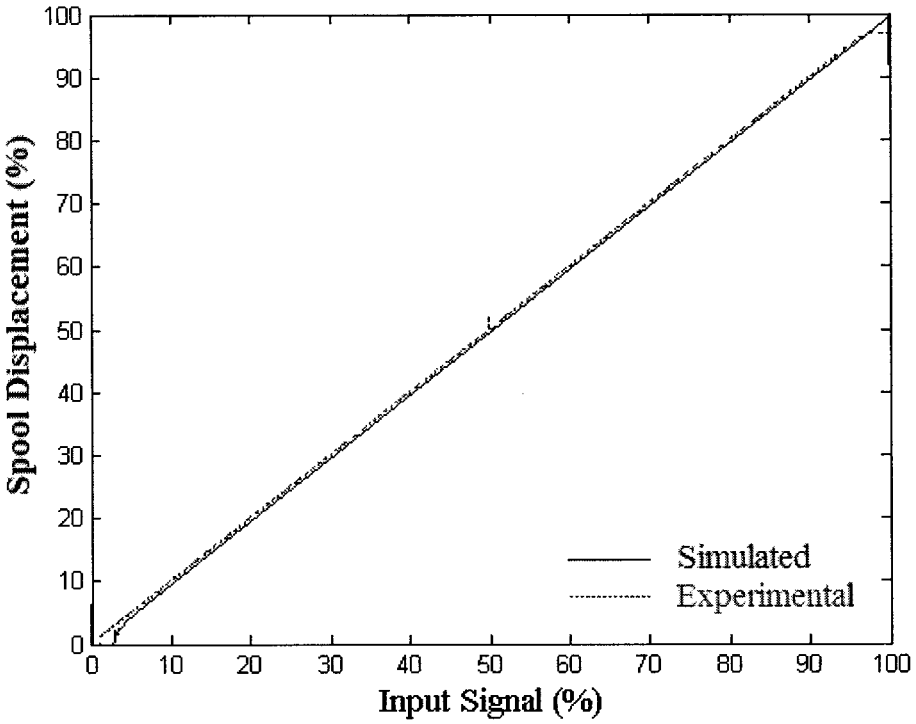

Fig.6.14 Measurement of the closed loop static characteristics of the proportional valve

(iv) Calibrating and Conditioning the Swiveling Angle Sensor: In this step, the voltage reading of the swiveling angle sensor is to be calibrated to the corresponding physical value of the swiveling angle. Finding the actual zero point of the proportional valve at which the swash plate is held at its current position is important for building control schemes.

The control supply pressure should be first adjusted and connected to the proportional valve for driving the swash plate. Module 5 shown in Appendix 6 is constructed to perform this function. A reference signal of a zero value is fed to the proportional valve. In this situation, the swash plate is driven to the position of the minimum inclination angle by the control pressure directed to one side of the control piston. The corresponding swiveling angle read by the swiveling angle sensor is recorded. A reference input signal sent to the proportional valve is increased smoothly while observing the swiveling angle. At the point where the swiveling angle starts to move, the value of the reference signal to the proportional valve represents its zero value. At this value of the reference signal, the valve spool is in the middle of its stroke and is in the steady state position of the valve during pump control. In the absence of the pump controller, any further increase in the reference signal to the proportional valve will completely drive the swash plate to the position of the maximum inclination angle. The corresponding swiveling angle read by the swiveling angle sensor is also recorded. Software conditioning for the swiveling angle signal read by its sensor is needed to match the range 0-10 Volts read by the sensor, to the 0-15 degrees that represent the actual value.

(v) Prototyping the first control scheme: Matlab real time workshop is used to construct the first control scheme, in which double negative feedback control loop with a PD pump controller is used. Module 6 in Appendix 6 shows further development of the real time control software to establish the double feedback control scheme. Without the pump running, the control pressure is supplied to the proportional valve and then some experimental trials were carried out to ensure proper control of the swash plate swiveling angle.

(vi) Testing the Pump Idle Running: During this step the pump will be tested for proper running under no-load. The safety of the operator is the highest priority. Therefore, the emergency button, shown in Fig.6.7, must be tested for proper functioning. The emergency stop button is designed to stop the pump and the control pressure supply pump when it is depressed. It is also essential to ensure that the electrical connections are properly connected and insulated.

For the safety of the pump, a review of some safety considerations of Fig.6.6 and Fig.6.7 should be considered each time before running the pump. The shuttle valves (30) and (31) should be kept open. The two-position button (21) should be kept OFF, by which the hydraulic directional unloading valve is kept in its initial position where it unloads the test pump. Control pressure is supplied to the proportional valve before, in order to ensure that the swash plate is driven to the position of the minimum inclination angle by which the pump provides the minimum volume of oil per unit time, and cooling water is to be supplied at this point. During this step of the test, the pressure relief valve (19) and throttle valve (22) integrated in the loading unit should be kept fully open.

The pump is then turned ON while listening for any unusual noises. The pump should be kept running for at least 15 minutes. For the safety of the testing operation, any leakage, oil volume in the tank, and oil temperature should be monitored from time to time during the test. Using module 6 of the real time control software, the swash plate is controlled to very gradually increase its inclination angle while watching for the increase of the pump discharge and monitoring for the zero load pressure read by the dial gauge (20). If there is a jerky movement of the swash plate, this indicates the presence of some air pockets. Swiveling the swash plate up and down in both directions smoothly may eliminate these air pockets. Some foaming usually appears at the beginning of the running of the pump; however, the foaming should stop at least an hour after start-up.

(vii) Calibration of the Load Pressure: The pump is first switched ON after following all safety considerations mentioned in the previous step. Again, using module 6 of the real time control software, the swash plate is controlled to very gradually increase its inclination angle to the maximum, while monitoring the zero load pressure read by the dial gauge (20). Thereafter, the throttle valve (22) is smoothly and fully closed while monitoring the load pressure read by the dial gauge (20), which should still be zero. In this situation, pump flow now has a single route to the tank through the pressure relief valve (19) that should be fully open. The next activity is the most dangerous one in the test procedure, and therefore needs special vigilance. By closing the pressure relief valve, the load pressure starts to increase very rapidly. Hence it is should be closed very carefully and smoothly while the load pressure is being monitored by the dial gauge (20). The process is continued until the maximum pressure of 15 MPa is reached. The pressure relief valve is then locked at

this position in order to protect the pump physically against any overloading in case of a control malfunction. The physical load pressure read by the dial gauge (20) could be linearly calibrated by reading the pressure sensor (5). The pump now unloaded by opening the throttle valve (22).

(viii) Prototyping the Alternative Control Schemes: The real time control software is used again to construct the alternative control schemes: In Appendix 6, module 7, the fuzzy controller replaces the PD controller with the double negative feedback control loop. The third control scheme, in which a single feedback control loop is implemented, is shown in Appendix 6, module 8.

6.4 Testing of the Pump Performance

The Experimental setup is now complete and ready to measure the pump static and dynamic characteristics with the three proposed control schemes shown before in Figs. 5.1 and 5.2. In this section, the pump mathematical model will be experimentally verified and the pump characteristics, found analytically in Chapter 5, will be validated.

6.4.1 Measurement of the Pump Step Response at Constant Load

Pump step response was simulated earlier in Chapter 5. The simulation program was fed with successive step input command signals equal to 25%, 50%, 75% and 100% of the full range of the swash plate swiveling angle. Each command signal will be reduced to zero in a stepwise manner after reaching the steady state, . The same sense

of input signals is used for measuring the actual step response of the pump. In order to adjust the value of the constant load pressure equal to 10 MPa, the throttle valve (22) in the load disturbance unit should be kept closed, and the pressure relief valve (19) should be used to set the required value of load pressure. The throttle valve is not used to adjust the constant load because the pump flow rate is changing, which means that we would have to change the setting of the throttle valve each time the step input changes. Modules 6, 7 and 8 are used successively to measure the pump step response with the three control schemes.

The first control software module considered in the testing process is the one shown in Appendix 6 Module 6, in which double feedback control loops are used with the PD pump controller. The same PD parameters that resulted from the analytical investigation, K_p=1 and T_d= 0.02, are implemented in the real time control software.

Figure 6.15 illustrates a comparison between the measured and simulated response of the pump to successive step inputs at a constant load pressure and a 9 second time span. The measured response shows that the swash plate follows the successive input signals along the span of testing time very closely. The measured results in [60] confirm the presence of the steady state vibration of the swash plate. This vibration could the effect of the lateral moment acting on the swash plate and the selected PD parameters that leads to a reduced settling time in order to limit power shocks on the prime mover. The measured responses shown in Fig. 6.15 show that the steady state vibration may be different in magnitude and frequency from what is obtained through simulation. This could be fairly justified by the effect of the loading unit, sensor

dynamics and the change in oil parameters during the test, which are not considered in the modeling. However, both results fell within acceptable limits.

Figure 6.16 and 6.17 show an enlarged view of the measured transient periods of the pump response when the swiveling angle increases from the zero position to different percentages of its maximum value and vise versa, as compared to the simulation results. Both cases show a close agreement between the measured and simulated results.

Figure 6.18 shows the measured behavior of the proportional valve spool during the testing of the pump as compared to the simulated one. The figure shows that the measured spool impact on the ends of its stroke is practically less than what is found by simulation. This could be due to the slight difference between the estimated and the actual system parameters such as spring stiffness, damping coefficients, moving masses and the moment of inertia of the rotating masses.

The pump mathematical model is now fairly validated based on the agreement between the simulated and measured response of the pump.

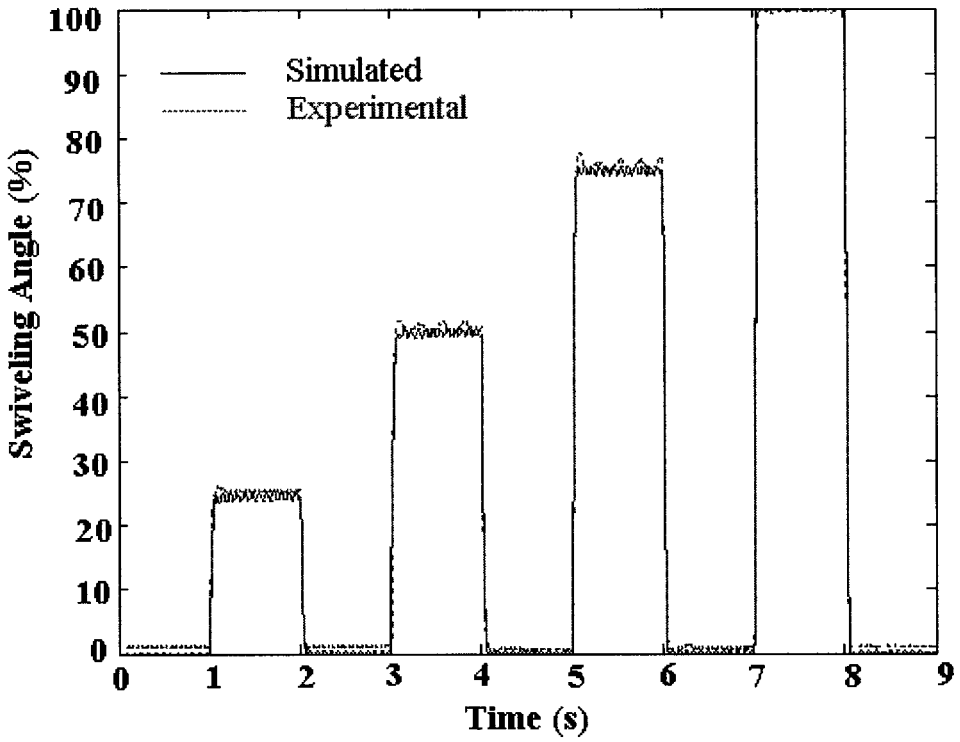

Fig. 6.15 Measured pump step response at constant load pressure using double feedback control loop with PD controller as compared with the simulation results

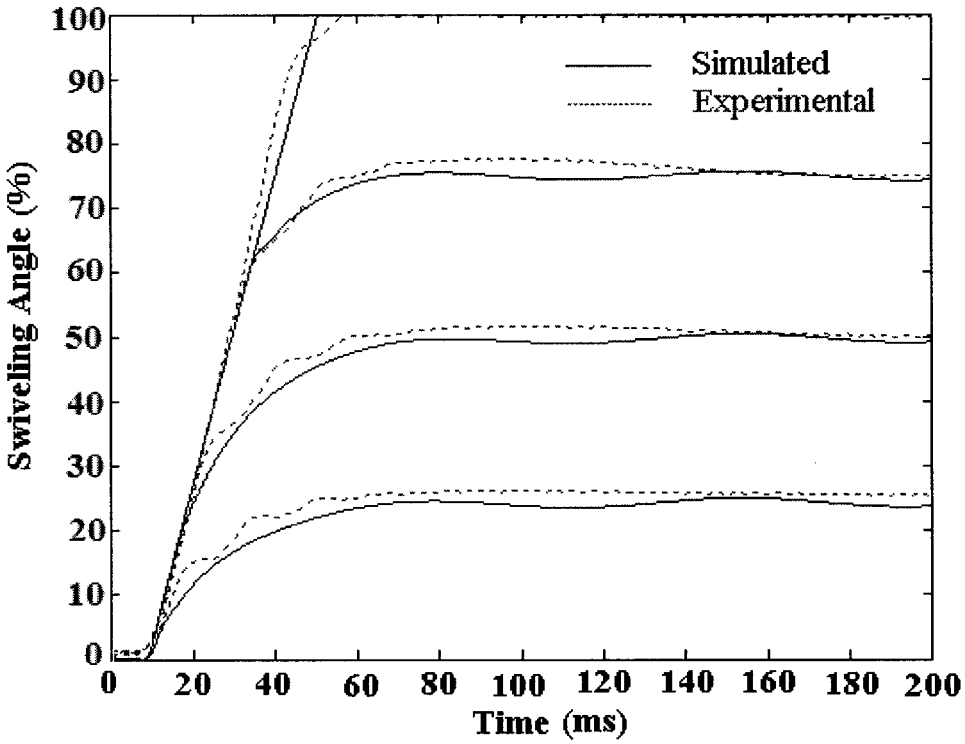

Fig. 6.16 Measured swiveling angle increasing from zero position to different percentages of its maximum value using double feedback control loop with PD controller as compared with the simulation results

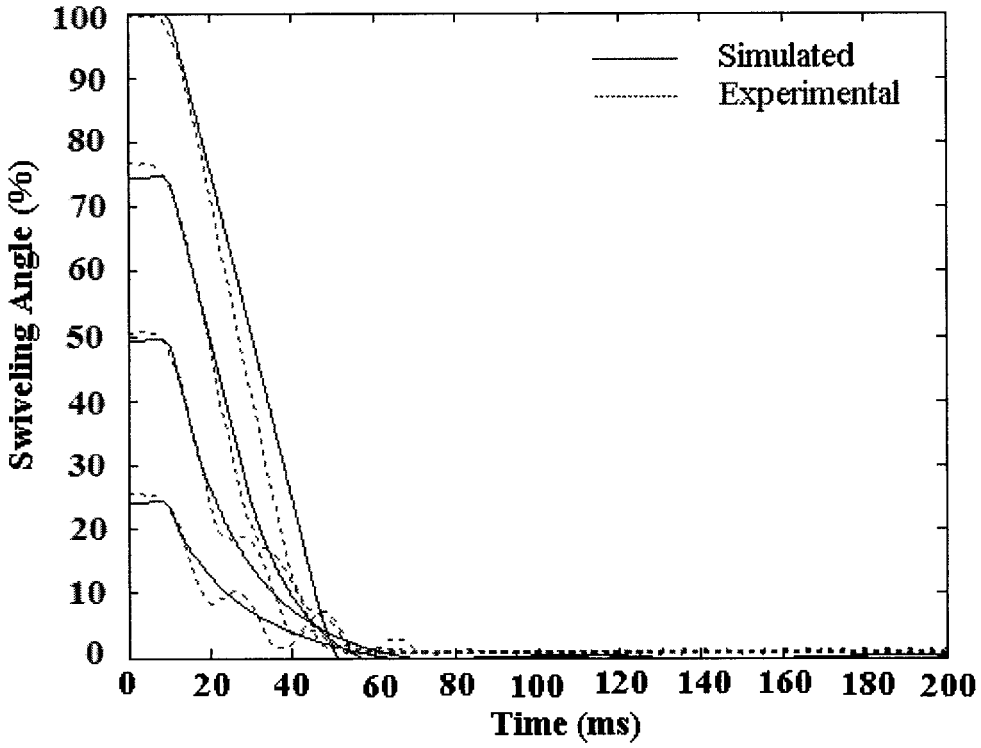

Fig. 6.17 Measured swiveling angle reduction from a position of different percentages of its maximum value to zero position using double feedback control loop with PD controller as compared with the simulation results

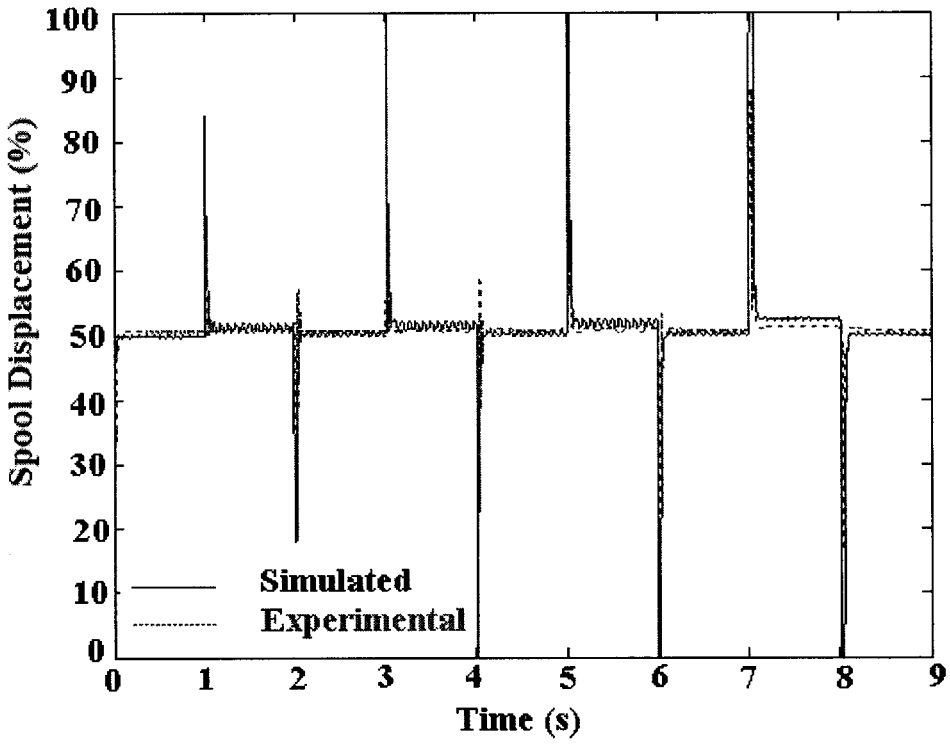

Fig. 6.18 Measured proportional valve behavior when the pump responses to step inputs at constant load pressure using double feedback control loop with PD controller as compared with the simulation results

The second control software module considered in the testing process is the one shown in Appendix 6 Module 7, in which a fuzzy logic controller is proposed as a replacement for the PD controller in double negative feedback control loops.

Fig. 6.19 shows the response of the pump to successive step inputs at a constant load pressure and during a 9 second time span. The transient periods, presented in Figs. 6.20 and 6.21, show satisfactory agreement between the simulation and the measured results, which confirms the suitability of replacing the conventional PD controller with a fuzzy controller.

Fig. 6.22 shows the measured behavior of the proportional valve spool during the testing of the pump compared to the simulated one. The figure shows better dynamic performance of the proportional valve when using a fuzzy logic controller. The spool has no impact with the side ends of its stroke, which tends to increase its service life.

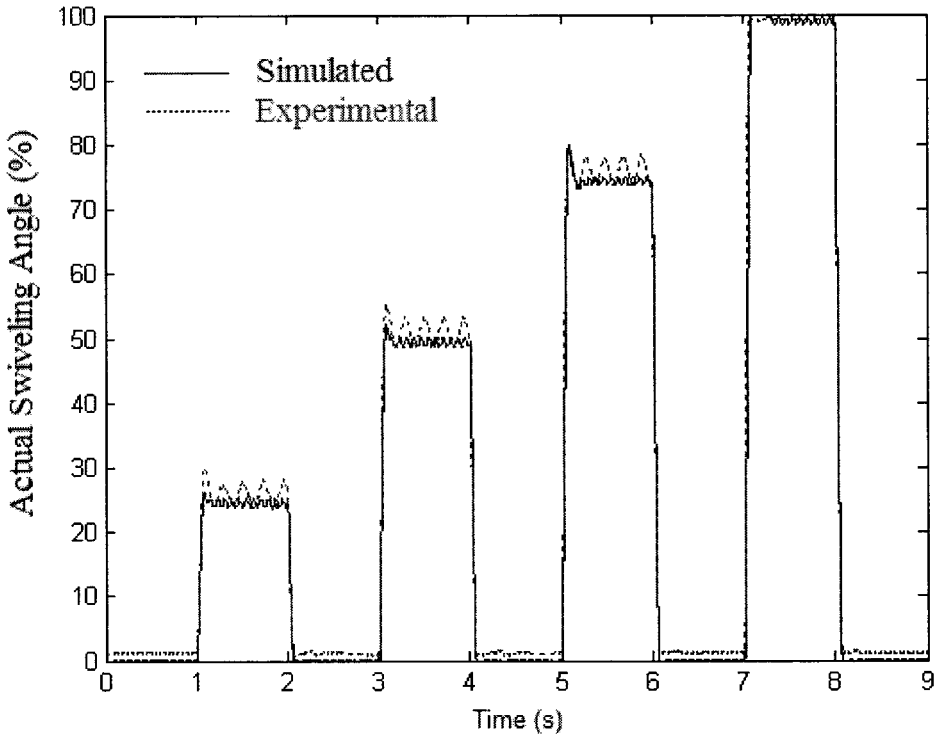

Fig. 6.19 Measured pump step response at constant load pressure using double feedback control loop with fuzzy controller as compared with the simulation results

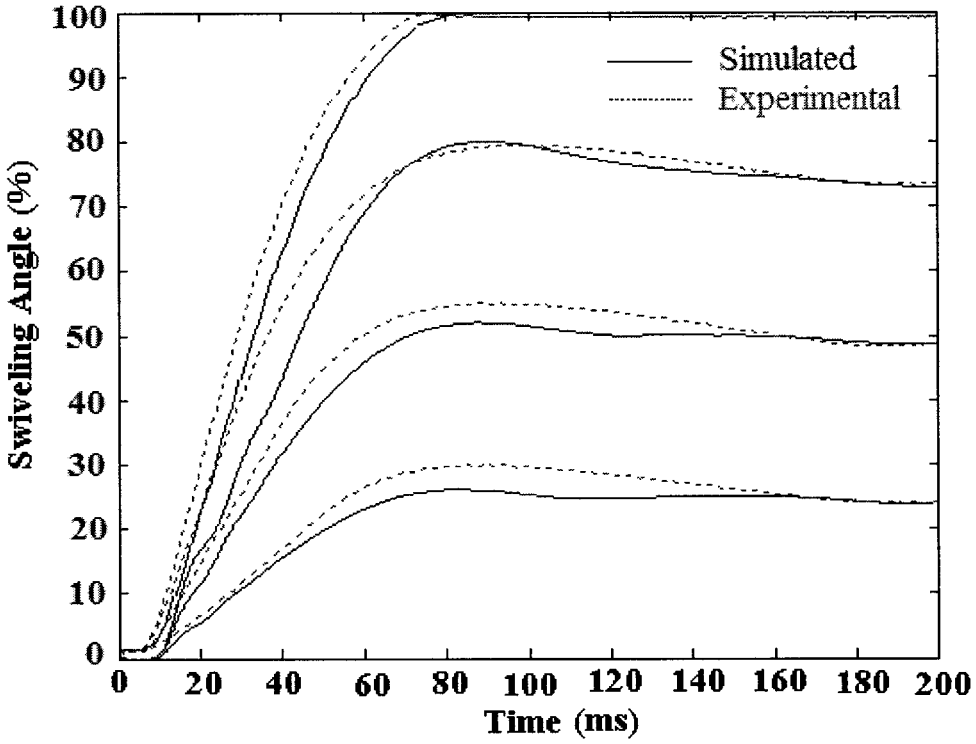

Fig. 6.20 Measured swiveling angle increasing from zero position to different percentages of its maximum value using double feedback control loop with fuzzy controller as compared with the simulation results

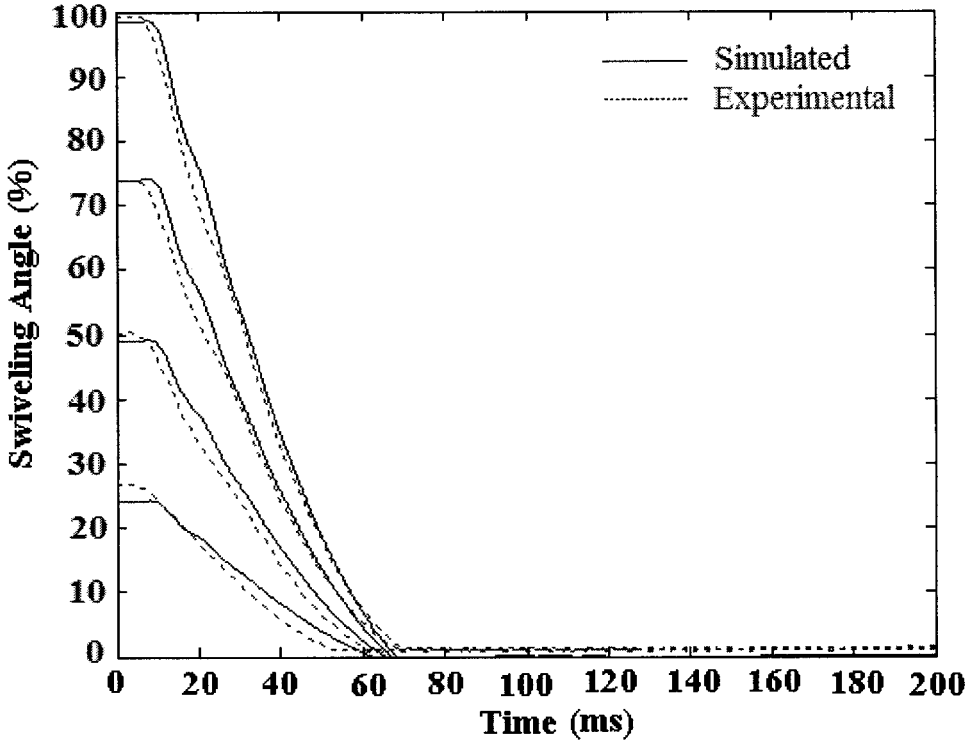

Fig. 6.21 Measured swiveling angle reduction from a position of different percentages of its maximum value to zero position using double feedback control loop with fuzzy controller as compared with the simulation results

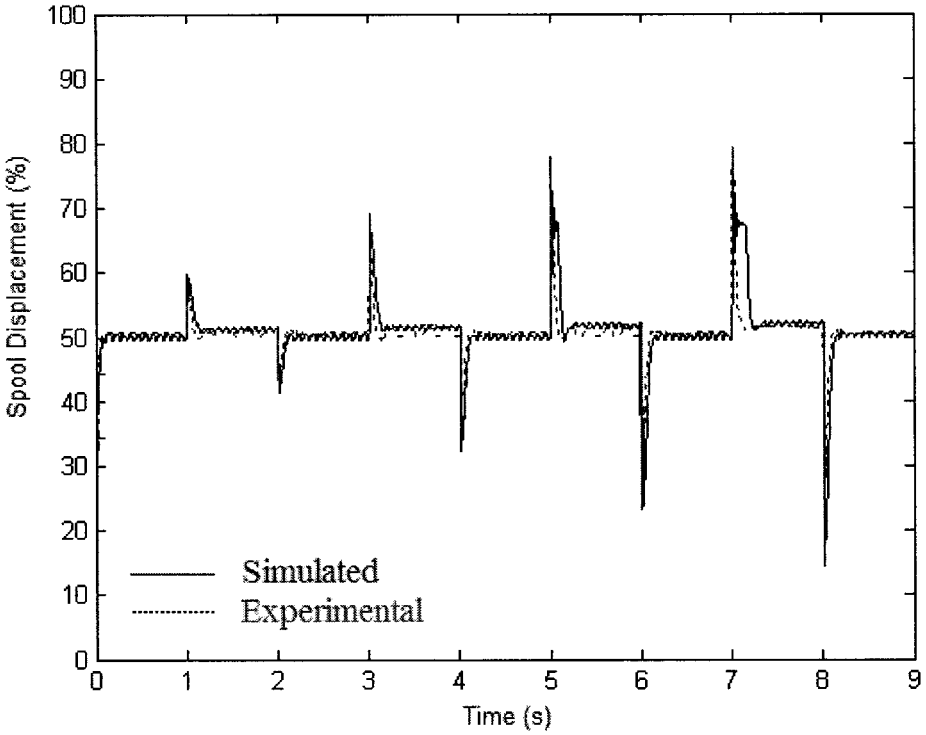

Fig. 6.22 Measured proportional valve behavior when the pump responses to step inputs at constant load pressure using double feedback control loop with fuzzy controller as compared with the simulation results

The third control software module considered in the testing process is the one shown in Appendix 6 Module 8, in which a single feedback control loop is used with the PD pump controller. The same PD parameters from the analytical investigation, K_p=1 and T_d= 0.01, are implemented in the real time control software.

Fig. 6.23 confirms the advantage of using a single feedback loop since the pump response is smoother and the swiveling angle steady state vibration is avoided.

Figures 6.24 and 6.25 show an enlarged view of the measured transient periods of the pump response when the swiveling angle increases from the zero position to different percentages of its maximum value and vise versa, compared to the simulation results. These figures reveal the pump response features discussed in Chapter 5 when using a single feedback loop. The pump response is more gradual and the settling time increases to 200 ms, inconvenient for the constant power operation of the pump. The control piston arrives with a nearly zero velocity to the end of its stroke, which reduces the impact on it.

The measured proportional valve performance shown in Fig.6.26 shows that there is no impact on its side, as in the case of using the fuzzy controller.

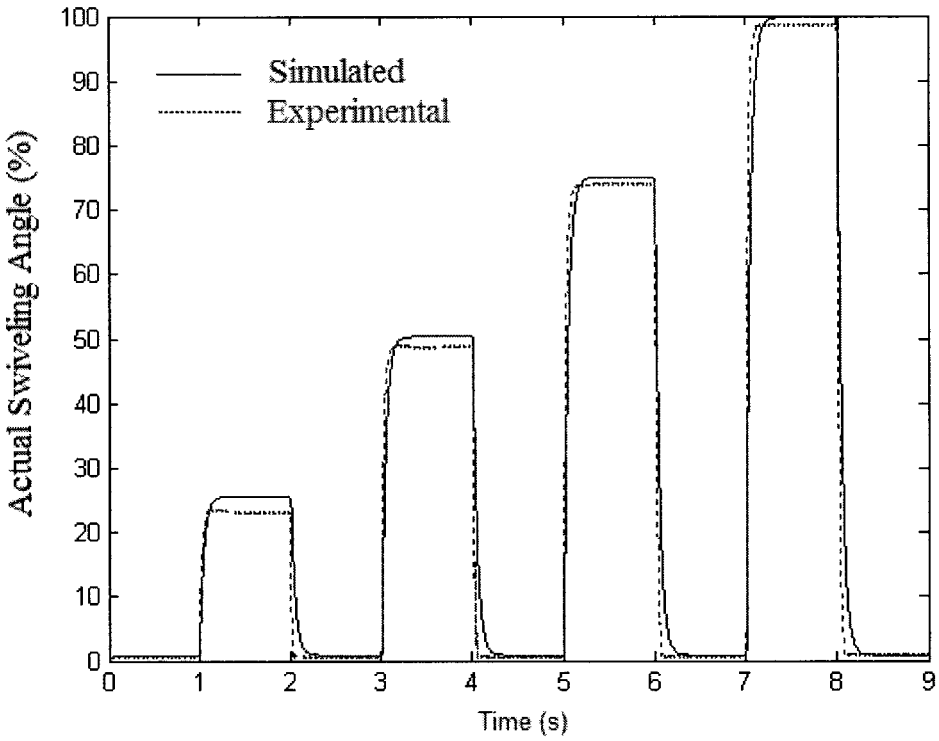

Fig. 6.23 Measured pump step response at constant load pressure using single feedback control loop with PD controller as compared with the simulation results

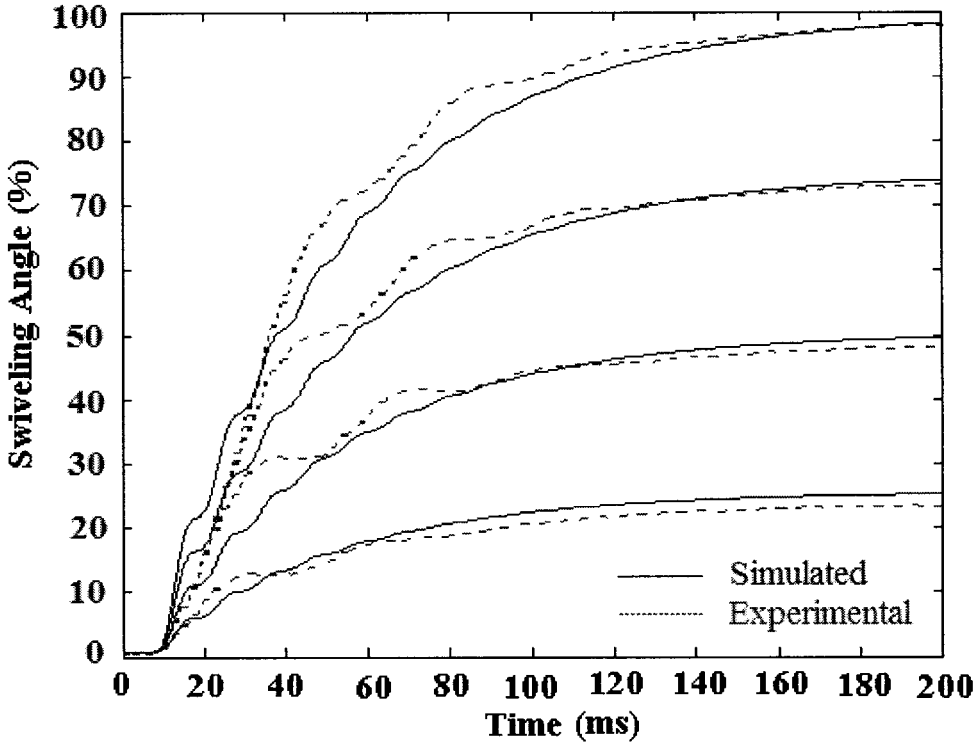

Fig. 6.24 Measured swiveling angle increasing from zero position to different percentages of its maximum value using single feedback control loop with PD controller as compared with the simulation results

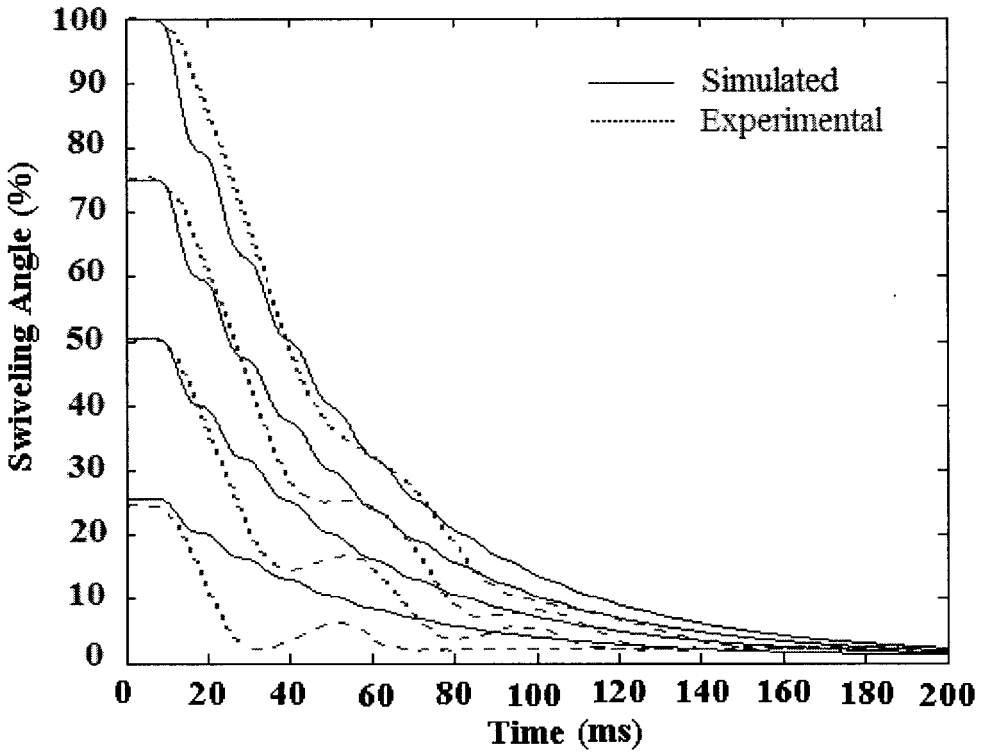

Fig. 6.25 Measured swiveling angle reduction from a position of different percentages of its maximum value to zero position using single feedback control loop with PD controller as compared with the simulation results

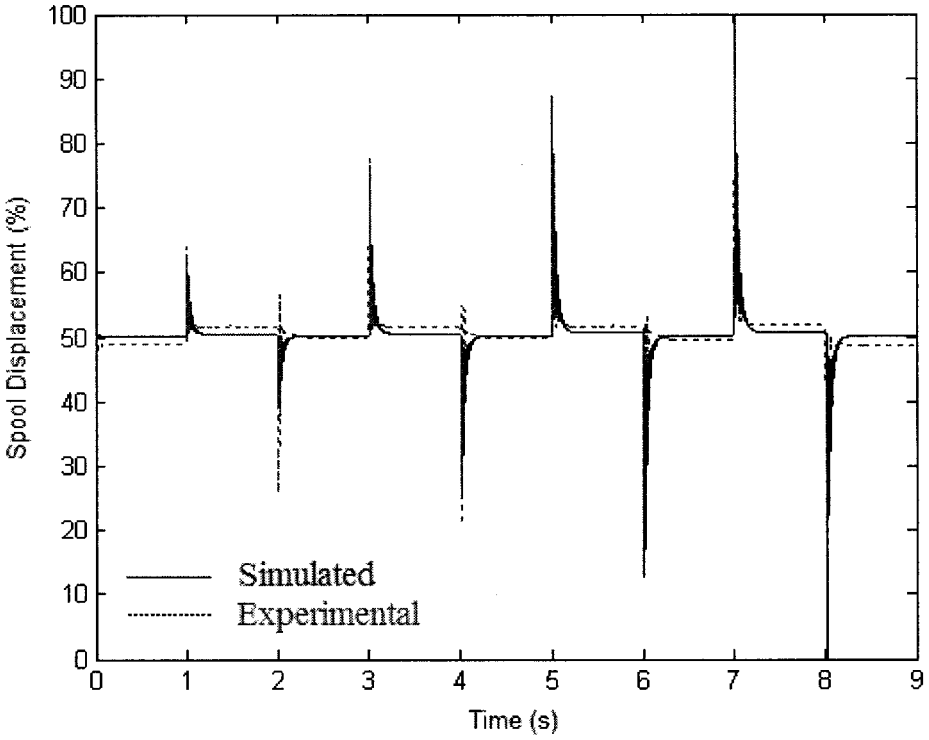

Fig. 6.26 Measured proportional valve behavior when the pump responses to step inputs at constant load pressure using single feedback control loop with PD controller as compared with the simulation results

6.4.2 Measurement of the Pump Static Characteristics at Constant Load

The real time control software modules 6, 7 and 8, shown in Appendix 6, are used successively to measure the pump static characteristics for the three different control schemes. The load pressure is kept constant at 10 MPa as before while measuring the pump step response. The step input command signals are replaced by a command signal assumed to change slowly and gradually from zero to 100%, while the corresponding normalized change in the swash plate swiveling angle is recorded.

The measured results in the case of the double feedback control loop scheme are presented in Figs 6.27 and 6.28, which represent the performance with a PD and Fuzzy controller, respectively. The measured results validate the simulated results and confirm the presence of the steady state vibration when the double negative feedback control loop is considered, either with a PD or fuzzy logic controller. Both cases exhibit linear static characteristics along the whole range of the command signal.

As shown in Fig. 6.29, using the single feedback control loop expresses the advantage of suppressing the swash plate steady state vibration observed with the previous control schemes. The measured results clearly show the non-linearity of the proportional valve open loop static characteristics on the pump static characteristics.

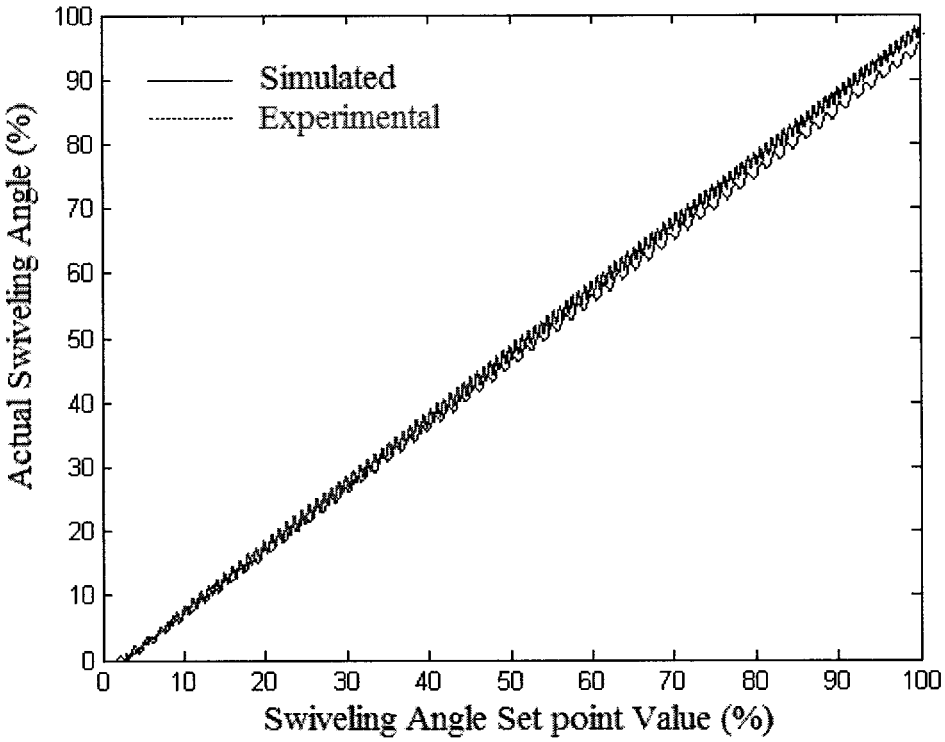

Fig. 6.27 Measured pump static characteristics at constant load pressure using double feedback control loop with PD controller

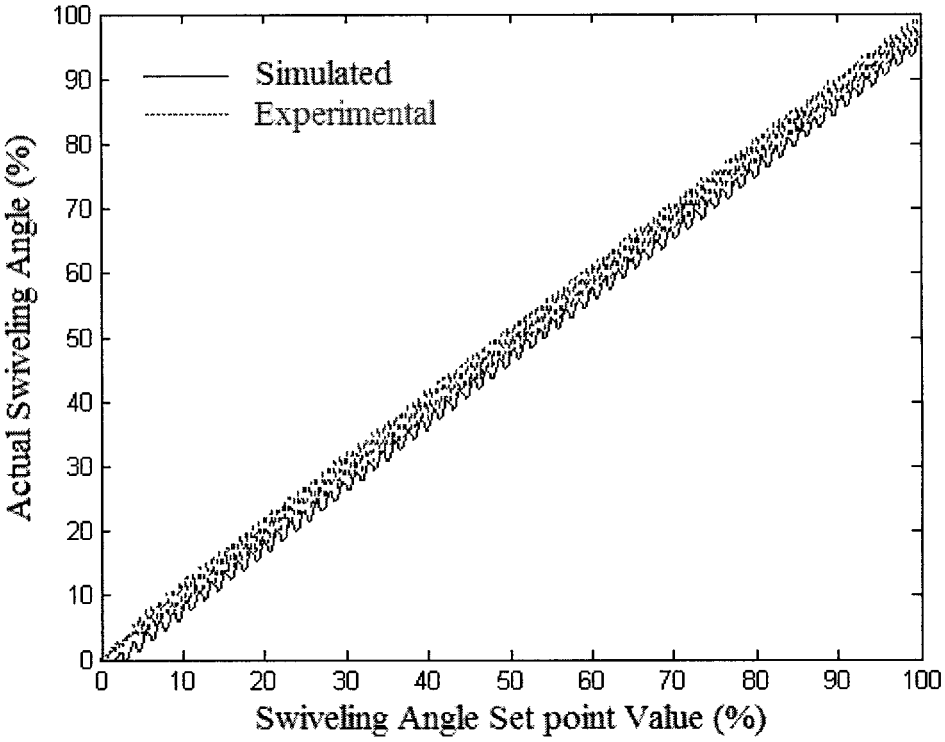

Fig. 6.28 Measured pump static characteristics at constant load pressure using double feedback control loop with fuzzy controller

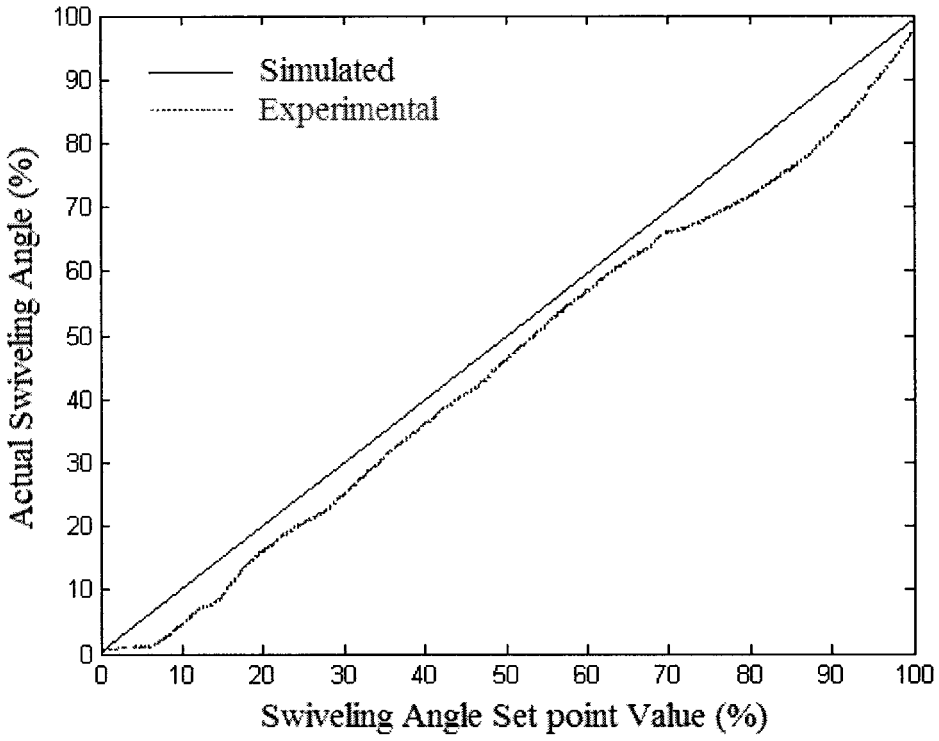

Fig. 6.29 Measured pump static characteristics at constant load pressure using single feedback control loop with PD controller

6.4.3 Measurement of the Pump Performance at Constant Power Operation

The real time control software modules are further developed in order to measure the pump performance during constant power operation. Modules 9 and 10 included in Appendix 6 are developed to measure the pump performance in constant power operation using double feedback control loops scheme with a PD and fuzzy controller, respectively. Module 11 is used for measuring the pump performance in constant power operation using a single feedback control loop.

In this test, the pump flow rate is recorded versus the load pressure, which will be increased linearly in order to test the constant power operation of the pump. Before starting the test, the throttle valve (22) should be fully opened. Testing starts by turning the pump ON at a zero load pressure when the throttle valve (19) is fully opened. The throttle valve is then gradually closed to increase the load pressure against the pump; the corresponding pump flow rate is recorded. The measured results are presented and compared with the simulation results in Figs 6.30 and 6.31 for the pump performance during constant power operation using a double feedback control loops scheme with a PD and fuzzy controller, respectively. Agreement between the experimental and simulation results validates the analytical findings and shows full utilization of the prime mover power. As shown in Fig. 6.32, using a single feedback loop in constant power operation releases the swiveling angle steady state vibration. On the other hand, the experimental results exhibit non-linearity due to the nonlinear proportional valve open loop static characteristics. The three figures show that the three control schemes respect the static characteristic limits, which are the maximum flow, the maximum pressure and the maximum power.

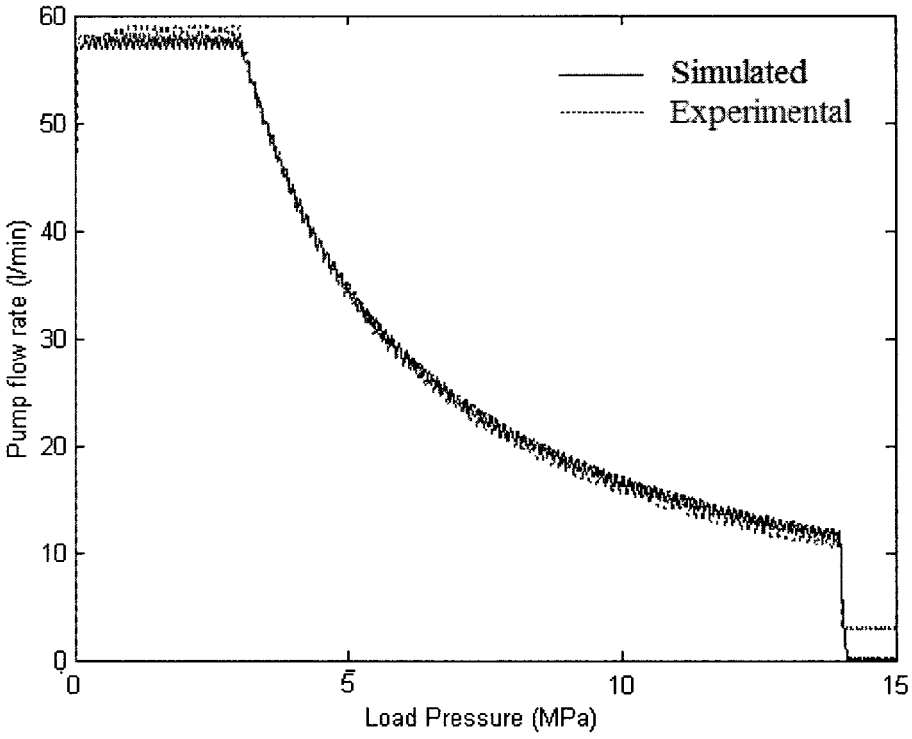

Fig. 6.30 Pump constant power operation using double feedback control loop with PD controller

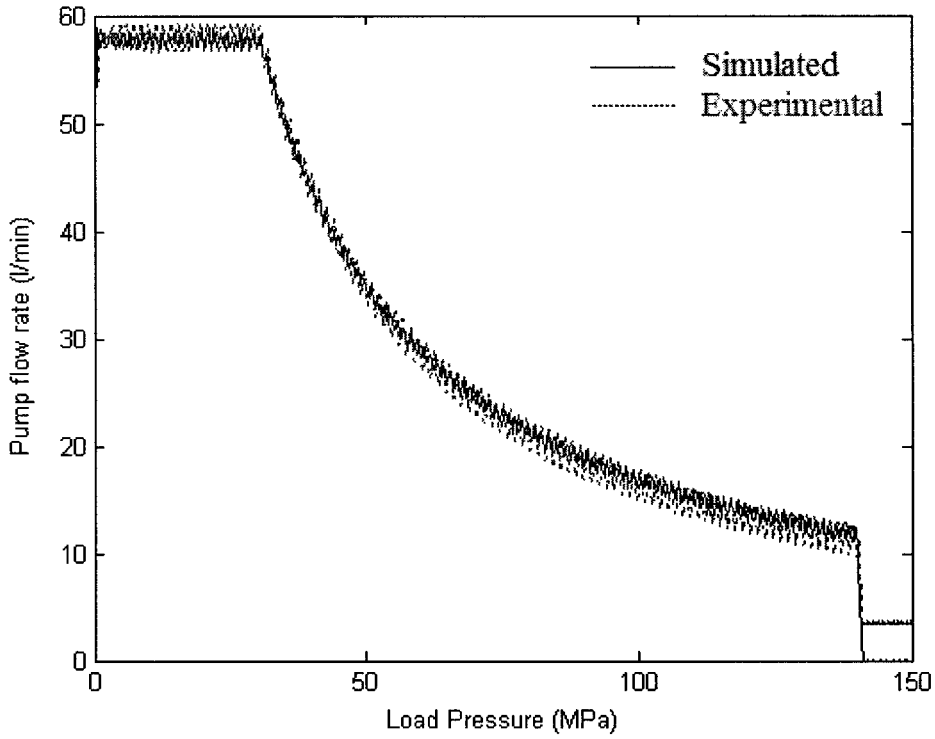

Fig. 6.31 Pump constant power operation using double feedback control loop with fuzzy controller

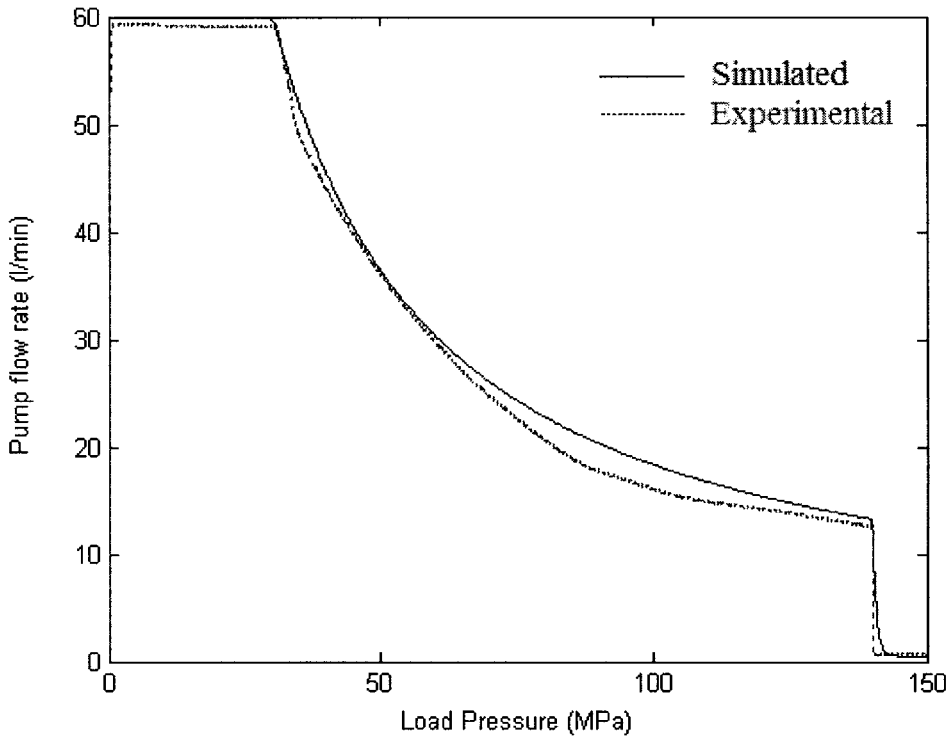

Fig. 6.32 Pump constant power operation using single feedback control loop with PD controller

6.4.4 Qualitative Evaluation of the Pump Performance in View of the Proposed Control Schemes

In this section, the previously conducted comparative study is used to qualitatively evaluate the pump performance with the three proposed control schemes. Results showed that the fuzzy controller could perform the basic control action of the PD controller during normal operating conditions. Further, the fuzzy controller exhibits more robust control action with deteriorated operating conditions, as shown in the analytical investigation. An additional advantage of using the fuzzy controller is the absence of the impact of the proportional valve spool at the end of its stroke. Using a single control loop results in having a relatively larger settling time, which reduces the bandwidth of the pump frequency response and reflects poorly on the pump constant power operation. Also, pump performance shows nonlinear static characteristics. On the other hand, using such a single loop suppresses the steady state vibration of the swash plate, and reduces the impact on the control piston on the ends of its stroke. The main advantage of using a single feedback control loop is to reduce pump production cost, while having reasonable performance that may be acceptable for various commercial applications.

Table 6.1 concludes the features of the pump performance with the three proposed control schemes. In the table, Case1 represents the double feedback control loop with a PD controller, Case2 represents the double feedback control loop with a fuzzy controller and Case3 represents a single feedback control loop with a PD controller. The check mark, ✔, indicates that the qualification is relatively better. The table

offers a quick selection criteria for one of the control schemes based on the convenience of the pump features for a certain application.

Table 6.1 Features of interest of the pump performance with different control schemes

Features of Interest of the Pump performance	Case1	Case2	Case3
1- Speed of response	✔	✔	×
2- Linearity	✔	✔	×
3- Convenience to constant power operation	✔	✔	×
4- Bandwidth	✔	✔	×
5- Valve performance	×	✔	✔
6- Robustness of the control action	×	✔	×
7- Vibration in the steady state conditions	×	×	✔
8- Production cost	×	×	✔
9- Impact at the control piston end strokes	×	×	✔

CHAPTER 7

CONCLUSIONS AND SUGGESTIONS FOR THE FUTURE WORK

A mathematical model has been developed to describe the performance of swash plate axial piston pumps with conical cylinder blocks. This model has been used to simulate the static and dynamic performance of the electrically controlled swash plate pumps. The model has been validated on the basis of the satisfactory agreement between the simulation results and the experimental results.

7.1 Conclusions

With the aid of specially developed auxiliary computer programs, the model has been used to investigate the pump kinematics. A comprehensive theoretical study has been carried out to investigate the effect of the port plate configuration on the variations of cylinder pressure and pump delivery flow rate. The study leads to a desirable port plate configuration, which yields a gradual rise and drop in the cylinder pressure, while cavitation inside the cylinders is avoided for the whole range of delivery pressures. Additionally, the noise of the pump can thus be significantly reduced. On the other hand, the determined valve plate configuration rendered relatively small fluctuations in pump delivery flow rate. This study could be applied to pumps of any size.

The moments acting on the swash plate have also been investigated. The investigation demonstrates that the lateral component of the moment is periodic and can be fairly represented by a mean value and twenty-seven harmonics. This mean value tends to drive the swash plate towards the pump minimum geometric volume position and it increases with the increase of pump delivery pressure and/or decrease of the swash plate inclination angle. The driving shaft torque is found to be nearly constant as compared to the lateral moment. The average value of this torque increases with the increase of pump delivery pressure and/or geometric volume. The component of the moment acting on the swash plate bearing system is seen to be nearly constant under constant delivery pressure and increases linearly with delivery pressure, and is not affected by the swash plate inclination angle.

Using a conical cylinder block reduces the force that tends to detach pistons from the swash plate during the period of piston acceleration in the first half of the suction stroke. It is verified that the detaching force is reduced almost linearly with an increase of the cylinder block cone angle, and that it is independent of the pump rotational speed. The conical cylinder blocks have a relatively larger geometric volume for the same piston diameter. From studying the pump kinematics, it is shown that for a cylinder block cone angle equal to 5 ^{o}, the piston stroke increased 4% more than the case in which the cylinder block arrangement is circular. The mathematical model has been used to evaluate the dynamic loads acting on the drive shaft bearings due to the pressure forces transmitted to the drive shaft bearing through the cylinder block. The bearing reactions along the three main axes are calculated. Simulation results show that each of the bearing reaction forces fluctuates periodically around the

mean value. While the bearing reaction along the X_0 direction is shown to change its sign during its fluctuation, the one along Y_0 is found to be always negative. The reaction in the direction of Z_0 helps in tightening the clearance between the cylinder block and the valve plate. The study can be used in the drive shaft bearing design and in investigating the drive shaft vibration, which has a direct effect on the positioning of the swash plate and hence on pump performance.

In an introductory study, two alternative control schemes were proposed to replace the currently used control scheme in which double negative feedback control loops are used with a PD pump controller. First, a fuzzy controller was proposed to replace the PD pump controller. Second, a single negative feedback control loop is proposed to replace the double feedback control loops. Fuzzy controller demonstrates the possibility of performing the same basic control action as the PD one. Fuzzy controller demonstrates also additional advantages of improving the proportional valve spool dynamics and robustness of control when the oil bulk modulus is decreased. Using a single control loop results in having a relatively larger settling time, which reduces the bandwidth of the pump frequency response and has poor constant power operation. Also, the pump performance shows nonlinear static characteristics. On the other hand, using such a single loop control suppresses the steady state vibration of the swash plate, and reduces the impact on the control piston on the ends of its strokes. The main advantage of using a single feedback control loop is to reduce the pump production cost while ensuring reasonable performance that may be acceptable for various commercial applications. The pump performance with the different control schemes was verified experimentally.

The pump frequency response was obtained and it showed that, in the case of using the double negative feedback control loop, the swash plate responds harmonically with the same amplitude of the harmonic input of frequency less than 5 Hz. The frequency response of the pump shows a slight amplitude attenuation in the range of 5 to 15 Hz, while the amplitude attenuation is significant afterwards. It reaches approximately 65% of the input amplitude at 30 Hz. The pump frequency response, in the case of using a single feedback loop, shows to have less bandwidth.

7.2 Main Contributions

The main contributions in this thesis could be summarized as follows:

(i) A mathematical model for a new design of swash plate pumps with conical cylinder blocks has been developed and experimentally validated.

(ii) A systematic methodology and auxiliary software are developed in order to obtain a desirable valve plate design that improves the pump performance. The method and software used can be applied to pumps of any geometrical size

(iii) Using the pump mathematical model, the forces and vibrations that affect the pump mechanism have been analytically investigated. The analytical findings are useful in designing the pump mechanism and the control unit.

(iv) An introductory study of the pump performance in view of three alternative control schemes has been conducted. The pump performance shows different features that suit requirements of different industrial applications.

(v) The newly proposed control schemes are experimentally prototyped, and pump performance with the different control schemes was verified experimentally.

7.3 Suggestions for Future Work

Some suggestions for future work are given below:

(i) Robustness of the control action when the fuzzy controller is used should be extended to include other operating conditions. Experimental validation is also needed.

(ii) Pump frequency response needs to be validated experimentally. In this regard, the loading unit in the experimental setup should be further developed using a proportional pressure valve instead of the manual throttle valve. By using such a valve, a harmonic load could be generated to simulate the conditions of load variations in many practical applications.

(iii) The cylinder block is supported by the drive shaft bearings. The cylinder block vibrations affect the swash plate positioning, and consequently affect pump performance. Therefore, it is important to study the effect of the design parameters of the drive shaft bearings on the pump performance.

(iv) In many industrial applications, the quality of a product depends on the feed speed and/or the applied load. If these conditions are hydraulically controlled, then such pumps could be implemented to perform the necessary functions.

(v) The validated pump model can now be easily integrated with an entire model of a hydrostatic transmission system in mobile machinery applications. The entire model could be used to study some dynamic aspects of a constant power regulated hydrostatic transmission system.

REFERENCES

A. Papers

1. **Green W. and Crossley T., (1971).** *An analysis of the Control Mechanism used in Variable Delivery Hydraulic Pump*, Proceedings of the Institution of the Mechanical Engineers, Vol. 185, 63-72.
2. **Helgestad B. O., Forster K. and Bannister F.K., (1974).** *Pressure Transients in an Axial Piston Hydraulic Pump.* Proceedings of Institution of Mechanical Engineers, Vol. 17, 189-199.
3. **Yamaguchi A. and Ishikawa T., (1979).** *Characteristics of Displacement Control Mechanism in Axial Piston Pumps*, Bulletin of the JSME, Vol. 22, No.165, 356-361.
4. **Zaki H. and Baz, A., (1979).** *On the Dynamics of Pressure Compensated Axial Piston Pumps*, Fluidic Quarterly, Vol.11, No.2, pp. 73-87.
5. **Baz A., (1980).** *Optimization of the Dynamics of Pressure-Compensated Axial Piston Pumps.* Journal of Fluid Control, Vo.20, Issue 2, pp. 64-81.
6. **Tatsuji Yuasa, (1980).** *Vibrational Force which Generates Noise in Bent-Axis Type Oil Hydraulic Pump*, Journal of Hydraulic and Pneumatic, Japan, Vol.11, No.2, 115-122.
7. **Hooke C. J. and Kakoullis (1981).** *The Effect of Centrifugal Load and Ball Friction on the Lubrication of Slippers in Axial Piston Pumps,* 6th International Fluid Power Symposium, Cambridge, England.
8. **Atsushi Y., (1983).** *Cavitation in an Axial Piston Pump*, JSME, Vol. 26 No. 211, PP.72-78.

9. **Lin S.J., Akers A. and Zeiger, G. (1984).** *The Effect of Oil Entrapment in Axial Piston Pumps*, ASME G00282, pp. 127-134.

10. **Zeiger G. and A. Akers, (1985).** *Torque on the Swash Plate of an Axial Piston Pump,* ASME Journal of Dynamic Systems, Measurement and Control, Vol.107, 220-226.

11. **Zeiger G. and A. Akers, (1986).** *Dynamic Analysis of an Axial-Pump Swash Plate Control*, Proceedings of Institution of Mechanical Engineers, Vol. 200, 49-58.

12. **Edge K. A. and Darling J., (1986).** *Cylinder Pressure Transients in Oil Hydraulic Pumps with Sliding Plate Valves*, Proceedings of the Institution of Mechanical Engineers, Vol. 200, pp. 49-58.

13. **Kim S. D., Cho H. S. and Lee C. O., (1987).** *A Parameter Sensitivity Analysis for the Dynamic Model of a Variable Displacement Axial Piston Pump*, Proceedings of the Institution of Mechanical Engineers, Vol. 201, 235-243.

14. **Kiyoshi I. and Masakasu, N., (1987).** *A Study of the Operating Moment of a Swash Plate Type Axial Piston Pump*, Journal of Hydraulic and Pneumatic, Japan, Vol.18, No.4, 67-74

15. **Akers A., and Lin, S.J., (1987).** *The Control of an Axial Piston Pump Using Single-Stage Electro-hydraulic Servovalve*, Proceedings of American Control Conference, Vol. 3, pp. 1865-1870.

16. **W. Backe and H. Ulrich, (1988).** *Design of a Hydraulic-Mechanical Pressure Control of Variable Displacement Pump*, Design, Modeling and Control of pumps, First Bath International Fluid Power Workshop, p. 47, Research studies.

17. **You Z., (1989).** *Interactions Between Two Pressure Compensated Pumps in a Single Load Circuit*, Proceedings of the 2nd International Conference on Fluid Power Transmission and Control, China, pp. 569-571.

18. **Mohamed S. A., (1989).** *Comparative Study of Control Systems for Constant Supply Pressure Operation of Variable Geometric Volume Axial Piston Pumps*, M.Sc. Thesis, Faculty of Engineering, Cairo University.

19. **Lu Y.Z., and Chen Z, (1989).** *Measurement and Simulation Model Study of Cylinder Pressure Transition in An axial Piston Pump*, Proceedings of the 2nd International Conference on fluid Power Transmission and Control, International Academic Publishers, Beijing, 471-476

20. **Edje K. A. and Darling J., (1989).** *The Pumping Dynamics of Swash Plate Piston Pumps*, ASME Journal of Dynamic System, Measurement and Control, Vol. 111, 307-12.

21. **Schoenau G., R. Burton and G. Kavanagh, (1990).** *Dynamic Analysis of a Variable Displacement Pump,* ASME Journal of Dynamic System, Measurement and Control, Vol. 112, 122-132.

22. **Hogan P. H., Burrows C. R. and Edge K A. (1990).** *Development of a Knowledge-Based System for the Diagnosis of Faults in Hydraulic Systems.* ASME Winter Annual Meeting. Dallas, Texas, Paper 90-WA/FPST-2. .

23. **Hu F. and Edge K. A. (1991).** *Constant Pressure Control of an Axial Piston Pump - a Simulation Study of an Adaptive Control Scheme.* Proceedings of Fourth Bath International Fluid Power Workshop, Bath, England.

24. **Jaecheon Lee, (1992).** *Robust Control of a pump with Single-Stage Electro-hydraulic Servovalve*, presented at the International Fluid Power Exposition and Technical Conference, Paper Identification Number N92-3.2

25. **Virvalo T. K. and Koskinon (1992).** *Fuzzy Logic Controller For Hydraulic Drives*, 10th Aachen Colloquium of Fluid Power Technology, Germany.

26. **Harris R M, Edge KA and Tilley DG, (1993).** *The Spin Motion of Pistons in a Swash plate-Type Axial Piston Pump.* Third Scandinavian International Conference Fluid Power, Linköping, Sweden, Vol 1, 95-111.

27. **Harris R. M., Edge K. A. and Tilley D. G. (1993).** *Predicting the Behavior of Slipper-Pads in Swash plate-Type Axial Piston Pumps at High Speeds.* ASME WAM, New Orleans, USA.

28. **Jong-Hwan Kim, Jong-Hwan Park, Seon-Woo Lee and Edwin K.P. Chong, (1993).** *Fuzzy Pre-compensation of PD Controller for Systems with Dead zones*, Journal of Intelligent and Fuzzy Systems, Vol.1, No. 2, pp. 125-133.

29. **Kaliafetis P. and Costopoulos, T., (1994).** *Modeling and Simulation of an Axial Piston Variable Displacement Pump with Pressure Control*, Mechanical Design and Control System Section & Machine Design Laboratory, Mechanical Engineering Department, National Technical University of Athens, Partition 42, 106 82, pp. 599-612.

30. **Hu F. and Edge, K. A. (1994).** *Constant Pressure Control of a Piston Pump Using a Model Reference Adaptive Control Scheme.* Proceedings of the 11th Aachen Colloquium on Fluid Power Technology, Vol. 2, 425-439.

31. **Harris RM, Edge KA and Tilley DG (1994).** *The Suction Dynamics of Positive Displacement Axial Piston Pumps.* ASME Journal of Dynamic Systems, Measurement and Control, Vol 116, 281-287.

32. **Noah D. Manring, (1994).** *Swivel Torque within a Variable-Displacement Pump,* presented at the Fluid Power West, The Expo and Technical Conference for Electro-Hydraulic and Electro-Pneumatic Motion Control, Paper Identification Number 94-3.2

33. **Gregory R., (1994).** *Pressure Compensated Pump Control for Forestry Logic Skidders,* Proceedings of the 46th National Conference on Fluid Power.

34. **Manring N.D. and Johnson, R.E., (1996).** *Modeling and Designing a Variable-Displacement Open-Loop Pump,* ASME Journal Dynamic Systems, Measurement, and Control, Vol. 118, pp. 267-271.

35. **Rodney D. Hugelman, (1996).** *A New Adjustable Stroke Control Module for Axial Hydraulic Pumps,* presented at the International Fluid Power Exposition and Technical Conference, Paper Identification Number II96-8.3

36. **R. Paoluzzi, L.G. Zarotti, M. Ruggeri, and C. Fantuzzi, (1996).** *Hybrid Multiple Control of Pump Displacement,* International Mechanical Engineering Congress and Exposition Fluid Power Systems.

37. **C. Fantuzzi, (1996).** *Robust fuzzy control of an industrial robot, Proc. ISIR '96,* Milano.

38. **Osama G., (1997).** *An Investigation into the Static and Dynamic Performance of a Class of Variable Displacement Axial Piston Pumps with Power Controller,* Ph.D. Thesis, Zagazig University, Faculty of Engineering,.

39. **Manring N.D., (1998).** *The Torque on the Input Shaft of an Axial Piston Swash Plate Type Hydrostatic Pump*, ASME Journal of Dynamic Systems, Measurement, and Control, Vol. 120, pp. 57-62.

40. **Wicke V., Edge K. A. and Vaughan N. D., (1998).** Investigation of the Effects of Swash Plate Angle and Suction Port Timing on the Noise Generation Potential of an Axial Piston Pump. ASME-IMECE, Anaheim, CA, USA.

41. **Noah D- Manring (1999).** *Friction Forces Within the Cylinder Bores of Swash-Plate Type Axial-Piston Pumps and Motors.* Journal of Dynarnic Systems Measurement, and Control Vol. 121, No.1.

42. **Bapiraju Surampudi, (2000).** *Modeling of Low-Speed Characteristics of Swash-Plate-Type Axial Piston Hydraulic Motor*, presented at the International Fluid Power Exposition and Technical Conference, Paper Identification Number I00-3.2

43. **Olems L., (2000).** *Investigations of the Temperature Behavior of the Piston Cylinder Assembly in Axial Piston Pumps*, International Journal of Fluid Power Vol.1, pp. 27-38.

44. **Wieczorek U. and Ivantysynova M. (2000).** *A Computer Aided Design Tool for Axial Piston Machines.* Bath Workshop on Power transmission and Motion Control PTMC2000, Bath, UK.

45. **W. Xiang, S. C. Fok and F. F. Yap, (2000).** *A Fuzzy Neural Network Approach to Model Hydraulic Component from Input/Output Data*, International Journal of Fluid Power.

46. **Harrison A. M. and Edge K A. (2000).** *Reduction of axial piston pump pressure ripple.* Proc. IME, Part I, Vol 214, 53-63.

47. **Qiu H., Q. Zhang, and J. F. Reid,(2000),** *Fuzzy Control of Electro-hydraulic Steering System.* ASAE Paper 00-1020, ASAE Ann. Int. Mtg.

48. **Edvard Deticek, (2000),** *An Intelligent Position Control of Electro-hydraulic Linear Drive*, STROJ - 1135, 181-189. Faculty of Mechanical Engineering, University of Maribor, Smetanova, Republic of Slovenia.

49. **Edward Lisowski and Grzegorz (2000),** *Application of Fuzzy Logic Controller in the Hydraulic Lifting System of the Self-Propelled Crane Jib,* Fluid Power Net International. 105-108.

50. **Kassem S.A. and Bahr M.K., (2000).** *Effect of Port Plate Silencing Grooves on Performance of Swash Plate Axial Piston Pumps*, Current Advances in Mechanical Design and Production, Pergamon Press, VII, pp. 139-148.

51. **Kassem S.A. and Bahr M.K., (2000).** *On the Dynamics of Swash Plate Axial Piston Pumps with Conical Cylinder Blocks*, Proceedings of the 6th Terminal Symposium on Fluid Control, Measurement and Visualization. Sherbrooke, Canada

52. **X. Zhang, J. Cho, S. S. Nair and N.D. Manring, (2001).** *New Swash Plate Damping Model for Hydraulic Axial Piston Pumps*, Journal of Dynamic Systems Measurement and Control, Vol. 123, pp. 463-470.

53. **Manring N. D., and Y. Zhang. (2001).** *The Improved Volumetric Efficiency of an Axial-Piston Pump Utilizing a Trapped-Volume Design.* ASME Journal of Dynamic Systems, Measurement and Control. Vol.123, 479-87.

54. **Manring N. D., and F. A. Damtew. (2001).** *The Control Torque on the Swash Plate of an Axial-Piston Pump Utilizing Piston-Bore Springs.* ASME *Journal of Dynamic Systems, Measurement and Control.* Vol.123, 471-78.

55. **Kassem S.A. and Bahr M.K., (2001).** *Fuzzy Logic Control of Constant Power Regulated Swash Plate Axial Piston Pumps*, Proceedings of the International Mechanical Engineering Congress and Exposition, ASME-ME2001, (FPST Division), New York.

56. **G. Carbone. L. Mangialardi, L. Soria, (2002).** *Bearing load on slippers in swash plate axial piston pumps,* 3rd AIMETA International Tribology Conference AITC 2002.

B. Papers Published from the Thesis:

57. **M. K. Bahr, V. Yurkevich, J. Svoboda and R.B. Bhat, (2002).** *Implementation of Single Feedback Control Loop for Constant Power Regulated Swash Plate Axial Piston Pumps,* International Journal of fluid Power, Vol.3 No.3, pp 27-36, December 2002.

58. **M. K. Bahr, J. Svoboda and R.B. Bhat, (2002).** *Vibration Analysis of Constant Power Regulated Swash Plate Axial Piston Pumps,* Journal of Sound and Vibration, Vol.259(5), pp. 1225-1236, January, 2003.

59. **M. K. Bahr, J. Svoboda and R.B. Bhat, (2002).** *Dynamic Loads on the Drive Shaft Bearings of Swash Plate Axial Piston Pumps with Conical Cylinder Blocks.* Proceedings of the CSME Forum2002, Queen's University, Toronto, Canada.

60. **M. K. Bahr, J. Svoboda and R.B. Bhat, (2002).** *Experimental Investigation On Swash Plate Axial Piston Pumps With Conical Cylinder Blocks Using Fuzzy Logic Control*, Proceedings of the International Mechanical Engineering Congress and Exposition ASME-ME2002, New Orleans, Louisiana,USA.

61. **M. K. Bahr, J. Svoboda and R.B. Bhat, (2001).** *Response of Constant Power Regulated Swash Plate Axial Piston Pumps to Harmonic and Random Inputs*, Proceedings of the International Conference on Multidisciplinary Design in Engineering, CSME-MDE2001, Concordia University, Montreal, Canada.

C. Books:

62. **Negotia C. V., (1991).** *Expert Systems and Fuzzy Systems*, ISBN 0-8053-6840-X, Benjamin / Cummings Publishing Company Inc., New York.

63. **Franklin, Powell and Abbas, (2002).** *Feedback Control of Dynamic Systems, Fourth Edition*, ISBN 0-13-032393-4, Prentice Hall, New Jersey, USA.

64. **Mannesmann Rexroth,** *The Hydraulic Trainer Volume 1- Basic Principles and Components of Fluid Technology*. Mannesmann Rexroth GmbH (1986). ISBN 3-8023-0266-4.

65. **Mannesmann Rexroth,** *The Hydraulic Trainer Volume 2 - Proportional and Servo Valve Technology*. Mannesmann Rexroth GmbH (1986). ISBN 3-8023-0266-4.

66. **Anthony Esposito,** *Fluid Power with Application,* Prentice Hall (2000), ISBN 0-13-060899-8.

67. **Paula Fitch**, *Hydraulic Component Design and Selection*, BarDyne (2001), ISBN 0-9705922-3-X.

68. **Meriovitch, L.,** *Methods of analytical Dynamics*, McGraw-Hill (1970)

D. Technical Catalogues:

69. **Rexroth Corporation,** (1997). *Electronic Control Systems for Closed Loop Control of Variable Displacement Axial Piston Pumps Type A4VS with HS3 Control*, Data Sheet RE 30021, pp. 6/20.

APPENDIX A

FRAME TRANSFORMATION

The first transformation is from the initial frame of reference $X_0Y_0Z_0$ to the first one $X_1Y_1Z_1$ that represents a translation along the Z_0 axis for a distance L_1. The matrix T_{01} represents this translation and is given by:

$$T_{01} = \begin{bmatrix} 1 & 0 & 0 & 0 \\ 0 & 1 & 0 & 0 \\ 0 & 0 & 1 & L_1 \\ 0 & 0 & 0 & 1 \end{bmatrix}$$

The second transformation is taken from the first frame of reference $X_1Y_1Z_1$ to the second one $X_2Y_2Z_2$. It represents a rotation around Z_1 by an angle θ_k. The matrix T_{12} representing this rotation is given by:

$$T_{12} = \begin{bmatrix} \cos\theta & -\sin\theta & 0 & 0 \\ \sin\theta & \cos\theta & 0 & 0 \\ 0 & 0 & 1 & 0 \\ 0 & 0 & 0 & 1 \end{bmatrix}$$

The third transformation is carried out from the second frame of reference to the third one $X_3Y_3Z_3$. This transformation represents a translation along the X_2 axis through a distance $R_2 = 0.5D_2$. Matrix T_{23} represents this transformation and equals:

$$T_{23} = \begin{bmatrix} 1 & 0 & 0 & R_2 \\ 0 & 1 & 0 & 0 \\ 0 & 0 & 1 & 0 \\ 0 & 0 & 0 & 1 \end{bmatrix}$$

The transformation from the third frame of reference $X_3Y_3Z_3$ to the fourth one $X_4Y_4Z_4$ is carried out by a rotation around the Y_3 axis through an angle β. The transformation matrix T_{34} represents this rotation and equals:

$$T_{34} = \begin{bmatrix} \cos\beta & 0 & -\sin\beta & 0 \\ 0 & 1 & 0 & 0 \\ \sin\beta & 0 & \cos\beta & 0 \\ 0 & 0 & 0 & 1 \end{bmatrix}$$

The final transformation from the fourth frame of reference $X_4Y_4Z_4$ to the fifth one $X_5Y_5Z_5$ is a translation along the Z_4 axis for a distance $-L_3$. The transformation matrix is T_{45} and is given by:

$$T_{45} = \begin{bmatrix} 1 & 0 & 0 & 0 \\ 0 & 1 & 0 & 0 \\ 0 & 0 & 1 & -L_3 \\ 0 & 0 & 0 & 1 \end{bmatrix}$$

Multiplying these transformation matrices gives the resultant transformation matrix from the initial frame of reference $X_0Y_0Z_0$ to the final frame of reference $X_5Y_5Z_5$. The transformation matrix T_{05} can be expressed as:

$$T_{05} = T_{01} \times T_{12} \times T_{23} \times T_{34} \times T_{45} = \begin{bmatrix} \cos\theta_k \cos\beta & -\sin\beta & -\cos\theta_k \sin\beta & L_{3k} \cos\theta_k \sin\beta + R_2 \cos\theta_k \\ \sin\theta_k \cos\beta & \cos\theta_k & -\sin\theta_k \sin\beta & L_{3k} \sin\theta_k \sin\beta + R_2 \sin\theta_k \\ \sin\beta & 0 & \cos\beta & -L_{3k} \cos\beta + L_1 \\ 0 & 0 & 0 & 1 \end{bmatrix}$$

APPENDIX B

CONSTRUCTIONAL AND OPERATIONAL PARAMETERS OF THE TEST PUMP

Symbol	Description	Value	Unit
A_{cp}	Area of the control piston	$8.1x10^{-4}$	m^2
A_p	Piston cross-section area.	$2.27\ x10^{-4}$	m^2
B	Effective bulk modulus	$1x10^9$	Pa
C_d	Coefficient of discharge.	0.611	-
D_1/R_1	Pitch circle diameter/radius of the cylinders' arrangement at the base of the cylinder block	0.07175/0.0359	m
D_2/R_2	Pitch circle diameter/radius of the cylinders' arrangement at the top of the cylinder block	0.0602/0.0301	m
f_v	Control valve equivalent viscous friction coefficient	90	N.s/m
f_α	Equivalent angular viscous friction coefficient of the swash plate	1.5	Nm/(rad/s)
I_e	Equivalent moment of inertia of the swash plate	.0039	$kg.m^2$
k_i	Proportional solenoid force-current constant	2.5	N/A

k_v	Proportional valve spring stiffness	20000	N/m
k_α	Equivalent viscous friction coefficient of the swash plate	72	Nm/rad
L_1/ L_2	Lengths, referred in Fig. 2.1	.0766/.0661	m
L_c	Cylinder length	.0573	m
L_p	Piston length	.0591	m
m_p	Piston mass	0.118	kg
m_v	Proportional valve spool mass	0.1	kg
N	Number of pistons	9	-
p_s	Pump suction pressure	$.05x10^5$	Pa
p_T	Tank line pressure	$1x10^5$	Pa
R_L	Leakage resistance	$1x10^{13}$	$Pa/(m^3/s)$
r_s	Radius of swash plate swinging	.055	m
$s_{v(max)}$	Proportional valve spool displacement (maximum)	(.001)	m
V_{ci}	Initial control volume	$13x10^{-6}$	m^3
V_o	Additional cylinder volume	$1x10^{-6}$	m^3
w	Proportional valve area factor	$4.8x10^{-3}$	m
$x_{cp\ (min,\ max)}$	Control piston displacement (minimum, maximum)	(0, 0.015)	m
β	Cylinder block cone angle	5	deg
ρ	Oil density	850	kg/m^3

APPENDIX C

CALCULATION OF THE PUMP KINEMATICS

A visual basic program is developed in order to obtain the k^{th} piston displacement as a function of its angular position θ_k during one complete revolution of the pump drive shaft. The visual basic program is developed in order to solve the equations that represent the pump kinematics and also to animate the piston movement relative to Z_5 direction during both the delivery and suction strokes. Figure 7.1 shows the program user interface that allows free choice, within the limits of the main dimensions of the pump. The figure shows the value of the piston displacement s_k versus the angle θ_k during one pump revolution, for the pump with the dimensions shown in the figure. This software was helpful in understanding the effect of the various pump constructional parameters, particularly the cone angle β, on pump kinematics. The program demonstrates that as the cone angle increases, the piston stroke increases, which means a higher pump flow rate for the same piston dimensions, which consequently increases the pump specific power.

As shown in the figure, through the input data section, the program allows selection of different combinations of the cylinder block dimensions as well as the swash plate inclination angle. When the "Auto" button is pressed, the piston and cylinder block starts to do one complete rotation. The corresponding piston stroke is then plotted. Different colors might be used to differentiate between different plotting. By pressing "Reset" button, the piston starts from the beginning.

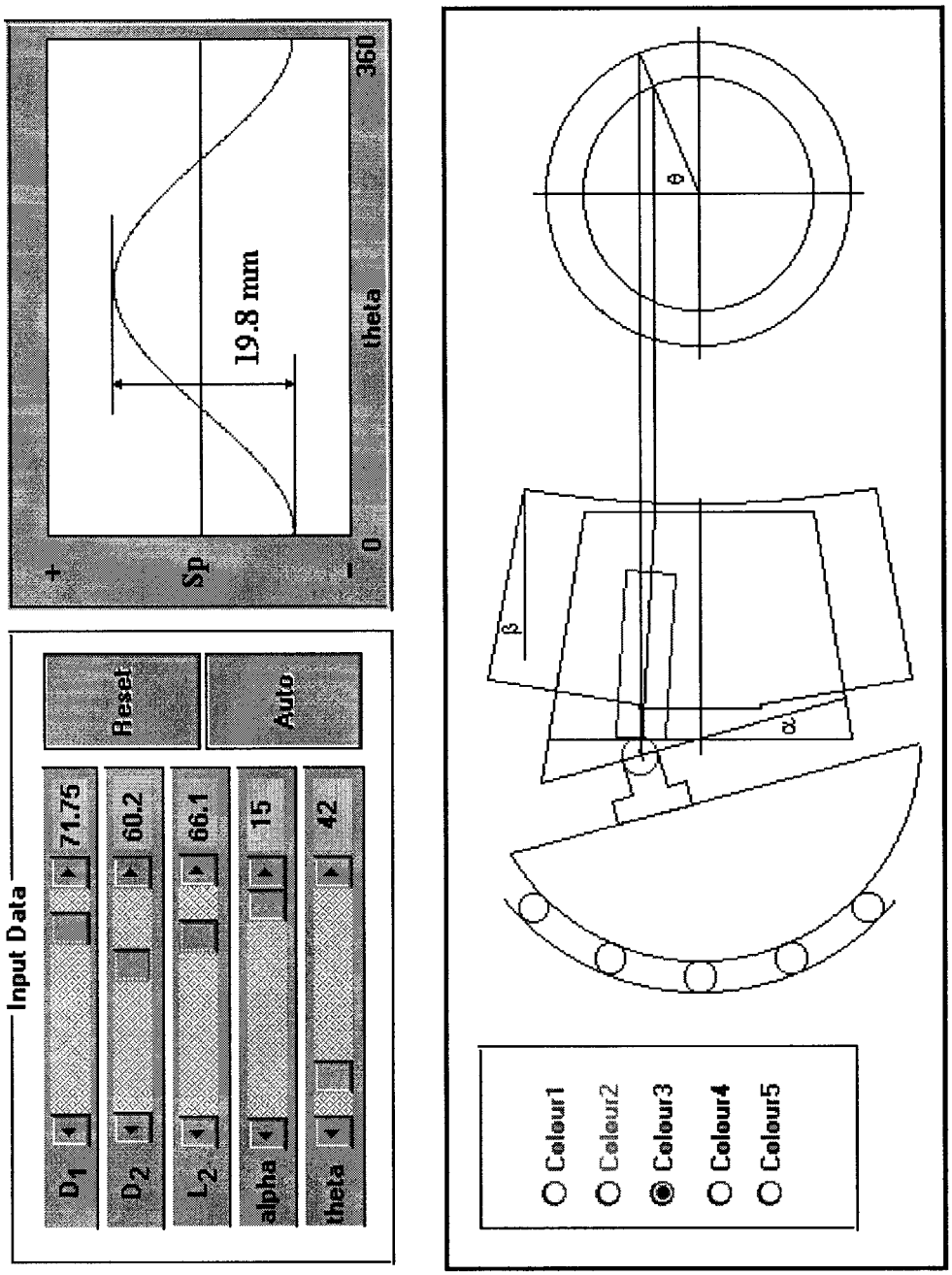

Fig.7.1 User interface Visual Basic program developed to calculate the piston displacement as function of its angular position

APPENDIX D

CALCULATION OF THE PORTING AREA

The figure shows the user interface of the visual basic program that is built to calculate the valve plate porting area for different combinations of silencing grooves dimensions. As shown in Fig. 8.1, through the input data section, the program allows selection of different combinations of the silencing grooves dimensions. The other sections on the user interface show projections of the notch, configuration of the valve plate based on the selected dimensions. When the "play" button is pressed, a circle represents the piston starts to do one complete rotation scanning the valve plate ports. The corresponding porting area is then plotted. Different colors might be used to differentiate between different plotting. By pressing "data to file" button, the plotted area is saved in a data file.

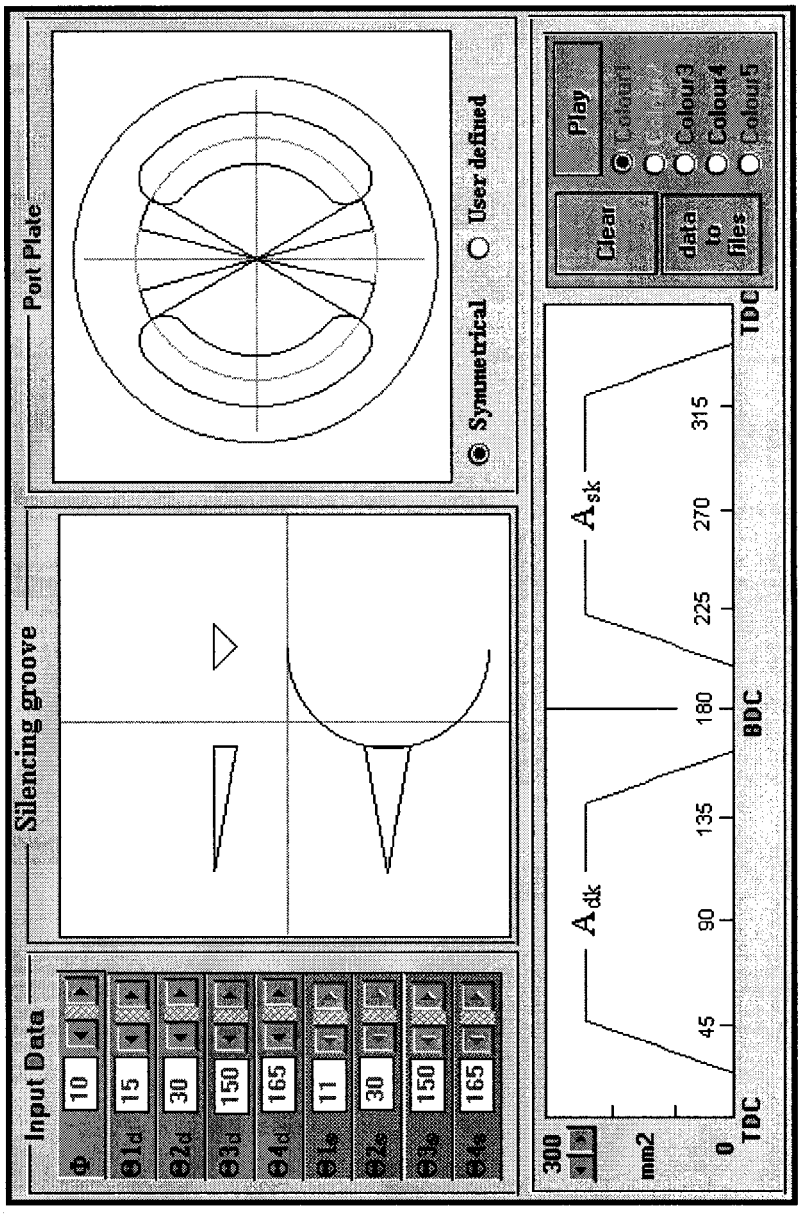

Fig 8.1 User interface of the Visual Basic program for calculating the porting areas

APPENDIX E

CONSTRUCTION OF FUZZY LOGIC CONTROLLER

The following five sequential steps explain how the fuzzy control mechanism works, as introduced in [62]:

(i) Defining the Non-Fuzzy Variables:

In this step, a decision is made regarding which non-fuzzy variables representing the system dynamics, (whether analog or crisp), shall be chosen as the input and output variables of the fuzzy controller. Since the fuzzy logic controller is proposed to replace the conventional PD, the error in the swash plate inclination angle α_e is chosen as the input signal to the fuzzy logic controller. The set point of the proportional valve spool displacement s_{sp} is the controlled output signal of the fuzzy controller. Oil bulk modulus B will be used as a disturbing parameter and it is represented by an input membership function and is considered in the inference unit.

(ii) Defining Fuzzy Variables:

This step describes some fuzzy linguistic variables that specify the quality of the control that can be achieved using the fuzzy controller. With the increase of the number of the fuzzy linguistic variables, the system dynamic performance improves; on the other hand, the computational time and the amount of required memory increases. The high (H), medium (M) and low (L) values are assigned as the linguistic

variables that will be used by the fuzzy controller. When these fuzzy variables are of positive or negative values, P or N designates them.

(iii) Fuzzification Process:

Fuzzification means the translation of the analogue input variables into the corresponding fuzzy values that are understood by the fuzzy controller. The part of the fuzzy controller structure that is responsible for performing this fuzzification process is called the input membership function. In general, the membership function consists of a group of fuzzy sets. Figure 5.4 illustrates a simple comparison between the ordinary set and the fuzzy set. An ordinary set allows only binary choices between the in or out of the set, while the fuzzy set allows a continuum of possible choices with a different weighting of membership. As shown in Fig.9.1.a, a value of 9 belongs to the ordinary sets L, M and H with weighting factors 0, 1 and 0, respectively. Figure 9.1.b is an example of a value of 9 that belongs to the fuzzy sets L, M and H with weighting factors of 0, 0.8 and 0.2, respectively. Engineering knowledge, as well as trial and error, is generally used to build up the membership functions in the fuzzy logic technique. Some recommendations must be considered during the construction of the membership functions in order to produce the best performance. Fuzzy sets are better when they are overlapped at a grade of 50%, and there should be no more than two intersecting fuzzy sets. Triangular, trapezoidal or bell-shaped functions are used. Asymmetrical shapes causing more crowding near the origin permit precise control near the steady state operating point. Among the many shapes available for membership functions, the triangular ones shown in Figs. 9.2 and 9.3 were found after extensive trial runs to be both simple and the shapes that yield the

best pump performance. Figures 9.1 and 9.2 show an example of the fuzzification process assuming an error in the swash plate inclination angle, α_e, equal to 1.75 and an oil bulk, B, equal to $1x10^9$Pa, as non-fuzzy inputs to the input membership functions. The input fuzzy variables corresponding to α_e are equal to MP and HP with membership grades equal to 0.25 and 0.75, respectively; and corresponding to B is equal to H with a grade of 1.

(iv) Rule-Based Decision Making

The control decision is made based on the inference unit which is a group of rules shown in Table 9.1. The inference unit is constructed in order to replace a skilled human operator. The outcome of this process is the output fuzzy variable corresponding to the input fuzzy variable. The output fuzzy variable will be corresponding to the proportional valve spool displacement set point value s_{sp},. Based on the inference unit and the algebra of fuzzy variables, the output fuzzy variable is equal to MP and HP with membership grades of 0.25 and 0.75, respectively.

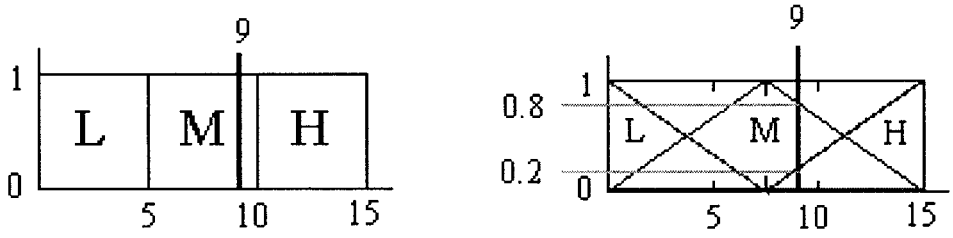

a- Ordinary Sets b- Fuzzy Sets

Fig.9.1 Ordinary sets and fuzzy sets

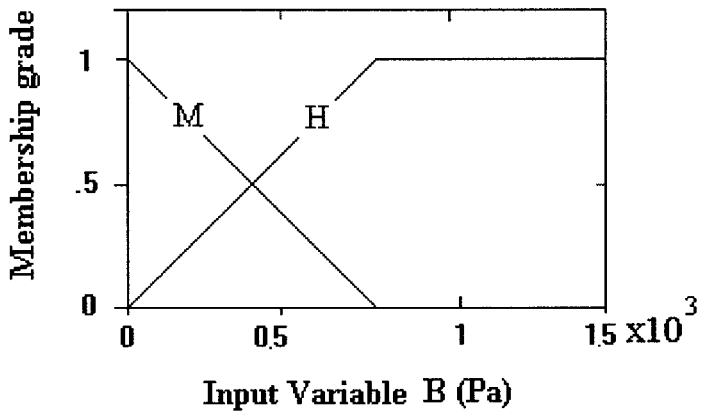

Fig.9.2 Input membership function, oil bulk modulus

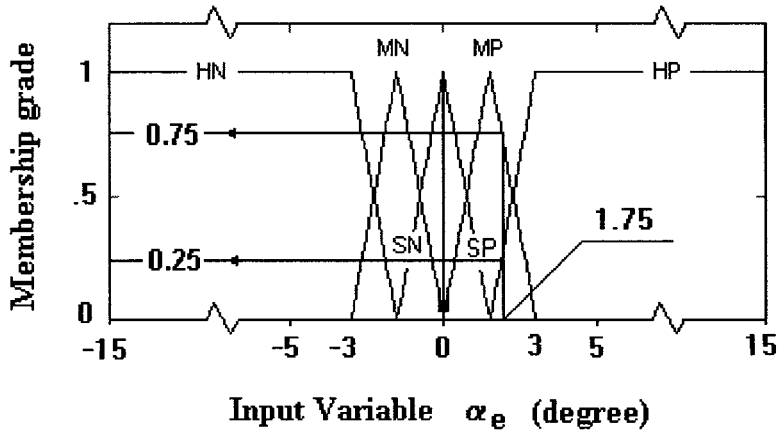

Fig.9.3 Input membership function, error in the swash plate inclination

Table 9.1 Inference unit

If α_e is HN AND B is H	then s_{sp} is HN	If α_e is HN AND B is L	then s_{sp} is HN
If α_e is MN AND B is H	then s_{sp} is MN	If α_e is MN AND B is L	then s_{sp} is HN
If α_e is LN AND B is H	then s_{sp} is LN	If α_e is LN AND B is L	then s_{sp} is MN
If α_e is LP AND B is H	then s_{sp} is LP	If α_e is LP AND B is L	then s_{sp} is MP
If α_e is MP AND B is H	then s_{sp} is MP	If α_e is MP AND B is L	then s_{sp} is HP
If α_e is HP AND B is H	then s_{sp} is HP	If α_e is HP AND B is L	then s_{sp} is HP

(v) Defuzzification Process:

The defuzzification process is the inverse of the fuzzification process. In this process, the output fuzzy variables that result from the decision-making processes are retranslated into a non-fuzzy output control signal. For this purpose, an output membership function is constructed. Figure 9.4 shows the widely used membership function for the output variable. Different techniques can be used to calculate the output control signal value but the most widely used method, Mamdani's method, is adopted in the following analysis.

The fuzzy sets of the fuzzy variables in the output membership function are to be truncated at the corresponding grades as shown in Fig.9.5. By using such a method, the centroid of the resulting truncated output fuzzy sets is considered to be the value of the output analogue control signal. The figure shows that the output controlled signal equals 0.8. The previously presented membership functions, as well as the inference unit, are used within the proposed fuzzy logic controller of the pumps studied in this thesis.

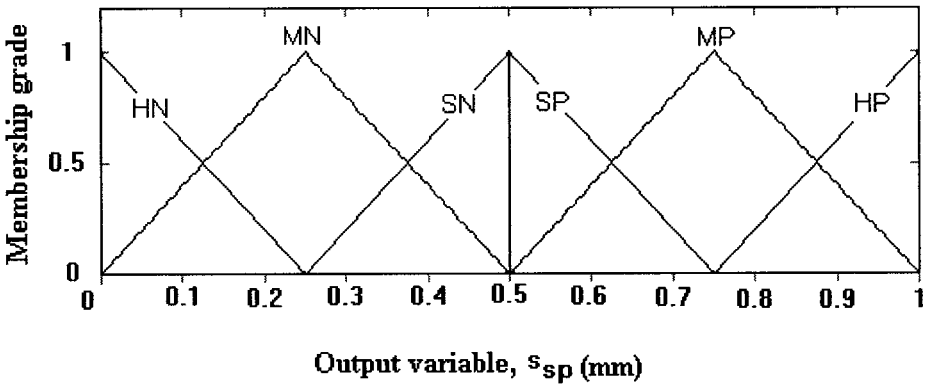

Fig.9.4 Membership function for the output variables

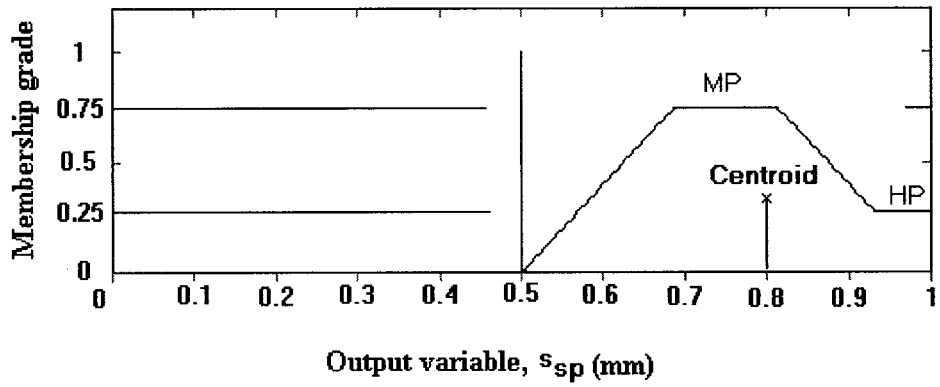

Fig.9.5 Defuzzification process

APPENDIX F

REAL TIME CONTROL SOFTWARE MODULES

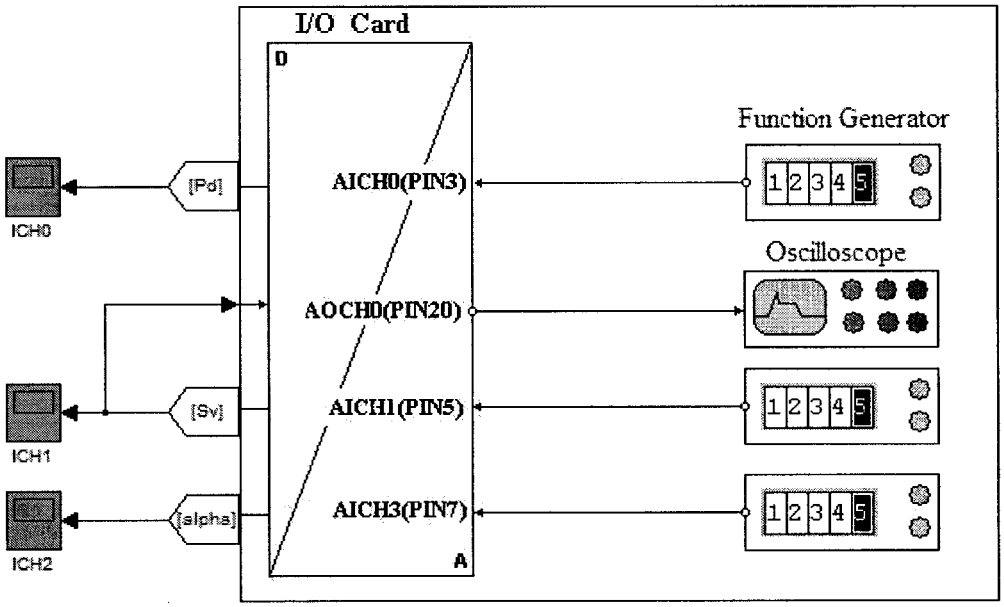

Module 1- I/O Card configuration

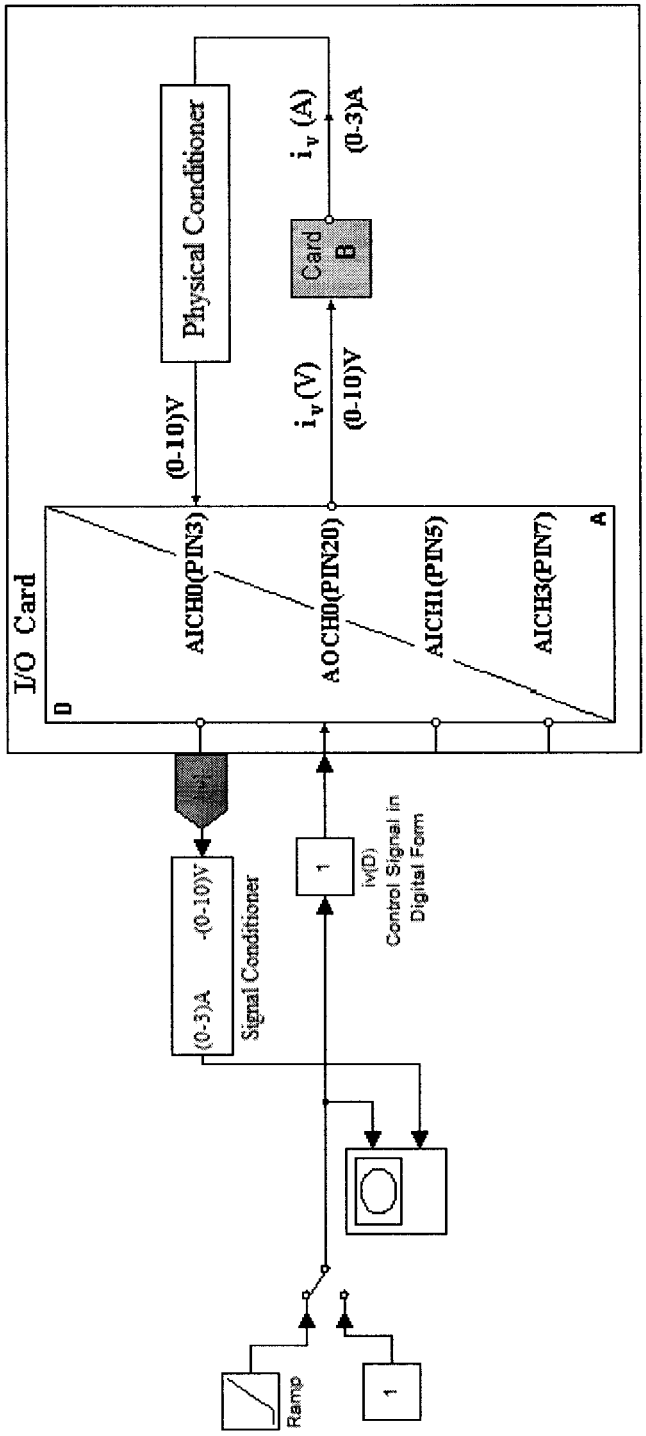

Module 2 – Card "B" configuration

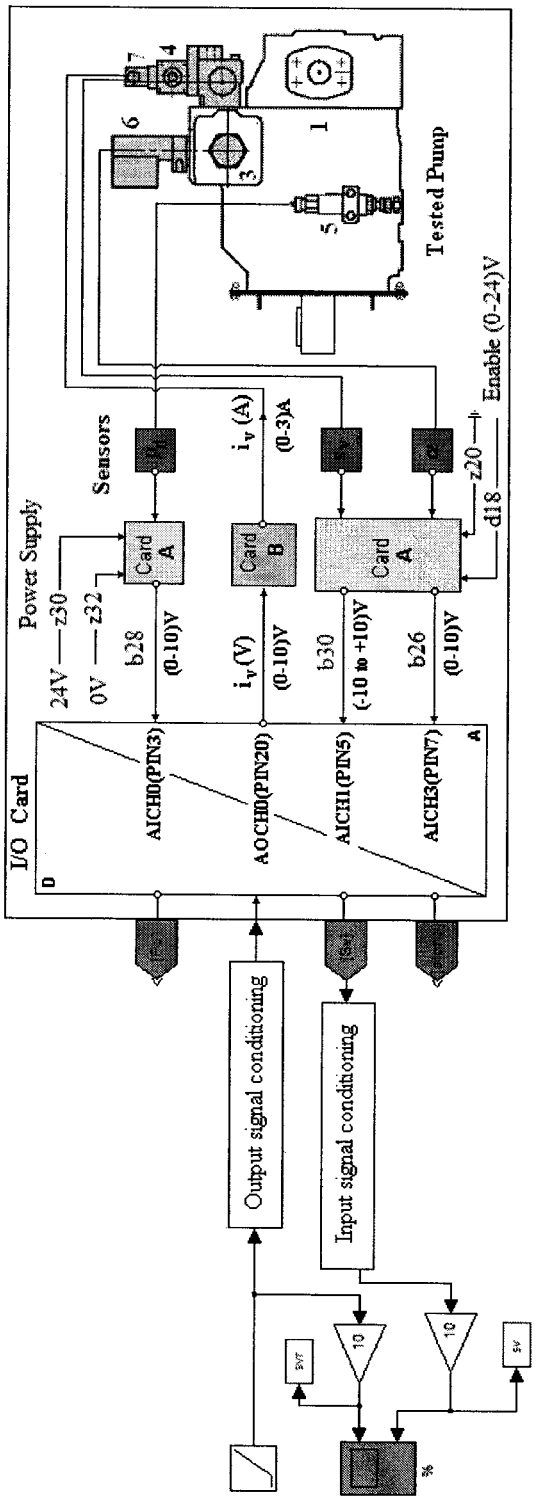

Module 3 – Conditioning of the proportional valve spool displacement signal in an open loop function

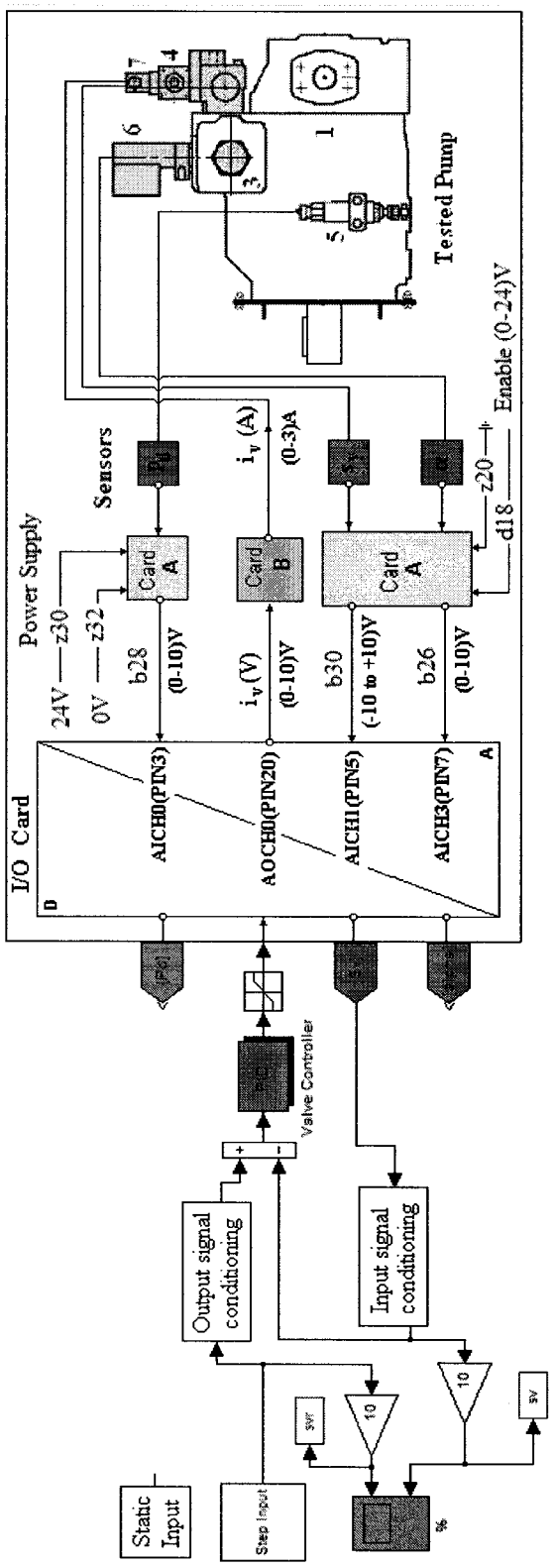

Module 4 – Closed control loop for position control of the spool

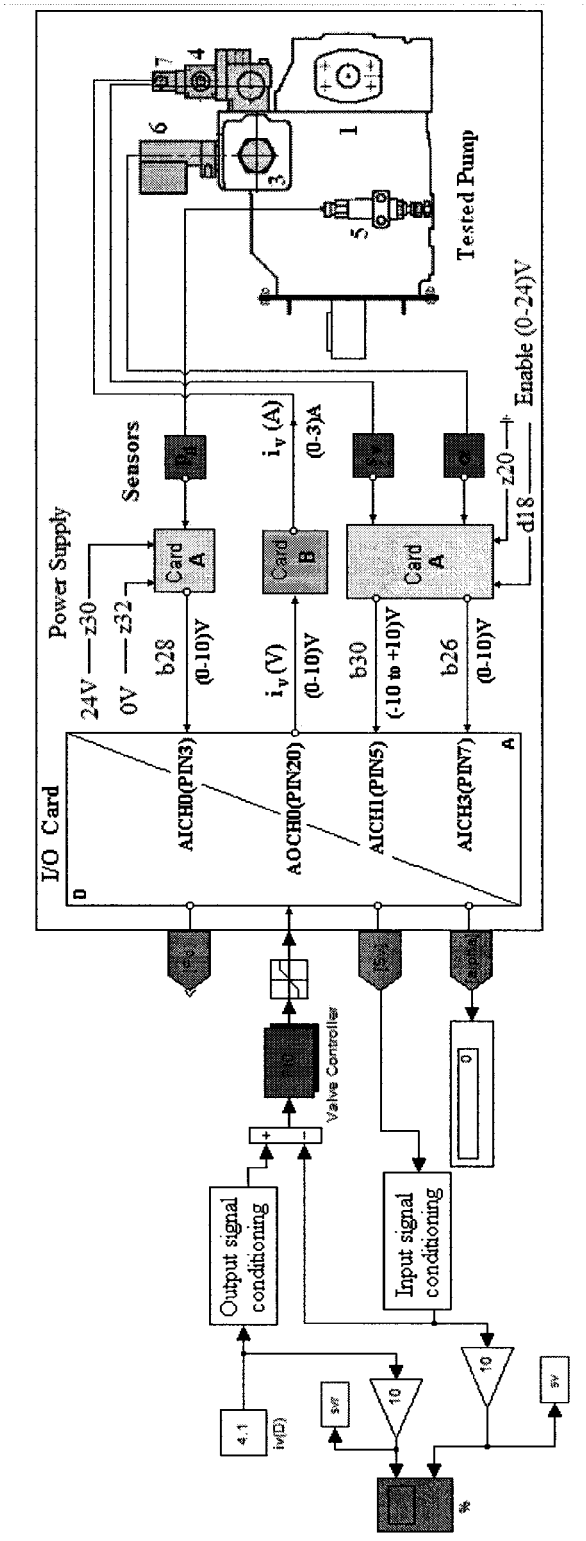

Module 5 – Calibration and conditioning of the swiveling angle and finding the valve zero point

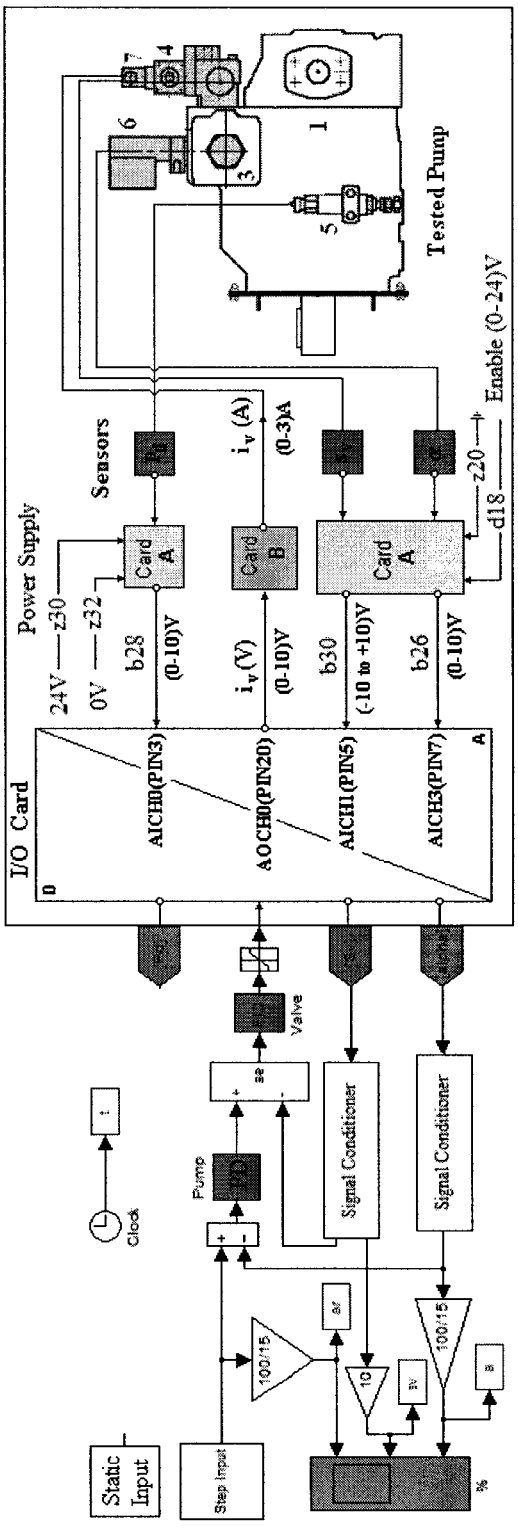

Module 6 – Double feedback control scheme with PD pump controller

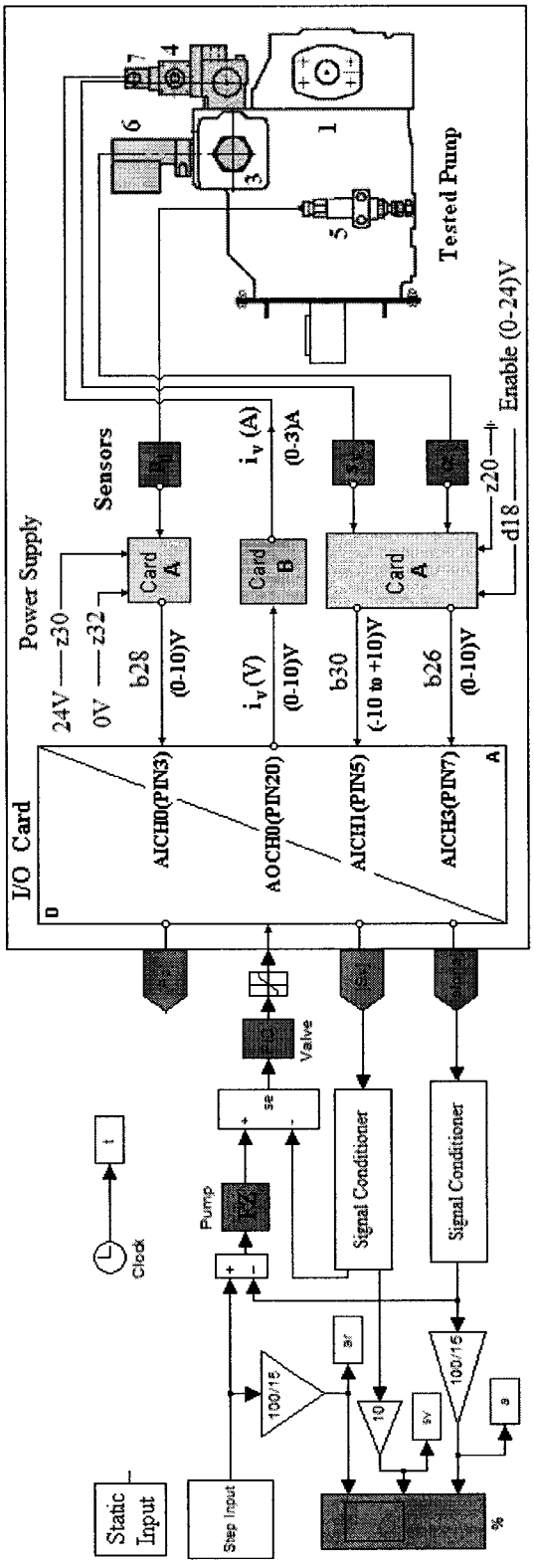

Module 7 - Double feedback control scheme with fuzzy pump controller

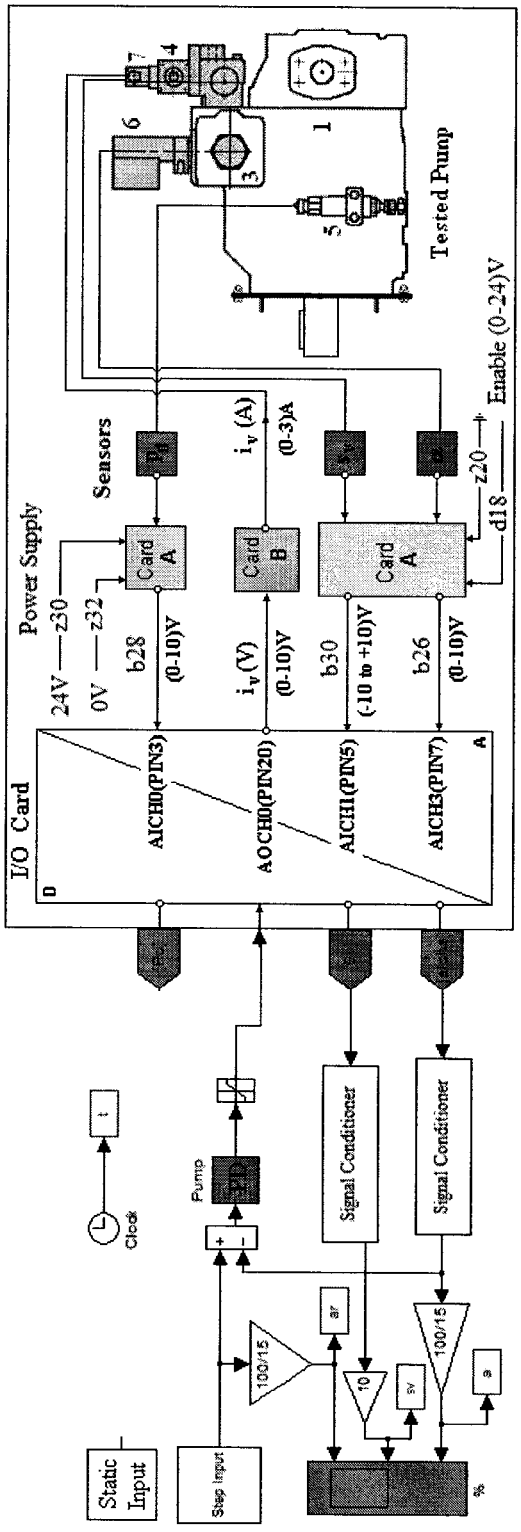

Module 8 – Single feedback control scheme with PD pump controller

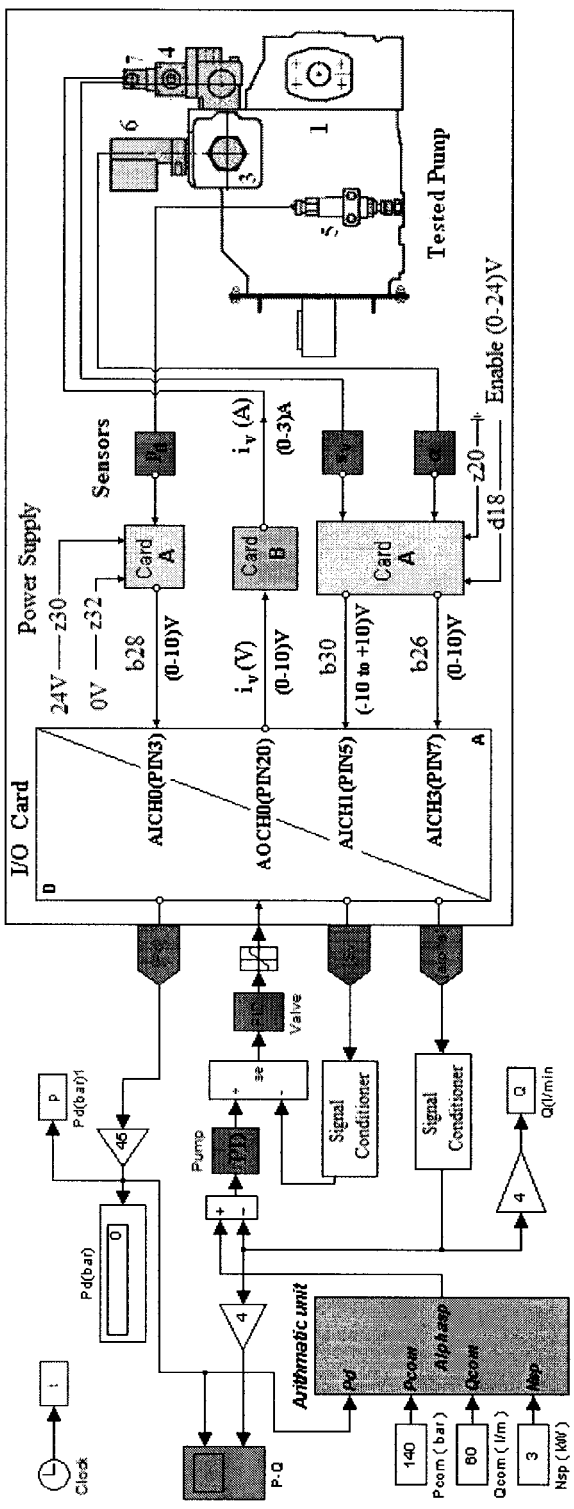

Module 9 – Constant power operation of the pump with PD controller in double feedback control loop

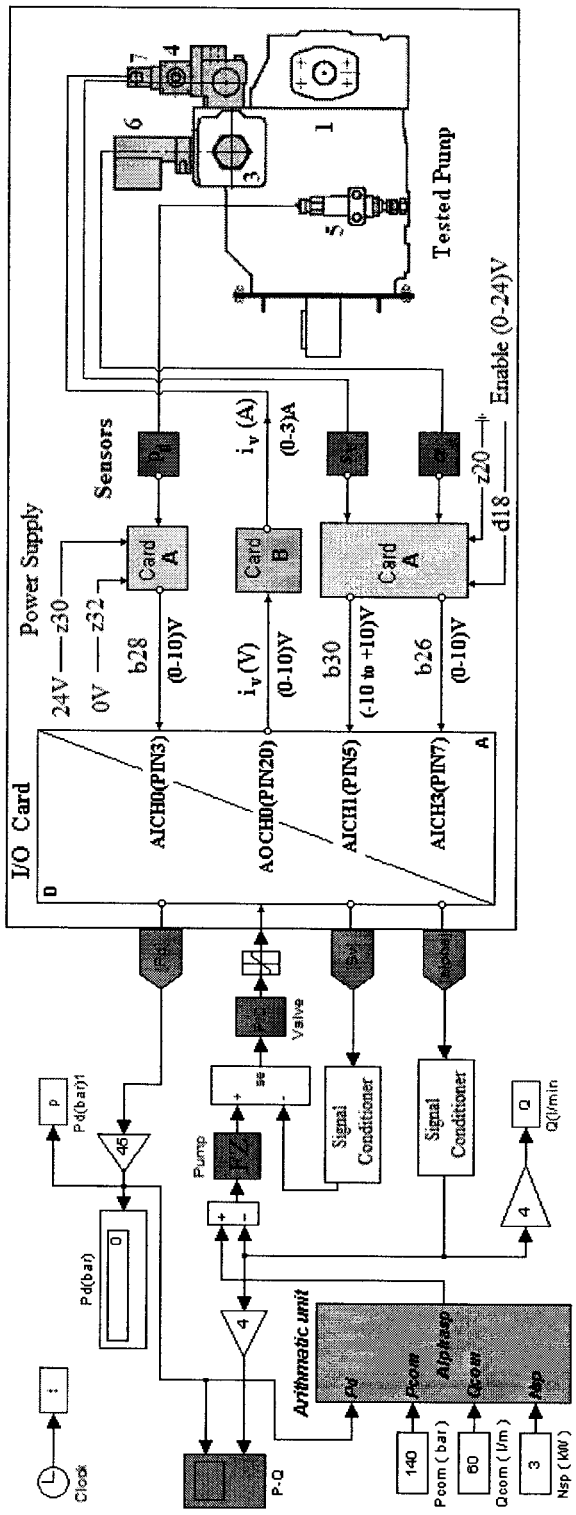

Module 10 - Constant power operation of the pump with fuzzy controller in double feedback control loop

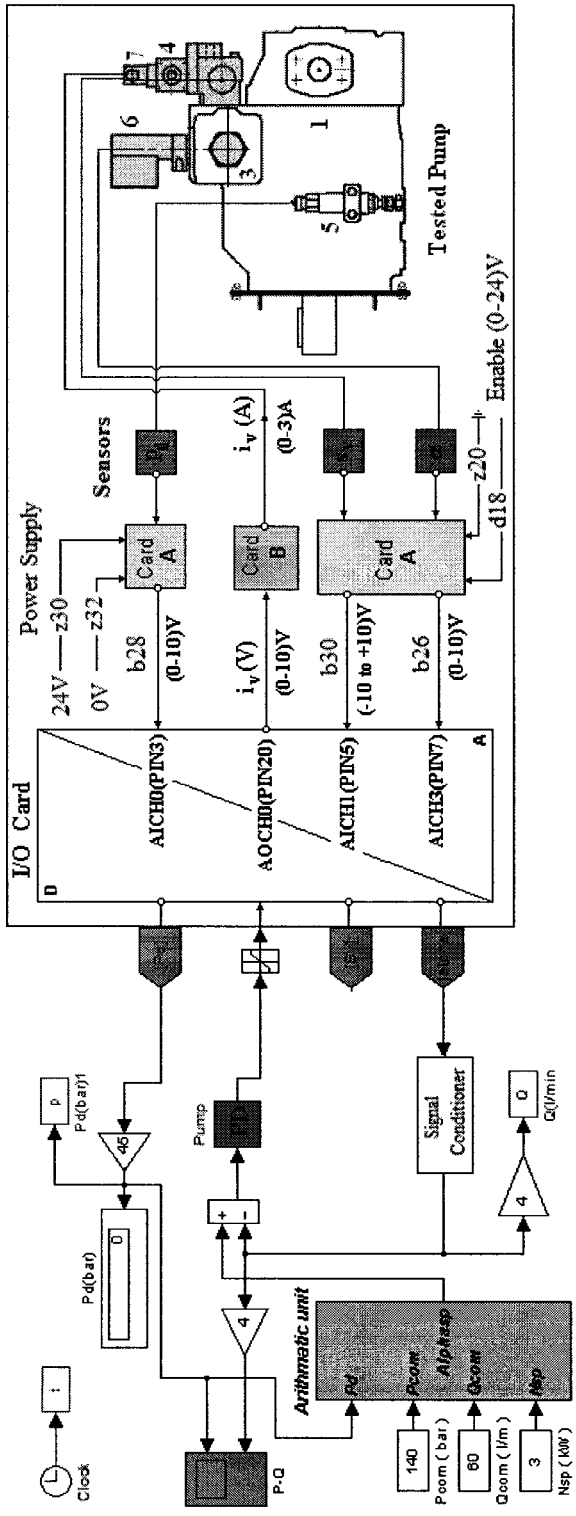

Module 11 - Constant power operation of the pump with PD controller in single feedback control loop